TIMED EXECUTION
IN DISTRIBUTED MACHINE LEARNING

BY

SAYED HADI HASHEMI

DISSERTATION

Submitted in partial fulfillment of the requirements
for the degree of Doctor of Philosophy in Computer Science
in the Graduate College of the
University of Illinois at Urbana-Champaign, 2020

Urbana, Illinois

Doctoral Committee:

Professor Roy H. Campbell, *Chair*
Professor William D. Gropp
Professor Philip B. Godfrey
Professor Volodymyr V. Kindratenko
Dr. Gregory F. Diamos

Abstract

Deep learning powers many transformative core technologies including Autonomous Driving, Natural Language Translation, and Automatic Medical Diagnosis. Its exceptional ability to extract intricate structures from high-dimensional data takes the credit for major advances in machine learning.

Essential ingredients that make Deep Learning possible include: the availability of a massive curated data, a well-designed model, and readily available high-performance computation. The computation used in training deep neural networks has doubled every 3.4 months since 2012, five times faster than Moore's law. Fulfilling this massive computational demand that has long outgrown the capability of a single high-end node is vital to keep extending the flow of innovations. For example, in 2018, the AlphaGoZero model trained with 1.89 ExaFlops/s times a day. The state-of-the-art GPU at the time, NVidia V-100, could only deliver 125 TeraFlops. In a meanwhile, Summit, the fastest supercomputer in the world, could sustain 1 ExaFlops/s using 27,360 NVidia V-100 GPUs through distributed computation.

This dissertation studies the challenges of scaling out an ML job to keep up with the computational demand, specifically the problems stemmed from the complex interplay of various resources in the distributed ML. In the first stage of this research, we developed methods and systems to properly observe a distributed ML environment by tracing a distributed execution, visualizing the results, and expanding the observability to the production infrastructure. Later we developed three systems to address scalability challenges using these methods and systems based on a precise execution timing of the spectrum of resources:

Network: `TicTac` reduces internal computation delays by enforcing a near-optimal order on network transfers, which results in up to 37.7% throughput increases.

Computation: `Caramel` increases the network utilization and decreases network congestion by modifying the order of computation and choosing the most fitted collective primitive for the workload. This result in cutting the training time up by a factor of up to 3.8. While computation and network scheduling suggest an order of execution, `TimedRPC` addresses the issue of correctly enforcing this order by implementing a priority-based scheduling through pre-emption where an on-going transfer can be paused when a transfer with higher priority is requested.

I/O: `Diot` maximizes the I/O throughput by tuning knobs such as number of concurrent I/O requests and read size on I/O pipeline. Additionally it detects the I/O delivery unfairness which may causes a struggling worker due to slow I/O through.

Thesis Statement

Heuristic timing of distributed machine learning execution leads to utilization optimizations for computation, network, and storage, which in turn improves the overall throughput. In general, any multi-resource optimization involving parallelism is at least NP-Hard.

To Shekoofeh, Reza, Akhtar, Amir, Azadeh, and Payam.

Acknowledgments

Firstly, I would like to express my sincere gratitude to my advisor Professor Roy H Campbell, for the continuous support of my research, for his patience, upbeat energy, motivation, and immense knowledge. He was not only an advisor who helped to shape this study, but more importantly, he was a mentor who forms me into a curious, confident, and independent researcher. It has been a privilege for me to work with him and I could not have imagined having a better advisor and mentor for my Ph.D. study.

Besides my advisor, I would like to thank the rest of my doctoral committee: Professor William Gropp, Professor P. Brighten Godfrey, Professor Volodymyr Kindratenko, and Dr. Gregory Diamos, for their invaluable feedback, insightful comments, and encouragement.

My sincere thanks also go to Dr. Bryan Catanzaro, Dr. Gregory Diamos, Dr. Paul Barham, Professor Volodymyr Kindratenko, and the fantastic people at Baidu's Silicon Valley Artificial Intelligence Lab, Google Brain, and National Center for Supercomputing Applications who provided me an opportunity to join their team. Without their precious support, it would not be possible to conduct this research.

I thank my fellow collaborators throughout my journey. Mainly, I would like to thank Dr. Sangeetha Abdu Jyothi for the inspirational discussions, and the sleepless nights, we were working together before deadlines. I was fortunate to be part of "Systems Research Group," and many thanks to its members, Dr. Faraz Faghri, Dr. Shadi A. Noghabi, Dr. Mohammad Babaeizadeh, Dr. Read Sprabery, Dr. Chris Cai, Dr. Imani Palmer, Dr. Reza Farivar, Konstantin Evchenko, and John Bellessa. I would also like to express my sincere gratitude to my many friends in Urbana-Champaign for all the fun we have had in the last five years. Many thanks to the staff of the Computer Science department, including but not limited to: Kathy Runck, Laura Thurlwell, Alice Needham, Kara MacGregor, Mary Beth Kelley, Viveka Perera Kudaligama, and Maggie Metzger Chappell for their continuous help and support during my studies.

Last but not least, I would like to thank my wife, my parents, my brothers and sister for the unconditional love, and supporting me spiritually throughout this journey and my life in general.

TABLE OF CONTENTS

CHAPTER 1: INTRODUCTION

Artificial intelligence and in particular Deep Neural Networks (DNNs) form the crux of the advanced solutions in a variety of fields such as computer vision, speech recognition, autonomous driving, and natural language processing. The availability of rich data, readily accessible distributed high-performance computing, and flexibility of development offered by modern machine learning systems fuel AI growth in the past decade.

The computational cost of training sophisticated deep learning models has long outgrown the capabilities of a single high-end machine, leading to distributed training being the norm in a typical AI pipeline. Scaling from a single machine to multi-node training brings exciting challenges on how to handle communication, which has a crucial impact on the performance and scalability of distributed ML applications.

Adding networking to a machine learning job creates a complex interplay of heterogeneous resources which demands precise timing of network transfers, computational operations, and I/O requests to sustain a full resource utilization.

This dissertation studies the challenges of scaling out the machine learning jobs from a system perspective. We address issues of:

- Observing the performance unobtrusively in a distributed environment.
- Finding the right order of execution which often requires fusing the application-level data with platform specification.
- Faithfully enforcing the timing of execution.

1.1 CONTRIBUTIONS

The main contribution of this work is identifying several performance issues caused by poor timing of execution. We have developed three **toolkits** to observe these issues at runtime, three **models** to explain the problem, and four **frameworks** to address the challenges.

1.1.1 Frameworks

In this research, we have developed three frameworks to find and enforce the optimized order of execution on Computation, Network, and I/O, respectively. Additionally, we develop one framework to enforce the order on network transfers correctly.

- **Network Transfer Timing**: We show that the order of network transfers in distributed jobs that use a Parameter Server has a significant effect on accelerator utilization [45] and that finding the right order is an NP-Hard problem. Our framework, `TicTac` [46] improves the performance of these jobs up to 37% by heuristically improving order of transfers and enforcing this order at runtime(§6).

- **Computation Timing**: We show that changing the order of computing operations in the Data-Parallel training jobs with Collective Transfers allows improvement in network utilization. Our framework, `Caramel`, increases the computation throughput by up to 3.84×(§7).

- **I/O Request Timing**: We show that I/O could quickly block the computation when the data pipeline is not properly tuned or the I/O delivery is not fairly distributed among workers. Our framework, `diot`, increase the I/O throughput up to 100× by automatically improving timing and configuration of the data pipeline as well as detecting any delivery unfairness (§5).

- **RPC Timing Enforcment**: We show that using TCP and its FIFO ordering for a single connection between nodes is not optimal for scheduling network transfers and causes computational slow down. Our proposed RPC framework, `TimedRPC` [43], addresses this issue by implementing priority-based scheduling with network transfer preemption. (§7.8)

1.1.2 Models

We introduce three performance models to explain the performance properties of distributed machine learning jobs:

- **Communication Model** [45]: This model predicts the performance of an ML job with regards to computation to communication ratio and computation/computation overlap. We use this model to explain why a higher bandwidth network does not always lead to higher overall performance. (§6.3)

- **Aggregation Model** [44]: We use this model to predict the total time required to aggregate parameter updates over the given network when a certain aggregation primitive is used. Later we use this predictor to choose the best implementation of collective primitives in `Caramel` system from the collection of Doubling-Halving, Ring, Shuffle, and Parameter Server. (§7.4)

- **Storage Model** [47]: We use this model initially to explain the poor performance of CNTK on BlueWaters where I/O was the bounding resource [47]. Later we use this model to predict when the I/O becomes a bottleneck in an ML job. (§5)

1.1.3 Toolkits

We have developed a collection of performance analysis toolkits to bring runtime transparency into the execution of distributed machine learning jobs:

- **Distributed Tracing**: We expand the execution tracing capability of the existing system to support multi-machine jobs. This toolkit [42] coordinate the tracing among all the workers, captures the network activities (encapsulated as RPC calls) on all workers, and collect all the traces without interfering with the execution. (§4)

- **Visualization**: We develop a visualization toolkit [42] to facilitate the examination of a large quantity of tracing data by providing fast navigation of events while retaining the event details. (§4.2)

- **Tracing in the Production**: We extend the distributed tracing to production infrastructures. `tensorflow-tracer` [48] allows system administrators to profile and trace ML jobs without any code modifications and exchange tracing sessions to developers. (§4.3)

1.2 MODERN DISTRIBUTED MACHINE LEARNING SYSTEMS

There has been many distributed ML system introduced in the past few years. TensorFlow [1], PyTorch [81], Microsoft Cognitive Toolkit [89], Keras [26], MXNet [21], and Chainer [104] to name a few. While there are many differences between these systems, they can be characterized by three main traits:

1. **Iterative**: Modern systems focus on training large ML models on a big dataset which requires more sophisticated optimizer such as the family of "Stochastic Gradient Descent" algorithms [15, 85, 62, 86, 16]. These optimizers are iterative; The training process is a series of iterations which read a batch of data and update a set of persistent parameters. All the modern systems are designed around this iterative workload.

2. **Compute Intensive**: The massive success of Deep Learning which requires substantial computation time on the training makes specialized accelerators, such as the GPU

and TPU [59], a standard part of ML infrastructure and natively supported by ML systems. To contain the steep learning curve of SIMD programming for these accelerators, the ML workload is represented as a DAG of predefined operations.

3. **Rapid Experimentation**: The fast pace of change in AI requires a shorter cycle of prototyping an idea to getting results. To this end, the current incarnation of ML introduces dataFlow DAGs to hide the steep learning curve of SIMD programming for specialized accelerators and gradient calculations in SGD.

1.3 RELATED WORKS

This section presents an overview of evolution of distributed machine learning from the early cloud computing era until present days.

MapReduce The success of *MapReduce* [32] computational models in cloud computing inspires early distributed machine learning systems. Examples of these systems are Apache Mahout [53] (2009) built on top of Hadoop ecosystem [107] and MLlib [72] (2013) built on top of Spark Ecosystem [115]. These systems are a collection of computationally-light ML algorithms implemented as Map/Reduce jobs. Using MapReduce in these systems allowed the ML algorithms to be applied to the massive data stored in the cloud.

Parameter Server The next wave of Distributed ML systems makes use of the Parameter Server (PS) architecture to support more customizable and complicated ML models and iterative training algorithms such as Stochastic Gradient Descent [85, 62, 86, 16]. Examples are DistBelief [31] in 2012 and Project Adam [24] in 2014 which are designed specifically for neural networks and Parameter Server[68] in 2014 designed for some simpler models. In this architecture, the ML parameters are stored and managed in parameter servers (PS) modeled after Key-Value systems with weak consistency. At the beginning of an iteration, a worker reads the recent version of parameters from PS, then sends the updates back to the PS at the end.

GPU and Deep Learning Breakthrough In 2012, AlexNet [64] substantially reduced the error rate in the "ImageNet Large Scale Visual Recognition Competition" using a neural network trained on the GPU. The success of this work made a paradigm shift to ML research: Use of higher capacity neural network models (dubbed as Deep Learning [67]) which required higher computation time that could be cheaply attained using the GPUs of the time. The

steep learning curve of developing GPU application led to a new DAG-based programming model introduced in Caffe [58] and MxNet [21]. In this model, the workload is represented as a DAG where nodes are operations and edges are data flow or control dependencies. The ML framework is shipped with predefined operations with GPU implementations. The user then define the data flow or dependencies without requiring any GPU programming. Using a DAG-based model has been widely adapted in recent iterative machine learning systems.

TensorFlow [1] in 2015 extends this representation by assigning nodes to each device as well as adding network transfers as nodes to the DAG. This unified representation permits compiler optimizations and simplifies deployment [17].

Collective Transfers Moving beyond PS architecture, DeepSpeech2 in 2015 [7] and CNTK in 2016 [89] proposed a new distribution architecture tailored toward high-performance networks such as Infiniband and Omnipath. In these systems, unlike PS architecture, there are no centralized servers. Each worker stores a copy of parameters and update to parameters as an aggregate through a collective transfer such as `MPI_allreduce` call in MPI[40]. This is accelerated by hardware and unlike PS, it does not induce network congestion.

Later in 2017, these collective transfers are added to the collection of predefined operations in data flow DAG as operations by Baidu Allreduce [11] and Horovod [90].

In 2017, Facebook [37] reduced the training time of ResNet-50 from 29 hours to less than an hour while maintaining the same level of accuracy by combining the collective transfer architecture with enormous mini-batch sizes increased from 256 to 8192. This work has been the basis of a large number of followup works pushing the computation boundaries further [57, 4, 112, 113] including *Exascale Deep Learning for Climate Analytics* [65] on Summit SuperComputer which broke the ExaFlop barrier of an Application for the first time.

Beyond DAG The DAG has been the dominant representation of ML workloads, search for alternatives continue. PyTorch [81] and other works [3, 77]introduce imperative DAG programming style. In this style, an operation is executed as soon as it is added to the DAG. This, in turn, improves the interactive experience of a developer by allowing just in time debugging and more natural flow of execution.

Yu et al. [114] propose a new graph-based representation which adds conditional branching and loops to dataflow DAGs while maintaining the support for automatic differentiation.

The DAG programming style with coarse hyper-optimized predefined operations is blamed for hindering ML research progress [12] by making it harder to experiment with new operation types. Addressing this problem inspires high-performance general-purpose numerical programming models coupled with device agnostics compilers [54, 22, 103].

CHAPTER 2: BACKGROUND

"All models are wrong; some models are useful."

George E. P. Box

The goal of this chapter is to introduce the computational model of distributed ML jobs. To this end, the chapter starts with the definition of ML and the optimization problem it needs to solve. Then, the stochastic gradient descent (SGD) is introduced as a promising solution. Later we discuss how distributed SGD is implemented in ML systems.

2.1 MACHINE LEARNING

Machine learning as a subset of Artificial Intelligence is the scientific study of making a system learn a task without being explicitly programmed to do so. Mitchell [76] defines learning as:

> "A computer program is said to learn from experience E with respect to some class of tasks T and performance measure P, if its performance at tasks in T, as measured by P, improves with experience E."

Tasks refer to how a machine should process an **example** [36]. For instance, a *Classification* task assigns a class, from a limited list, to a given example. An example is usually defined as a set of **features**.

Performance Measure quantitatively evaluates the performance of a machine learning algorithm. For example, in a classification task, *Accuracy* is a performance measure that shows the proportion of examples for which the model assigned the right class.

Experiments are a collection of examples, or methods used in obtaining the data or examples that an algorithm has access to during the learning process [36]. For example, in a *Supervised* environment, an algorithm has access to a labeled dataset, which is a collection of examples each associated with a class. A Experiment set in supervised learning is commonly called a *dataset*.

2.1.1 Example: Supervised Classification

To better understand the computation model of an ML job, this section describes a simple "Classification" learning task with a "Supervised" experiment. In this experiment, the dataset is:

$$X \in \mathbb{R}^n, Y \in C = \{c_1, c_2, \ldots, c_m\}, X \to Y \tag{2.1}$$

Where X is the set of **examples** with n features and Y is the set of classes. Each example is associated with a class.

The classification task is defined as function which assigns a class to a given example:

$$f(W; x) : \mathbb{R}^n \to C \tag{2.2}$$

f is the machine learning model, such as Neural Networks or Linear Class, and W is a set of parameters the model takes in addition to an example, x.

The goal of learning is to optimize performance measure. For example, Using a loss function as the measure, the optimization problem is:

$$\min_{f,W} loss(f(W; X), Y) \tag{2.3}$$

Training a given model f, is the process of optimizing W:

$$\min_{W} loss(f(W; X), Y) \tag{2.4}$$

2.1.2 Stochastic Gradient Descent

As the size parameters and dataset grow, it becomes harder to solve the optimization problem in 2.4. Stochastic Gradient Descent and its variations [85, 62, 86, 16, 67] are the de facto methods in these cases.

The main idea in this iterative optimizer is to follow the opposite direction of the performance measure gradient. In each iteration, randomly selected examples, X_{bs} and Y_{bs}, are used to calculate the gradient. Then a multiplier of the gradient is subtracted from the parameters:

$$W \leftarrow W - \eta \nabla loss(f(W; X_{bs}), Y_{bs}) \tag{2.5}$$

Where η is the learning rate, and bs is the mini-batch size. There are three tasks involved in machine learning:

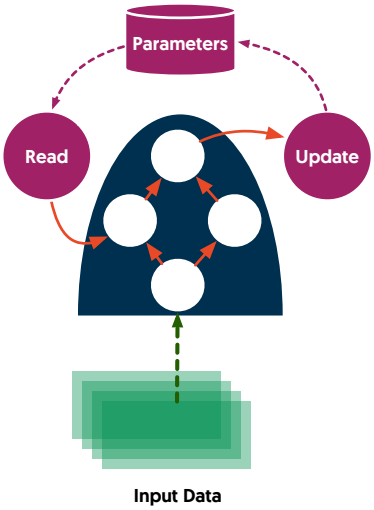

(a) Architecture

(b) Timeline

Figure 2.1: Abstract execution model of an iteration of ML training job on a single node

Training is the process of optimizing parameters W given the model f, the performance measure $loss$, the dataset X, Y, and hyper-parameters η, bs.

Hyper-parameter Tuning is the process of finding the right hyper-parameters for the learning process. This process is not a part of the training and does not use SGD directly to optimize.

Inference is the process of using the model f and parameters W to predict the result of the task on a possibly unseen example.

2.2 TRAINING COMPUTATION MODEL

The training computation model implements the SGD optimization algorithm in Equation 2.5. This model consists of a few components and several activities.

2.2.1 Components

The training computation model includes the following components (Figure 2.1a):

Stateless DAG: The logic of machine learning model, including calculating the loss function and gradients is represented by a stateless DAG where nodes are predefined operations and edges are data or control dependencies.

Stateful Parameters: The parameters are stored in a persistent object-store shared among ops in the DAG. Special nodes of the DAG can read and update parameters in this object-store.

Input Data: Dataset is stored in a secondary storage. Parallel to the training, the data is read from the storage and preprocessed. The DAG then reads this already loaded and transformed data in each iteration.

2.2.2 Activities

In each iteration, the DAG reads a batch of examples from the dataset and parameters from the persistent object-store. Then loss function and gradients are calculated, and the gradients are applied to the parameters.

Figure 2.1b shows the timeline of the execution. There are five distinct activities in this timeline. Each activities consist of multiple ops which are part of the DAG:

Loading Input Data: The first step of the iteration is to load the input data from memory to the accelerator memory. The data is loaded and preprocessed from a storage asynchronously with the computation (§5.1).

Reading Parameters: This starts in parallel to loading the input data; Each parameter is read individually from the persistent object-store.

Forward Pass: This calculates the loss function using the input data and parameters. The execution of forward-pass, like the rest of the DAG, follows topological order. An op is ready to execute if all its dependencies are available. Therefore, some ops in forward pass may start before all the parameters are loaded. Forward pass also temporary keeps the intermediate data to be used in backward propagations.

Backward Propagation: This calculates the gradients of each parameter following the chain rule. This component runs after the forward pass finishes and uses the loss function value and the intermediate data. Gradients of parameters are calculated roughly in the reverse order the parameters are used in the forward pass.

Updating Parameters: This implements the rule of SGD or other optimizers to update the parameters using the gradients. In this component, the updated value is stored in the persistent object-store. Whenever a gradient is calculated, its corresponding parameter may be updated without waiting for the rest of the Backward Propagation finishes.

An iteration finishes when all the nodes in the DAG are executed.

2.3 DISTRIBUTED TRAINING COMPUTATION MODEL

Distributing a ML jobs introduces network ops and device associations, where each node in the dataFlow DAG is associated with a device. There are three major ways to divide the computation load on multiple devices: Examples, DataFlow DAG, and Operations, or a combination of these three.

Examples In this approach, the mini-batch input is divided among workers. Each worker has a replica of the dataflow and aggregates the parameter changes with other workers. This approach is known as Data-Parallel or Model-Replica. Scaling a model using a Data-Parallel approach is easier compared to other distribution approaches and does not require any placement or human intervention. For example, Data-Parallel DeepLabv3+ [20] has been scaled out to 27360 GPUs while sustaining parallel efficiency of 90.7% [65].

DataFlow DAG In this approach, the dataflow DAG is partitioned on multiple devices. Each worker hosts a part of the DAG. If two ends of an edge are located on different devices, the data is transferred using network or other communication channels (e.g. PCI Express). This approach is known as Model-Parallel. Model-Parallel is shown to have a better performance than Data-Parallel [74, 75]. However, partitioning and placement of the DAG is a non-trivial task that has to be done either manually or by approximation algorithms which in practice can not handle more than a few workers (4 GPUs in [74] and 8 GPUs in [75]).

Operations In this approach, one operation is divided over multiple devices. This approach is mainly used when an operation is disproportionally compute-expensive or exceed

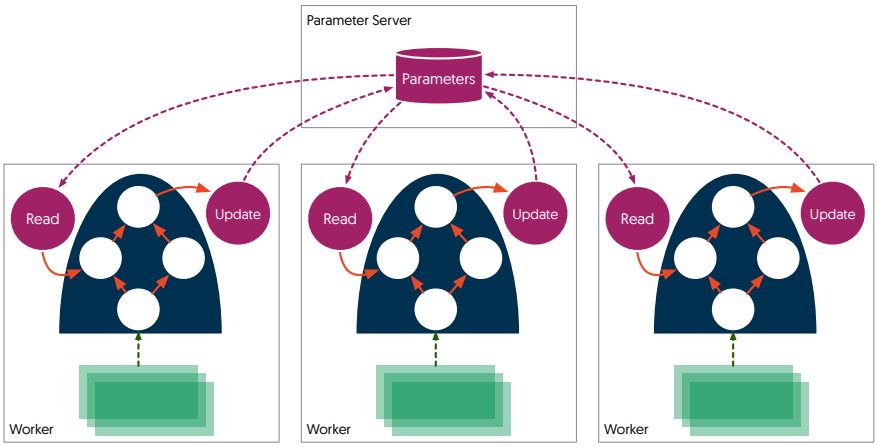

(a) Architecture

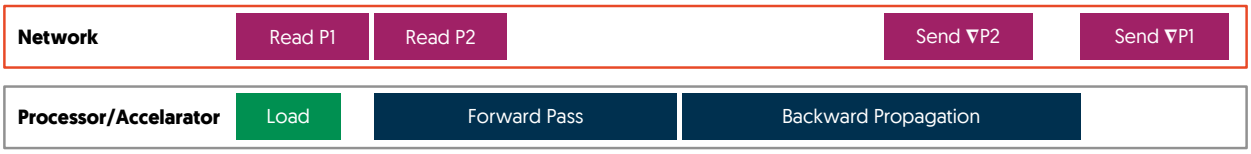

(b) Timeline

Figure 2.2: Abstract execution model of an iteration of a Data-Parallel ML training job with Parameter Server

the size of memory on one device. This approach is known as split network [111] and is implemented by splitting the op into multiple ops, while maintaining the semantics of the operation and applying a Model-Replica approach. In practice, this approach has not scaled beyond a few devices [111].

2.4 DATA AGGREGATION IN DATA-PARALLEL DISTRIBUTION

In the data-parallel distribution there is a need to aggregate the parameter changes among multiple workers and this can be as many as 10s of thousands changes. There are two main implementations:

Parameter Server: In this pattern, the persistent object store is located on a special node, parameter server (Figure 2.2a). In an iteration, workers fetch a recent version of parameters over the network from the PS and send their gradients back to the PS at the end of the iteration (Figure 2.2b). The PS then is responsible for updating the parameters accordingly.

The PS architecture is fault-tolerant: When a worker dies, the training job can continue.

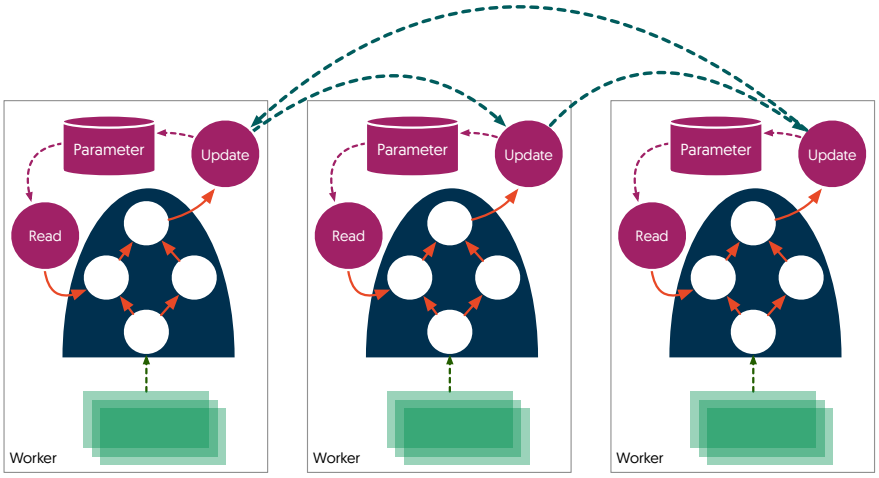

(a) Architecture

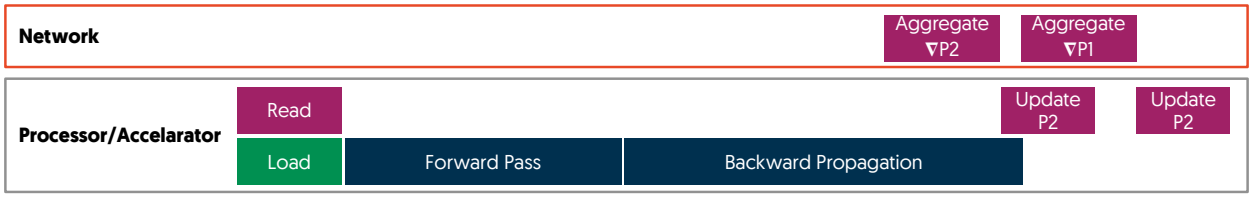

(b) Timeline

Figure 2.3: Abstract execution model of an iteration of a Data-Parallel ML training job with Collective Transfers

Fault tolerance makes PS a perfect fit for clusters with job preemptions such as Borg [108]. However, the all-to-one, one-to-all network patterns in PS induce in-cast/out-cast congestion (§7) which in turn limits scalability.

Collective Transfer: In this pattern, workers collectively aggregate the parameters without requiring additional servers (Figure 2.3a). In an iteration, each worker reads the parameter from a local copy. When a parameter gradient is calculated, it is aggregated through a collective primitive such as Bucket (Ring) [13] or Vector Halving and Distance Doubling [102]. The result of aggregation is then used to update the local parameters (Figure 2.3b).

Collective primitives do not induce congestion in the network and are accelerated through hardware in High-Performance Networks such as Infiniband or Omnipath. As a result, the collective transfer pattern is exclusively used in highly scaled jobs. On the other hand, the collective transfer is not fault-tolerance and relies on mechanisms such as checkpointing for error recovery.

CHAPTER 3: DISTRIBUTION CHALLENGES

"You can have a second computer once you've shown you know how to use the first one."

Paul Barham

Distribution allows more computational resources to be made available for a job. However, fully utilizing the resource increase is quite challenging. This chapter is a summary of such challenges, many have been reported first by this work. We classify these issues into three categories:

- **Scaling Out Challenges:** These appear when the network is added to a ML job including Slow Network, Poor Timing, and Network Underutilization.
- **I/O Challenges:** These are about reading the data from the storage. Slow Storage, Storage Underutilization, and Delivery Unfairness.
- **Methodological Challenges:** These limit the available options to address a performance issue. These options are bounded by how intrusive the solution is to the underlying ML logic.

Furthermore, this chapter describes how the rest of this dissertation addresses these issues.

3.1 SCALING OUT CHALLENGES

Scaling out an ML job does not always improve the overall performance despite the added capacity. In this section, we discuss some of the reasons and how to mitigate them.

The transfer window of a parameter is a period on DAG from when the parameter gradient is calculated in back-propagation to when the updated value is read which could be in the next iteration. If the gradient aggregation among multiple workers finishes after the end of the transfer window, the computation on workers will be stalled waiting for the aggregation to finish. Therefore, for the maximum computational utilization the network transfers should finish within the parameter windows. Figure 3.1 shows the transfer window of VGG-19 [95] running on a slightly modified TensorFlow (§7). Each arrow represents the transfer window of one parameter. As long as all the parameters are updated in their window, the ML job can be perfectly scaled as far as the network concerns. Updating the parameters faster does not speed up the training; however, missing the window slows down the training since the accelerator has to stay idle waiting for the parameter.

Figure 3.1: Transfer window of parameters in a VGG-16 training job. Each arrow represents one parameter: starts when an update to a parameter is available and ends when the parameter value is needed to progress the computation.

The size of transfer windows is independent of the underlying network performance. Instead it depends on dataflow DAG structure, hyper-parameters such as mini-batch size, or the computational performance of the system. There are different reasons why a deadline is missed, see below.

3.1.1 Slow Network:

One obvious reason for missing a deadline is if the network is just too slow keeping up with the computation due to high latency (e.g., WAN) or low bandwidth. A slow network can be described as:

$$Latency + \frac{Total\ Parameters\ Size}{Bandwidth} > Total\ Computation\ Time \tag{3.1}$$

If the Equation 3.1 does not hold, in theory, the network is fast enough to handle the transfer windows. Mini-batch size and computation precision affect the total computation time. However, total parameters size is independent of these factors and is solely depends on the structure of the DAG.

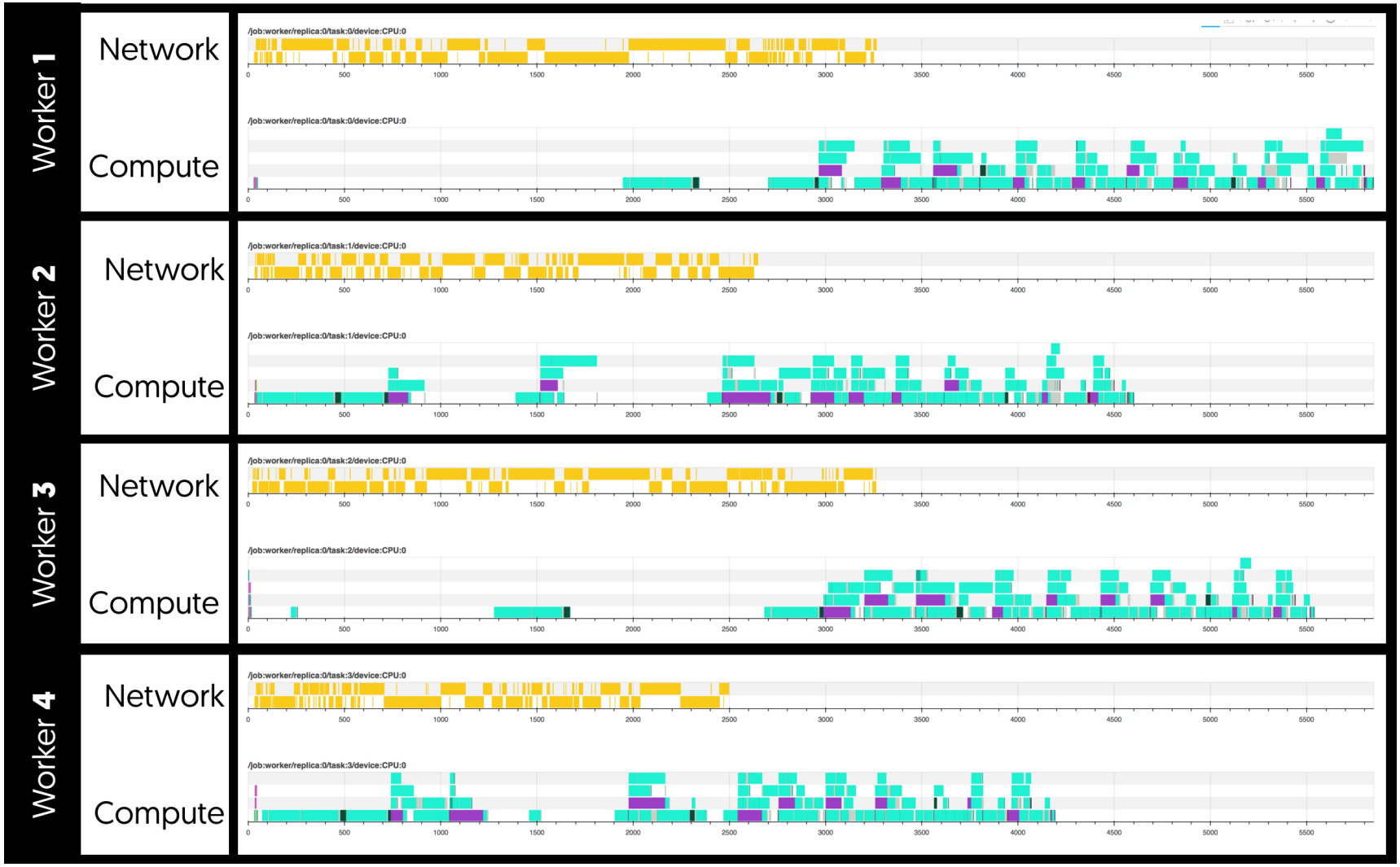

Figure 3.2: The execution timeline of a training iteration. The horizontal axis represents time; each box represents an op execution. The arbitrary transfer timing in default TensorFlow causes processing to stale waiting for network transfers.

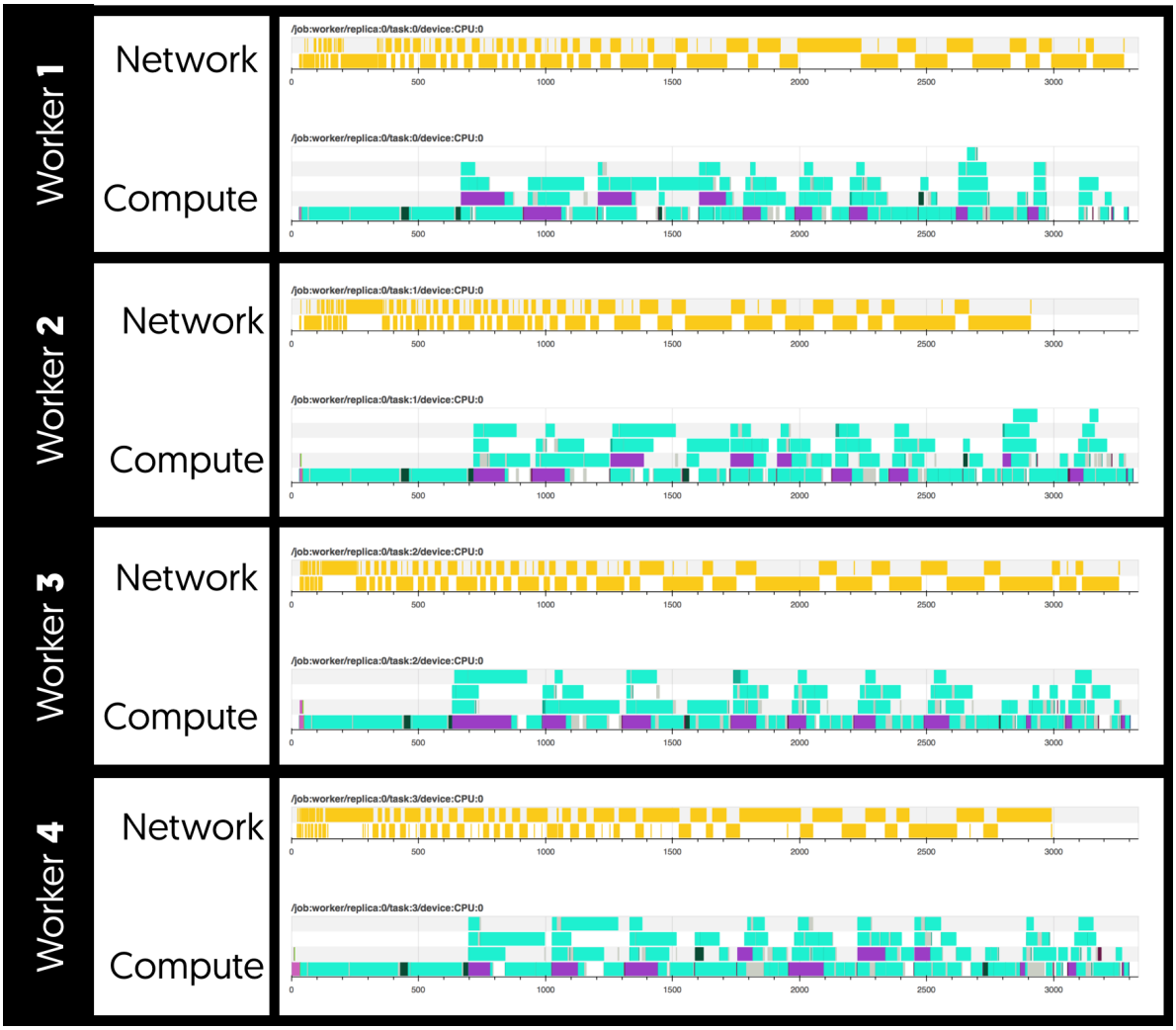

Figure 3.3: The execution timeline of a training iteration. The horizontal axis represents time; each box represents an op execution. TicTac timing achieves near-optimal overlap between computation and network transfers.

3.1.2 Poor Timing

Poor timing of network transfer may cause some parameters to miss their windows while some others finish earlier than necessary. As a result, the computation has to stall waiting for a specific parameter to transfer while some other received parameters are staying unused.

Figure 3.2 and Figure 3.3 show the effect of the timing on a Data-Parallel with PS training job of Inception V2 [55]. The vanilla timeline (Figure 3.2) shows an iteration with arbitrary order of transfer, the default behavior of TensorFlow. The missing parameter stalls the computation several times in the iteration. In comparison, the TicTac timeline (Figure 3.3) shows the identical training step with a near-optimal transfer order. While the network and computation load is identical to the vanilla timeline, the iteration is substantially faster due

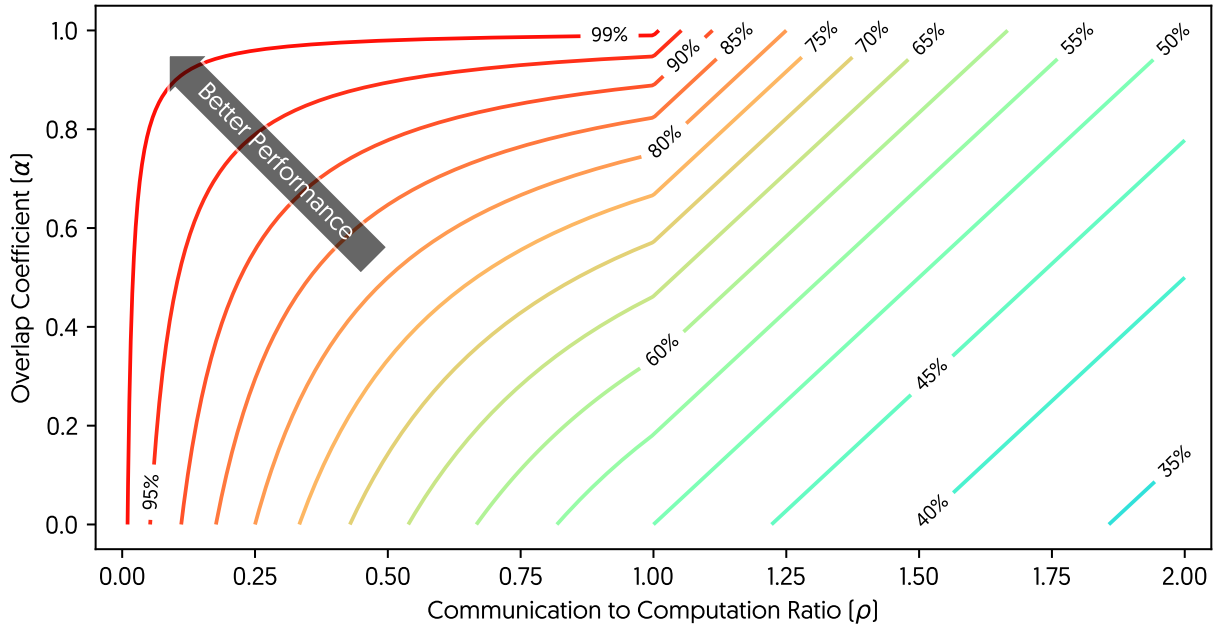

Figure 3.4: Impact of overlapping and communication to computation ratio on computation utilization. Contours in the background shows processing units utilization.

to fewer computation stalls.

To measure, quantitatively, the effect of poor timing on the performance, we use the Amdahl's argument [6] to calculate the average accelerator utilization as follow:

$$\begin{aligned} Utilization &= \frac{Computation}{Step\ \ Time} \\ &= \frac{Computation}{Computation + Network - Overlap} \\ &= \frac{1}{1 + \rho - \alpha * min(\rho, 1)} \end{aligned} \tag{3.2}$$

Where ρ represents the total *Computation* time to *Network* time ratio and α shows the overlap coefficient where $\alpha = 0$ means there is no overlap between *Computation* and *Network* (worst case scenario) and $\alpha = 1$ means total overlap (best case).

Higher *Utilization* results in shorter iteration time where utilization of 100% is the best iteration time achievable.

Figure 3.4 shows the dynamic of performance with regard to ρ and α. The ML model and style of distribution dictate the value of ρ while the runtime scheduling mandates the α. Properly addressing the poor timing problem requires finding the best transfer order and enforcing this order in the execution.

Finding the Best Order The DAG representation of ML workloads creates a complex resource interdependency which in turn, complicates the process of finding the best order. Following the notion in [83], the scheduling problem of finding the best execution order in a Data-Parallel job with identical nodes is formally defined as:

$$P_m|M_i, prec|C_{max} \tag{3.3}$$

In this formulation, P_m represents multiple parallel resources with identical performance. M_i assigns the operations to specific resources, i.e., computation ops vs. communication. *prec* describes the dependency relation of ops that is the DataFlow DAG. The C_{max} represents the goal of scheduling is to minimize the last node completion time.

This problem is still open [19] and simpler cases are proven to be NP-Hard. While there exist approximations for relaxed versions of this problem, to the best of our knowledge, there is no solution or approximation with guaranteed bounds for our original problem.

In §6, we present two approximations to this problem with empirically near-optimal results.

Enforcing the Best Order: Using TCP would imply an in-order delivery of the data, which is irrespective of priorities based on best transfer order. To enforce a transfer order beyond FIFO, a priority-based scheduling is needed where priorities are the order of execution. This scheduling scheme should additionally support pre-emption to pause a transfer if a higher priority transfer is requested. Our application-aware RPC framework, `Timed RPC`, implements the priority-based scheduling on top of the existing TCP based network stack. It mimics the transfer pre-emption by splitting each transfer into smaller pieces. (§7.8).

3.1.3 Network Underutilization

The ML job may not be able to use the full network bandwidth for the whole duration of the iteration. For example, if p is the average portion of full network bandwidth that a job uses during an iteration, the transfer windows are missed if:

$$Latency + \frac{Total\ Parameters\ Size}{Bandwidth \times p} > Total\ Computation\ Time \tag{3.4}$$

As the network to computation ratio increases, which naturally happens in scaling out, the effect of underutilized network becomes more severe.

There are two common root causes for the network underutilization:

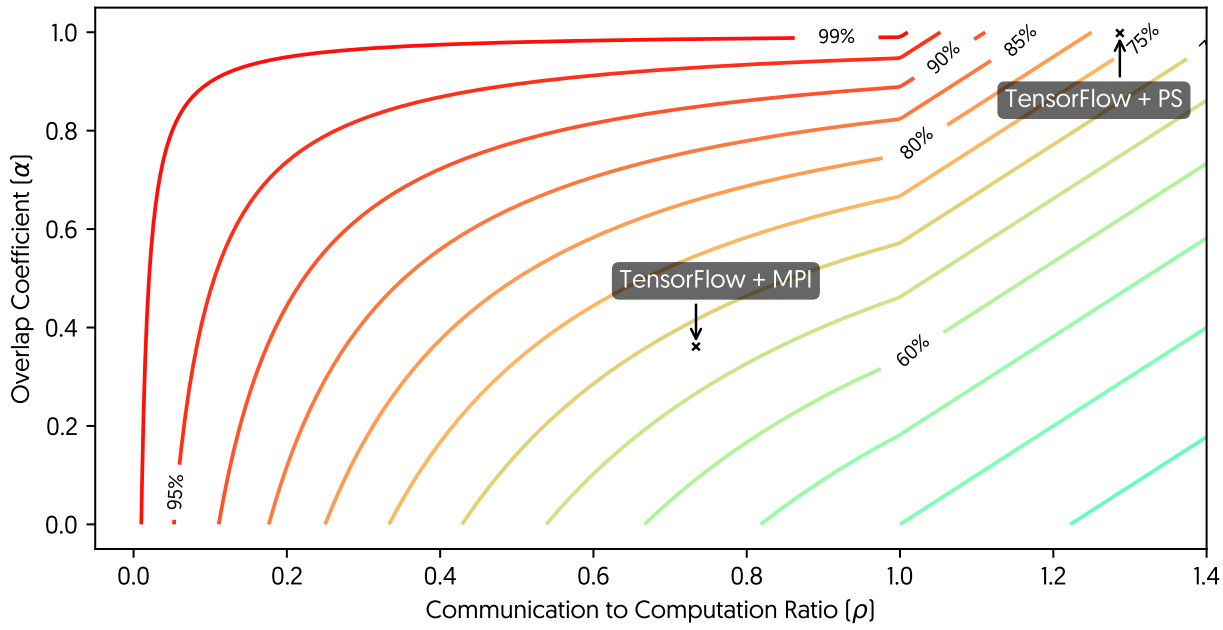

Figure 3.5: Example of having faster communication (MPI) but worst overall performance due to inferior overlapping. Contours in the background shows processing units utilization.

Idle Network Some distribution patterns do not use the network throughout an iteration. For example, in Data-Parallel with Collective Transfers, the network is idle during the Forward Pass, which accounts for 30% to 40% of total computation time (Figure 7.4a). Figure 3.5 compares the performance of training Inception v2 on PS vs Collective Transfer using the communication overlap model (Equation 3.2). While collective transfer has halved the cost of communication (α), the network underutilization makes it slower than PS with the double network cost.

Throughput Collapse Network congestion drastically reduces the effective bandwidth by triggering the TCP multiplicative decrease behavior. For example, Data-Parallel with PS extensively uses all-to-one and one-to-all network transfer pattern, which causes in-cast/out-cast network congestions [23]. In our experiment, in a 16-node PS job had 3.8 times smaller effective bandwidth compare to a similar job with collective transfer (§7).

3.2 I/O CHALLENGES

I/O is another resource vital to an ML job. The implementation of I/O in the current systems has three distinct processes:

1. Reading examples from a storage instument
2. Preprocessing examples
3. Loading the data to the accelerators

Only the third process, "loading the data to the accelerator", is a part of the dataflow DAG and is on the critical path. The first two processes are executed asynchronously separated from the main training thread. As long as reading the data and preprocessing can keep up with the iteration, I/O is not a performance bottleneck.

I/O in a distributed job is implemented in different ways:

- Offline Replication: In this design, a replication of the dataset is permanently replicated on each worker. Each worker reads the data from the local disk. There is no network activity involved in reading data.
- Remote Storage: In this design the dataset resides on remote file systems such as NFS [91], GPFS [87], Lustre [88] or a remote file storage such as Google File Server [35] and Hadoop Distributed File System [93]. Each worker reads the data over the network during the training.
- Online Replication: In this design, the portion of the dataset a worker needs to process is copied on the worker at the beginning of the job [65]. The worker reads the data from the local storage for the duration of the training. The network is used in setting up the job before the start of the training.

The I/O may become a bottle-neck in a job for various reasons, see below.

3.2.1 Slow Storage

If the storage through can not keep up with the pace of training, it becomes a bottleneck:

$$Latency + \frac{minibatch\ Data\ Size}{Throughput} > Iteration\ Time \tag{3.5}$$

If the order of processing the examples in the dataset is known in advance, which is very common in Deep Leaning jobs, the I/O requests are pipelined which hides the read latency. In this case the storage throughput is the only factor in keeping up with the iteration time. In other word, the storage is slow if:

$$\frac{minibatch\ Data\ Size}{Throughput} > Iteration\ Time \tag{3.6}$$

if the Equation 3.6 does not hold true, in theory, the I/O is fast enough to handle the training job.

3.2.2 Storage Underutilization

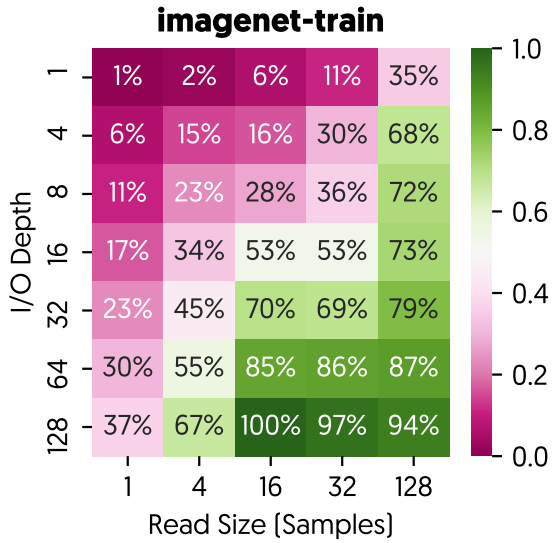

Figure 3.6: Impact of I/O depth and Batching on the I/O Performance of ImageNet dataset on a 12-Disk array HDD storage. Percentiles in the matrix represents Storage Utilization (%).

Sustaining a high throughput from a storage device requires careful tuning. Two major configurations impact I/O performances:

Read Size: The read size of an I/O operation has a significant impact on the performance. The data is read and transferred in a block of a certain size (e.g., 4KB). If the size is too small to fit a block, filler data completes the block wasting the bandwidth. Additionally, in a storage device with an array of disks, a larger read size activates more disks at the same time, improving the throughput.

The read size follows the distribution of example sizes. When examples are too small, a common practice in the ML systems is to store a batch of examples together in a file.

I/O Depth: I/O depth is the number of concurrent I/O operations sent to a device. Higher throughput increases the utilization of the disk and hides the latencies. Additionally, taking advantage of a multi-disk storage requires a high I/O depth.

The I/O throughput is very sensitive to these two performance knobs. Figure 3.6 shows the impact of these variables on the throughput of an 12-disk array reading some ML datasets. In all cases, reading the data without batching or with I/O depth of one significantly degrades the throughput up to 99%. These variables are set through the application by the developer and cannot be enforced through the operating systems or hardware. In our survey of top 10 Deep Learning jobs in MRI-DL project in NCSA [34], we have observed I/O misconfigurations in 8 jobs.

Impact of Distribution: Achieving higher I/O throughput to serve multiple workers requires a larger number of disks arrayed together. This increase in the number of disks makes the I/O misconfiguration even less forgiving results in higher performance loss due to misconfigurations.

3.2.3 Delivery Unfairness

Uneven I/O throughput distribution in a remote storage could cause performance issues even if the storage is fully utilized and is fast enough to deliver the examples.

Figure 3.7 shows the I/O performance of an NFS server with 8 workers serving the ImageNet [33] dataset. The total I/O throughput required to train a Resnet-50 v1.5 on these workers is 6509 image per seconds, well below what this NFS server sustains. However, not all workers get a fair share of this throughput. The fastest worker takes more than 85% of the throughput while the slowest takes merely 3.4%. As a result, the computation in the worker with the slowest I/O is bounded by I/O performance. In turn, the rest of workers have to stay idle waiting for this struggling worker to keep up which slows down the overall distributed training job.

3.2.4 Deep Learning I/O Toolkit

To address the underutilization problem, we introduce Diot, an automated framework to benchmark and tune the I/O performance (§5). Our framework finds the best configuration for the storage as well as evaluating the delivery fairness of the remote filesystem.

3.3 METHODOLOGICAL CHALLENGES

Addressing the performance issues often mandates changes in the underlying ML algorithm. However, these changes may have a non-trivial impact on the number of iterations

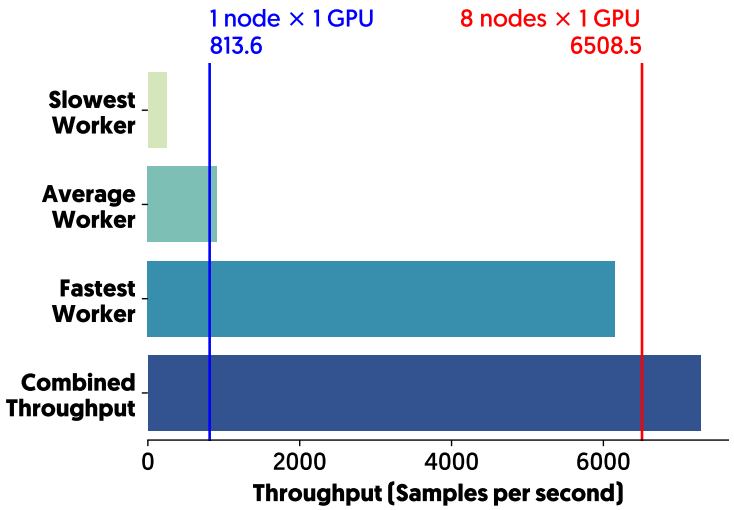

Figure 3.7: Example of Delivery Unfairness in Remote File Storage. Throughput of a NFS server feeding the ImageNet dataset to 8 workers. The vertical bar shows the required I/O throughput to train a Resnet-50 v1.5 on these workers with a V-100 GPU.

required to reach a training goal (e.g., certain accuracy target). A training job time can be simply modeled as:

$$Training\ Time = Average\ Step\ Time \times Number\ of\ Steps \tag{3.7}$$

Decreasing *Average Step Time* is often the goal of system performance optimizations and reducing the *Number of Steps* to train a model is often a function of the underlying ML algorithm.

The challenge is these two disciplines are not entirely independent; trying to improve one may damage the other one [14]; in some cases, the damage defies the benefits gained by the optimization leading to overall lower performance. This trade-off often limits the available options to address a performance issue or mandates extra steps to fix what is broken.

System-level optimizations can be divided into intrusive and unobtrusive depending on whether the underlying algorithm/logic of training is modified or not. This dissertation only focuses on unobtrusive solutions to keep the results as generally applicable to any machine learning system as possible.

CHAPTER 4: PERFORMANCE OBSERVABILITY IN DISTRIBUTED MACHINE LEARNING

> *"It is a capital mistake to theorize before one has data. Insensibly one begins to twist facts to suit theories, instead of theories to suit facts."*
>
> Arthur Conan Doyle
> *in* The Adventures of Sherlock Holmes

The promise of *Systems performance* is to study any physical entity or software components affecting the performance. This study not only requires a disciplined methodology but relies heavily on specialized tools to collect performance events. These events happen on different entities at different time. There are two ways to collect these events:

Profiling records the events bar the timing and order of the event, which helps to find load imbalance in the system and excessive resource uses.

Tracing records the event with timestamps and/or ordering of the event, which helps to examine timing issues in the system. In exchange, tracing has a larger memory and overhead footprint.

For a distributed job, capturing events additionally requires coordination among nodes, dealing with network overhead caused by coordinations, and accurate deduction order of internetwork events

In this chapter, we discuss our work in filling the gap in tracing and profiling toolkits for distributed ML jobs. First, we explain our work to scale out the ML execution tracing specially capturing network events. Later, we explain the design of a new visualization tailored for performance analysis of distributed ML jobs. Lastly, we expand our effort to fulfill the shortcomings of tracing and profiling ML jobs in the production.

Our work in tracing is implemented on TensorFlow and publicly available. Throughout this chapter, TensorFlow conventions are extensively used.

4.1 DISTRIBUTED TRACING

Tracing ops in a dataflow DAG is quite straightforward. It can be done simply by record the time of start and end of each op. However, a vast majority of ops do not execute in the main process but trigger events in different execution environment outside of the main process. For example:

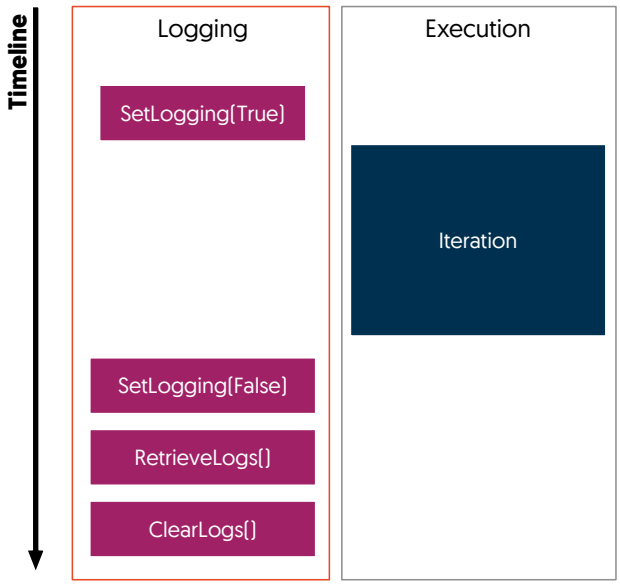

Figure 4.1: The timeline of distributed tracing RPC calls in an iteration

- GPU execution: the main process starts a set of kernels on the GPU. However, the GPU is the one deciding on the exact timing of computation.
- Network: the network operations are part of the DAG. In a peer to peer communication, there are a pair of send and receive ops on both peers. When both of these ops executed, this triggers an RPC call in the RPC framework.

Tracing this "out-of-band" processes is challenging and needs extra effort. TensorFlow supported collecting GPU events through NVidia's CUPTI and CPU events but not the network activities and RPC calls. The rest of this section explains our effort to add network tracing to TensorFlow.

4.1.1 Design

The network tracing uses the existing logging mechanism in TensorFlow. To support distributed tracing we modify the master node to coordinate the logging and collect the traces. Figure 4.1 shows the timeline of activities in a tracing session.

Coordination Before the start of an iteration, the master node notifies other nodes to start the tracing through a `SetLogging` RPC call. Each node then starts the execution while tracing the DAG and, if applicable, the GPU for the duration of iteration. The network activity is traced by logging the `RecvTensor` RPC call which is responsible for transferring data between nodes during the execution.

Managing the Network Overhead Tracing data is not immediately collected over the network and is stored locally during the iteration. When the iteration finishes, the master turns off the logging through another `SetLogging` RPC call. Then the logs are collected by an `RetrieveLogs` RPC call to each node followed by a `ClearLogs` call to remove the local storage of the logs.

Even though this collection phase between iterations significantly slowdowns the overall job time; it does not have a noticeable impact on the execution of iteration.

4.1.2 Implementation and Availability

We have implemented the network tracing module on TensorFlow. The implementation adds the gRPC RPC events to the TF standard tracing format. The network tracing module is 115 lines of C++ code[1] and has been a part of standard TensorFlow from v1.5.0.

4.2 VISUALIZATION

Visualization is an effective way to examine a large quantity of data and find patterns and correlations in the traces, which may be difficult to achieve through other means [39].

A distributed training job trace commonly contains a sizable number of events, which makes a visualization tool a necessity for the performance analysis of distributed jobs. For example, a 4-worker training of Inception V3 [99] contains 8937 events.

While there are many visualizations specifically design for ML performance analysis purposes, there are two tools specifically designed to visualize TensorFlow runtime traces. TensorFlow includes a tool to convert traces into *Chrome Tracing Format* which is visualized with Google Chrome internal tracer. Since this tool has not been designed for ML jobs, it does not retain much essential information in the tracing. For example, this visualization discards the network activity details such as size, source, and destination the transfer, and the other metadata. TensorBoard [18] includes a visualization of tracing data in a graph format where each node represents an op and is colored proportional to its elapsed time. This visualization discards the timing of visualization, implicitly converting the tracing data to a profiling data.

[1] `https://github.com/tensorflow/tensorflow/pull/14604`

4.2.1 Design

We design our system based on Shneiderman's principle [92], "Overview first, zoom and filter, then details-on-demand". Our visualization has implemented six out of seven information visualization tasks:

Overview Our main view is an overview of the execution consist of several timelines for each resource. Timelines are horizontal bar charts with X-axis as the relative time. Events are represented as boxes. Many events occur at the same time especially on the GPU with many cores; therefore we use Y-axis to stack the concurrent event using a bin packing placement algorithm. Figure 4.2 shows the main overview view.

Relate We have used two techniques to represent relations in the visualization. First, box colors represent operation types. We use a consistence hashing algorithm on the op type, to assign a color to each operation. Second, we group out-of-bound events such as GPU kernels and RPC calls in separate timelines.

Zoom Navigation in the system is done through changing the time range visible on the timeline. This can be done by either zooming in and out or dragging the time range directly. This time range syncs with another timeline.

Details-on-demand Details of events are shown on demand. We show an abridged version, on hovering on a box, and the full version, on the click, through a separate pop up window. Figure 4.3 shows the full details display.

Filter Event resource groups can be filtered out of the visualization, which helps to remove the clutter caused by a noisy resource.

History We take advantage of the underlying visualization framework, `bokeh`, to let the user go back to a previous view or fully reset the view back to the initial state.

4.2.2 Implementation and Availability

We have implemented our system using the `bokeh` [100] framework. The implementation has 360 lines of Python and 300 lines of HTML/Javascript code. The code is publicly available[2].

[2]https://github.com/xldrx/tensorflow-runtime-metadata-visualization

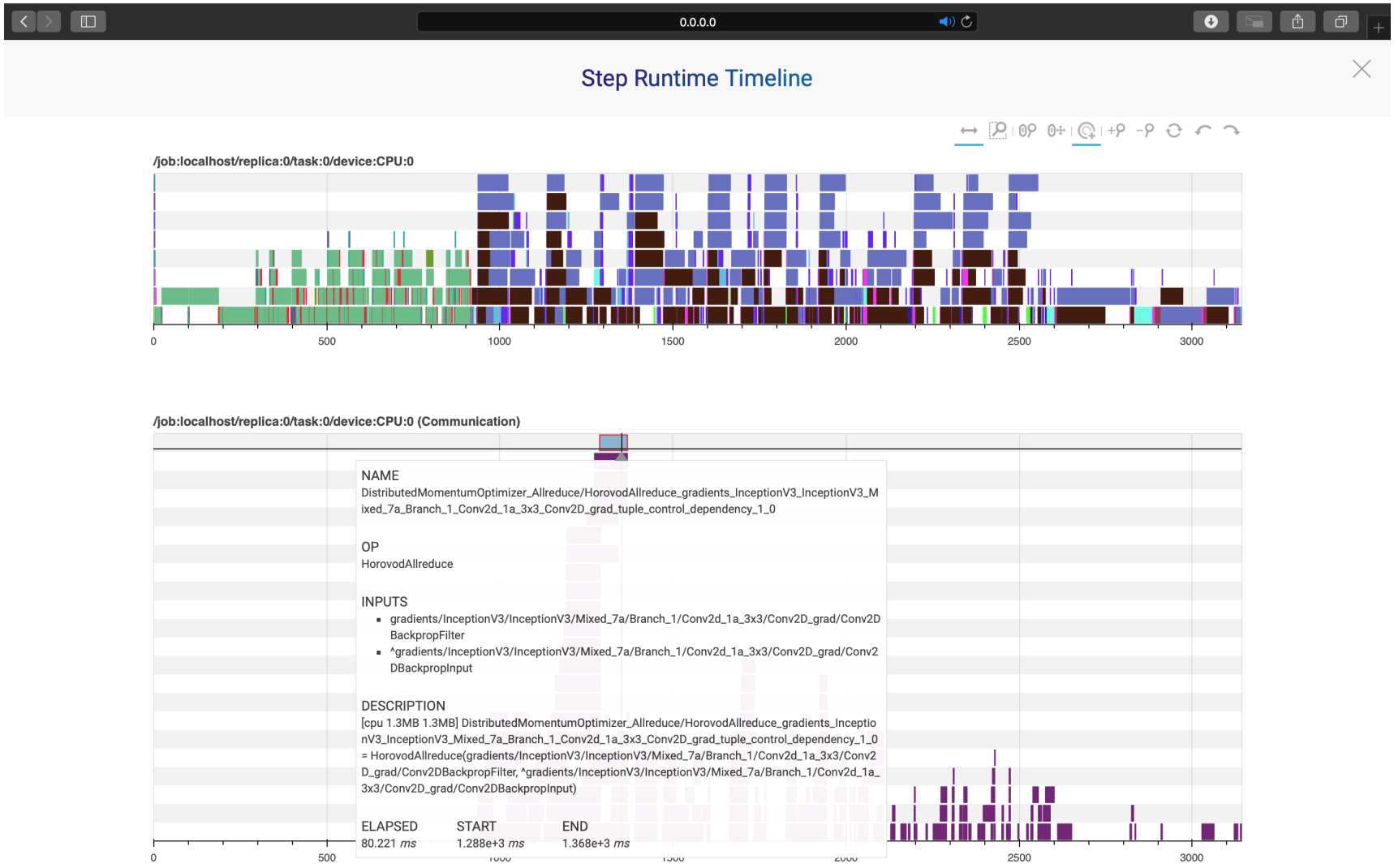

Figure 4.2: TensorFlow Runtime Tracing Metadata Visualization: Overview

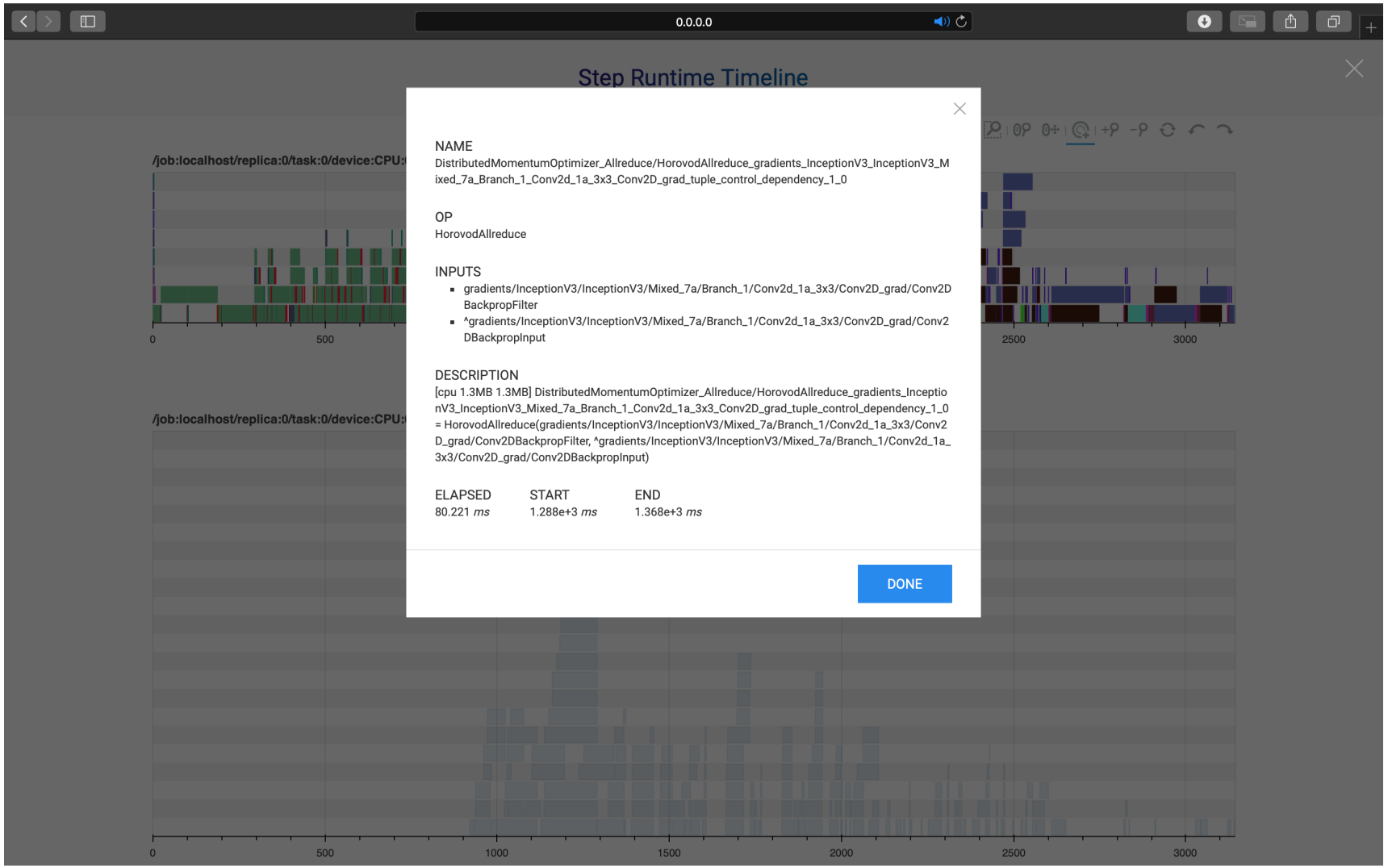

Figure 4.3: TensorFlow Runtime Tracing Metadata Visualization: Details View

4.3 TRACING IN PRODUCTION

The growing popularity of Deep Neural Networks (DNN) within the mainstream [94] has had a rapid transformative effect on clusters and data centers. DNN training jobs are becoming one of the largest tenants within clusters, and often take hours to weeks to complete, and even a slight performance improvement can save substantial runtime costs. Despite this fact, the DNN specific performance tuning tools are yet to keep up with the needs of the new changes in production environments.

On the one hand, the existing application-agnostic resource-level tools such as top, Nvidia Nsight (for GPU utilization), IPM (for MPI network monitoring) are too limited to predict or explain the behavior and performance of a job accurately. In DNN applications, there exists a complex relationship among resources. Even though measuring coarse metrics such as bandwidth, latency, and GPU/CPU utilization can draw an overall picture of cluster performance, these metrics are not easily translatable to application-level metrics and do not provide actionable insights on how to handle performance bottlenecks.

On the other hand, the shortlist of application-aware tools, such as MLModelScope [30], TensorBoard [18], and `tf.RunOptions` [3], while able to provide actionable insights, are mainly designed for the need of application developers and are not intended for production use. Such tools require substantial modification to applications and early planning as to what, when, and how data should be collected.

We introduce `tensorflow-tracer` to fill the gap between these two classes of performance tuning tools. The `tensorflow-tracer` addresses the following technical challenges:

- Collecting the application-level runtime metrics, such as the timing of each operation or the total iteration time, required application source code modification. To avoid application-level modification, `tensorflow-tracer` *monkeypatches* the `tensorflow` library at the system level allowing on-demand application tracing.
- Collecting some metrics is expensive and has a significant overhead on the runtime. `tensorflow-tracer` treats metrics differently; it collects low-overhead metrics automatically, while expensive ones are collected on demand through an admin interface.
- There is no easy way to exchange runtime metrics among users and admins — our system facilities this through a portable file format and supporting tools to explore these metrics offline.

[3] `https://www.tensorflow.org/api_docs/python/tf/RunOptions`

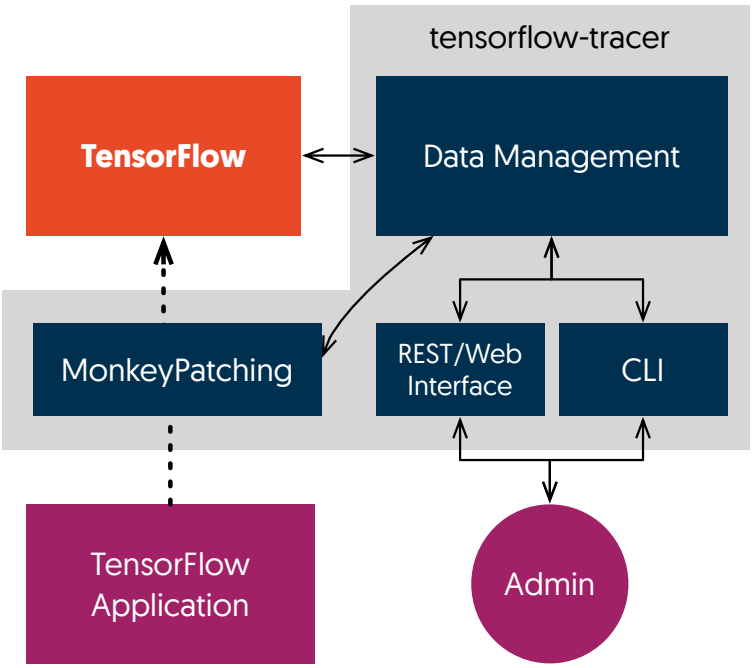

Figure 4.4: The architecture of `tensorflow-tracer`

4.3.1 Design

Figure 4.4 shows the building blocks of `tensorflow-tracer`:

MonkeyPatching In order to provide tracing without code modification, our system injects a proxy function into the `tensorflow` library using a *monkeypatching* scheme to intercept the calls to certain functions and redirects them to the *Data Management* module. While *monkeypatching* the library at the system-level automatically enables tracing for any DNN application, `tensorflow-tracer` also supports per-application patching.

Data Management This module is responsible for collecting event data as well as making online decisions as to whether a task should be traced[4]. This module is also responsible for serializing/deserializing tracing sessions from/to a file.

REST/Web Interface This interface is the main portal for interacting with the system. `tensorflow-tracer` starts a web server whenever an application is executed which is accessible either through a web browser or a REST API client (possibly from a terminal). The interface provides two logical views:

[4] `MonitoredSession.run` function calls

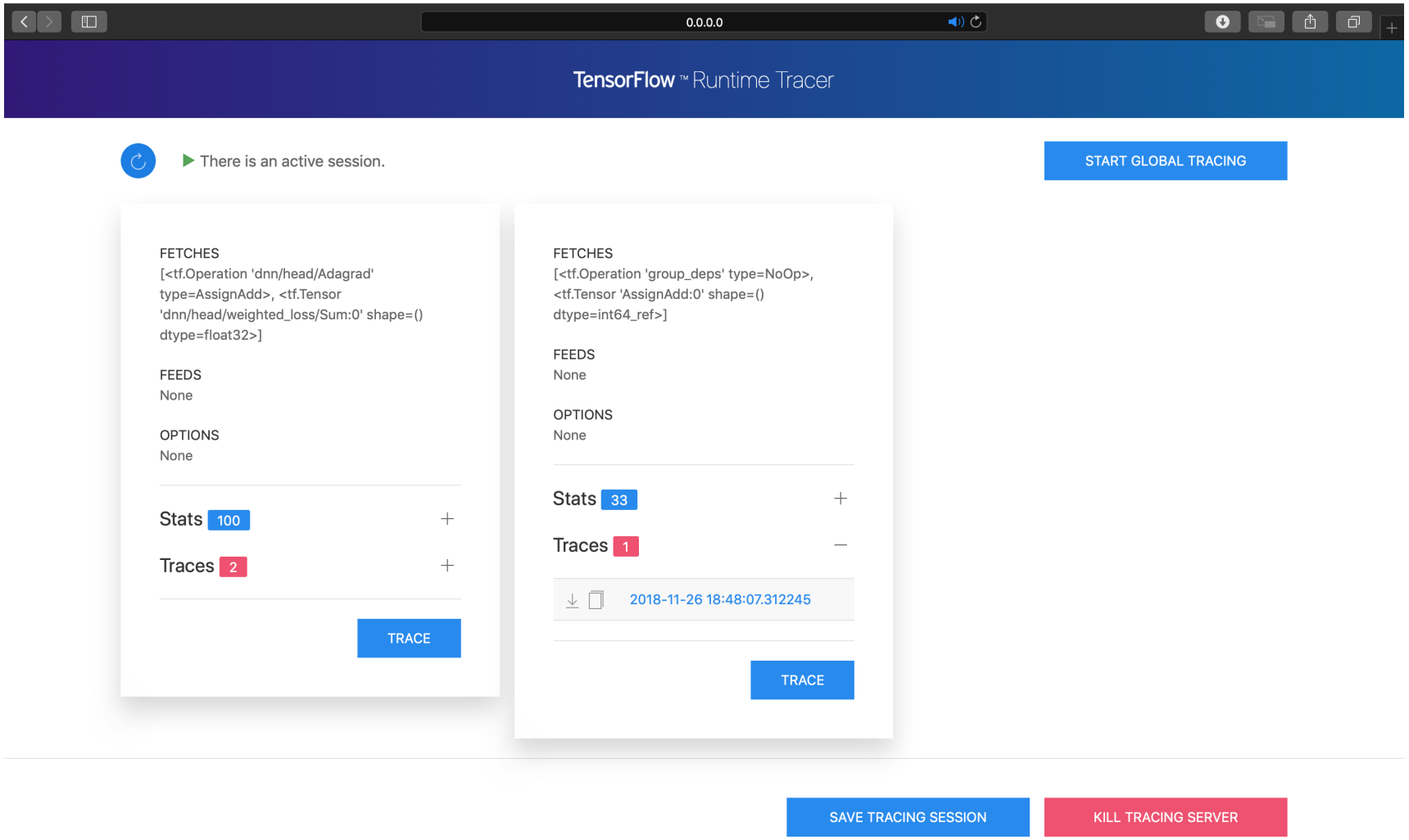

Figure 4.5: The main web interface of `tensorflow-tracer`. Each entry represents a separate task in the DNN session.

Figure 4.6: The timeline interface provides details of the execution of one iteration step. Each box represent an operation in the DataFlow DAG. There is a timeline for every resources on each machine. The trace is collected from `next_frame_sv2p`[10] model in `tensor2tensor` library [106].

1. *Main Interface* shows the list of tasks and their associated profiling/tracing data. This interface allows request tracing. (Figure 4.5)
2. *Timeline Interface* visualizes an instance of a task trace as a series of timelines, one for every resource (e.g., CPU, GPU, Network Interface) on each machine. Each box represents operation in the DataFlow DAG of DNN application. (Figure 4.6)

CLI It loads a tracing session offline and enables exploring through a web interface.

4.3.2 tensorflow-tracer in action

Overhead We observe no performance hit on collecting low-overhead metrics such as iteration times, 'session.run' call names and frequencies. We observe less than 3% runtime overhead to iteration time when individual operations in a call are traced. CPU Memory requirements varies for different models. For example: an *Inception v3*[99] trace consumes 718KB while **next_frame_sv2p** [10] consumes 2.4MB.

Case Study We have used `tensorflow-tracer` on different workloads to find the performance issues on application, framework, and infrastructure level. This is the main tool we used in §6, §7 and §7.8.

4.3.3 Implementation and Availability

We have implemented `tensorflow-tracer` in Python. The implementation is Python 1100 LOC and 800 LOC of HTML/JavaScript. it is publicly available under `Apache-2.0` license[5]. It supports native TensorFlow [1], Horovod [90], and IBM PowerAI [25] applications.

The correctness of the `tensorflow-tracer`'s distributed traces relies on the precision of the clocks on the different machines. Currently, it relies on external sources to synchronize the clocks.

[5] `https://github.com/xldrx/tensorflow-tracer`

CHAPTER 5: I/O IN DISTRIBUTED MACHINE LEARNING

Large scale computation in deep learning training demands the loading of a high volume of data. Consequently, I/O has become an integral part of an ML training iteration with a critical impact on the overall performance. Ever growing computational demand of ML workloads not only has introduced accelerators in enterprise clusters but also has evolved the storage infrastructure from off-the-shelf local disks to highly parallel storage systems.

On the software side, frameworks like Tensorflow and Pytorch have harness next-generation storage system by evolving their I/O pipeline with optimizations such as batching and parallelism. However, the behavior and efficiency of these optimizations are controlled by multiple I/O knobs, such as the number of concurrent I/O operations (IOP) sent to a storage device and the read size of each IOP. In the absence of a sufficiently comprehensive understanding of the effect of these knobs on the I/O throughput, the task of tuning these settings is wholly left to end-users in existing systems.

In this chapter, we attempt to provide an extensive experimental study on the effects of I/O tuning on modern ML systems. In order to achieve this goal, we have implemented `Diot`, a Deep Learning I/O toolkit, to automate and accelerate I/O benchmarking on distributed clusters. Contributions of this work are as follow:

- **Diot:** We observed that adjusting I/O knobs in current ML systems requires time-consuming data transformation. To accelerate the process of searching for optimal parameters, Diot models the example size distribution in a target dataset, which removes the need to work with the whole dataset. Additionally, Diot coordinates the experimentation over multiple workers in the network (§5.2). We have evaluated the Diot on seven datasets on four different storage systems. Diot increases the sustained I/O throughput up to 3 orders of magnitude compared to default settings, achieving nearly full utilization on all jobs.

- **Performance Impact:** We show that there is a wide performance gap between the optimized and default I/O parameters. Our measurement shows up two orders of magnitude I/O throughput difference in commodity storage devices and up to three orders of magnitude in highly parallel storage systems (§5.3.2). Additionally, the choice of filesystem could cause an imbalance of I/O delivery on the worker levels (§5.3.4).

- **Default Parameters:** We show that the optimal I/O parameters do not consistently follow any simple relationships with the I/O depth and I/O batch size and do not hold across all datasets or across all storage setups. Consequently, using the default

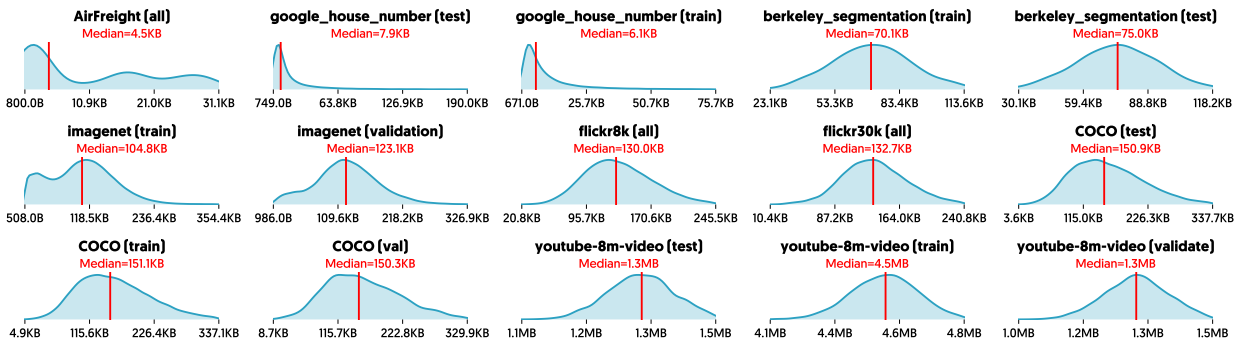

Figure 5.1: Example Size Distribution in select Datasets

I/O parameters results in suboptimal performance on a different dataset or storage setup. For example, compared to our optimized parameters, the default TensorFlow I/O settings have 94% lower I/O throughput, and the TF's official Resnet Model settings have 17% loss of throughput while reading the ImageNet dataset on 4-Disk array SSD over NFS storage. (§5.3.3)

- **User Behavior:** By surveying the top 10 workloads on an academic Deep Learning cluster, we show that the default I/O parameters are rarely tuned and are far from optimal. (§5.3.5)

5.1 BACKGROUND

During an iterative training job, the I/O subsystem feeds the input data to the accelerators. This process can be characterized as follow:

- I/O operations to the disks are random reads with varied sizes.
- Multiple examples are batched in the same file on an I/O storage, and I/O operations are parallelled.
- The I/O is pipelined with the computation and preprocessing.

The ML training input data is organized as a dataset, which consists of a set of examples. A training job has multiple epochs; in each epoch, all examples are read and processed. As shown in Figure 5.1, some datasets such as Youtube-8m have consistent example sizes, while size differences in other datasets such as ImageNet and Flicker8k are about an order of magnitude. Additionally, the order of examples is shuffled between epochs, which effectively forms a random read I/O pattern.

After an example is read from an I/O storage, it may go through a preprocessing phase, including transformation (e.g., resizing images [49], or "Fourier transform" on speech [7]) and augmentation (e.g., cropping or adding noise). Later, the preprocessed example is loaded on the accelerator and processed by the ML model.

In the current modern ML systems, these phases, 1) reading from an I/O storage, 2) preprocessing examples, and 3) computation on an accelerator are pipelined to improve the computation utilization (Figure 5.2). The intended behavior of the I/O pipelining is to make the computation the only bounding resource. However, if the I/O storage is too slow to deliver the examples, it becomes the bottleneck in the job wasting computational resources.

5.1.1 I/O Optimizations

There are two common practices to improve the I/O throughput in the current implementations: Parallelization and Batching. Both optimizations are essential to achieving high I/O throughput and are controlled by performance knobs: I/O depth and batch size, respectively.

Parallelization: In parallelization, multiple I/O requests are sent to storage simultaneously, which in turn increases the chance of activating more disks at the same time in disk arrays and allows better scheduling and pipelining at disk-level. The number of concurrent I/O requests is referred to as I/O depth. While increasing I/O depth is shown to improve the I/O performance, huge I/O depth could cause contention in the storage and kernel, which in turn hurts the I/O performance.

Batching: In batching, examples are grouped to form larger blocks; blocks are accessed randomly, but examples in a block are read sequentially and get shuffled in the memory afterward. This optimization improves the I/O throughput and effectively converts the I/O pattern from the random read to the sequential read. Additionally, it avoids the I/O channel underutilization of small I/O requests.

Current ML systems achieve batching through merging dataset files into larger sequence files. This transformation is statically done prior to the training, and depending on the dataset size could take a long time to finish.

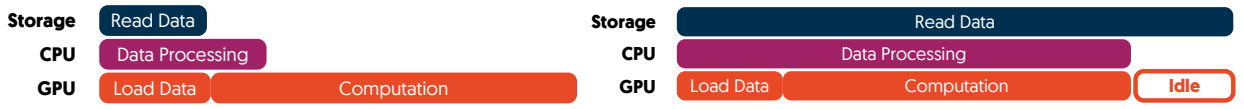

(a) Expected Behavior; Computation is the bottleneck.

(b) Unexpected Behavior; I/O is the bottleneck.

Figure 5.2: I/O Pipeline in a Deep Learning Workload

5.2 DIOT

I/O batching and parallelization are integral to the performance of ML systems. However, the efficiency of theses optimizations depends on correctly tuning their performance parameters. However, searching for the optimal I/O parameters in current ML systems is very time-consuming. Changing the I/O batch size requires applying an expensive data transformation on the whole dataset. In the same way, reading the whole dataset could take a long time.

Diot is an attempt towards automating I/O tuning in Modern ML systems. Diot provides a fast and accurate I/O performance measuring for a given parameter set in a distributed environment. Using this measuring capability, Diot can be used to find an optimal I/O parameter set through the parameter grid search. Instead of reading the actual dataset, Diot reads from a large contiguous block following the dataset example size distribution, which eliminates the need for dataset transformation to change I/O batch size.

5.2.1 Workflow

Diot takes an input dataset, a target I/O storage, and a list of I/O parameter sets and measures sustained I/O throughput for each set. The execution model has the following phases:

1. Extract Dataset Size Distribution: In the first phase, Diot generates a discrete size distribution model from examples in the given dataset. Figure 5.1 shows the distributions generated by Diot.

2. Generate Experiments: Next, Diot generates a set of experiments for the target I/O storage. Each experiment is detailed I/O specifications for a short run. Two kinds of experiments are generated in this phase:

- **Saturation**: The goal is to measure the maximum sustainable I/O throughput for given storage and network connectivity independent of the dataset. A saturation test uses a sequential read pattern with a constant read size.

Figure 5.3: Diot Runtime. Diot executes each steps sequentially with global barriers in between.

- **I/O Tuning**: The goal is to measure the sustainable I/O throughput for a given I/O parameter set. An experiment uses a random read pattern with I/O read sizes sampled from a given distribution. For the I/O batch size of 1, this distribution is the dataset size distribution. The distribution for larger batch sizes is calculated from dataset size distribution.

3. Execution: The execution is divided into a few steps; each step runs on all workers. As shown in Figure 5.3, there are global barriers between steps to coordinate the execution among multiple workers. On each worker, experiments are carried on locally by an I/O benchmark engine according to the test specification. Chronologically, the steps are as follow:

1. Write data file: Each process creates a sizable contiguous file with random data. The file size is set as twice as the size of memory to minimize the impact of file system caching on the measurement.

2. Saturation Test: After creating the data file, a saturation test is executed to calculate the maximum sustainable I/O throughput.

3. I/O Tuning: Lastly, each tuning experiment is executed sequentially with global barriers in between.

The performance measurement in an experiment starts after an initial warmup period to ensure all workers have been reached to their sustained state.

4. Reporting: Diot reports the raw performance numbers such as throughput in MB/s and IOP/S utils as well as the following metrics:

1. Normalized Sustained Throughput: Diot normalizes the throughput using the results of the saturation test. This metric reflects how far is the throughput from the empirical best.

2. Example per Seconds: Diot also reports the throughput in terms of the number of examples per second. This metric is particularly is useful when it is used with computation performance metrics in ML training.

5.2.2 Implementation

Diot is implemented in Python (900 LOC) and is publicly available at `https://github.com/xldrx/diot` under GPL-3 open-source license. The implementation uses OpenMPI [38] to spawn local processes and global barrier implementation. It also uses fio[9] as the local I/O benchmark engine.

5.3 EXPERIMENTAL STUDY

We have conducted an experimental study on the effect of parameter tuning on I/O throughput. More specifically, we try to answer the following questions:

- What is the performance gap between the best and the worst I/O parameters?
- Do optimized parameters hold across all datasets or storage setups?
- What is the impact of a distributed filesystem?
- How well are I/O parameters tuned in real applications?

5.3.1 Setup

We have used Diot to study on the effects of I/O tuning on modern ML systems. This experimental study uses eight ML datasets: AirFreight [73], Berkley Segmentation [71], Flickr8k, Flickr30k [84], Google Street View House Numbers [78], ImageNet [33], and YouTube 8m [2].

Four different storages on two clusters have been evaluated: (1) Single Disk NVMe SSD, (2) 4-Disk Array NVMe SSD, and (3) 12-Disk SATA HDD on NCSA Hal Cluster [34] shared through an NFSv4 remote filesystem using Infiniband 2-port EDR network. (4) a 60-Disk Array SATA HDD on UIUC Campus Cluster [79] shared through a GPFS distributed filesystem using Infiniband 2-port FDR network.

We explore two I/O parameters: I/O Batch Size with search space of $\{1, 4, 8, 16, 32, 128\}$, and I/O Depth with search space of $\{1, 4, 8, 16, 32, 64, 128\}$. Using these ranges, we could

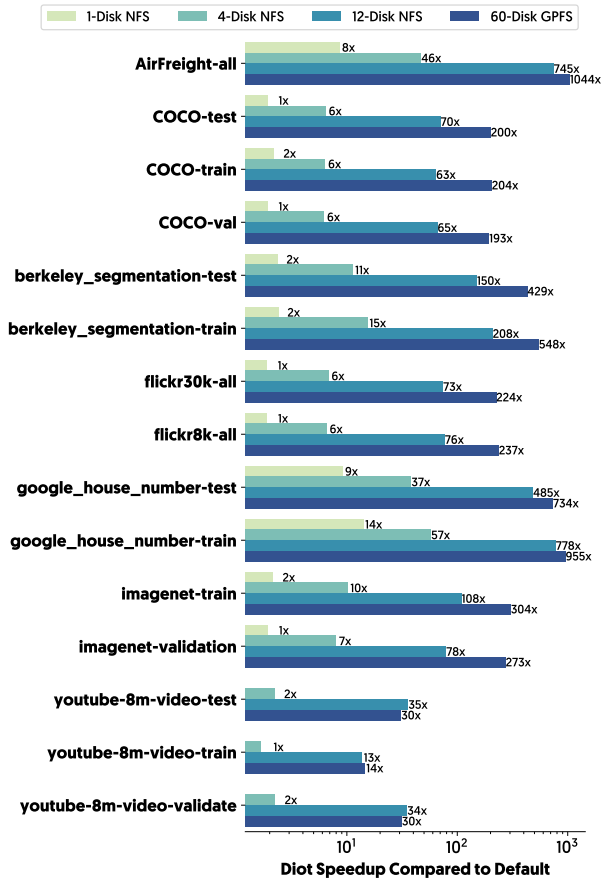

(a) Performance Gap between Default (Depth=1,Batch=1) and Optimized (by Diot) Parameters

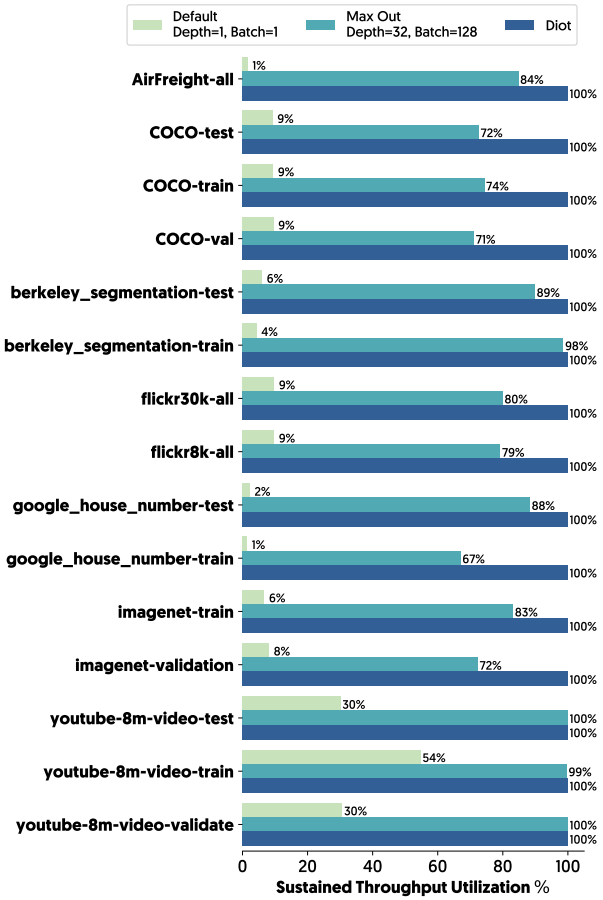

(b) Performance Gap Between Default, Max Out, and Optimized (By Diot) Parameters. Data is collected on a 4-Disk SSD over NFS

Figure 5.4: Performance Gap between optimized I/O parameters and default values. Diot optimized parameters achieve 100% throughput utilization in all cases.

find a combination that achieves a full throughput utilization in all datasets and storage setups.

Lastly, Each benchmark uses four workers. The reported throughput is the aggregation of throughput on all workers.

5.3.2 Performance Gap

Our evaluation shows a wide gap between default I/O parameters and optimized settings (Figure 5.4a). As the size of a disk array increases, the performance gap widens. For example, in the Imagenet training dataset, the optimized setting the optimized speed up over default setting are 2x, 10x, 108x, and 304x on 1-Disk, 4-Disk, 12-Disk, and 60-Disk

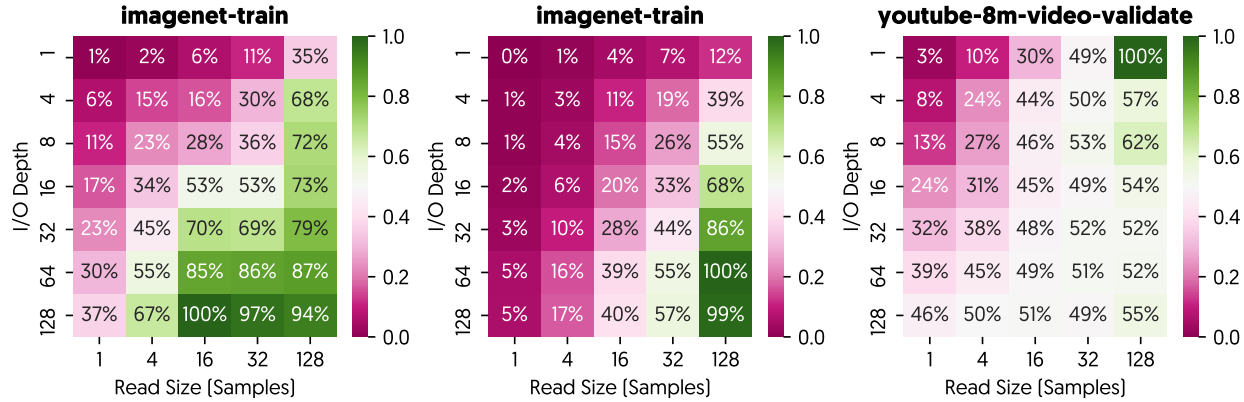

(a) ImageNet (Train) on 12-Disk HDD

(b) ImageNet (Train) on 60-Disk HDD

(c) YouTube-8m-video on 12-Disk HDD

Figure 5.5: Comparison of I/O performance on different datasets and storages. Percentiles in the matrix represents "Sustained Throughput Utilization (%)."

array respectively. The same trend is observed on other datasets.

Finding optimized parameters is not as straightforward as maximizing values. Figure 5.4b shows the performance gap on a 4-Disk SSD over NFS between Default (bs=1, depth=1), MaxOut (bs=128, depth=128), and optimized settings. The gap between max-out and optimized is not as wide as the default setting but still significant (up to 33%).

5.3.3 Parameter Transfer

Our evaluation shows the optimized settings on a dataset or storage do not hold across all datasets and storage setups. Take the sustained throughput utilization of ImageNet(train) on the 12-Disk HDD storage as an example (Figure 5.5a). The 100% utilization can be achieved by the I/O batch size of 16 and the I/O depth of 128.

Using these values to read the same dataset on 60-Disk storage penalizes the utilization down to 40%. Likewise, using the optimized values on the 60-Disk array (bs=64, depth=128) reduces the utilization by 13% on 12-Disk storage.

Similarly, optimizations do not hold across datasets either. Using ImageNet(train) optimized values (bs=16, depth=128) to read the YouTube 8m dataset on the same 12-Disk storage, reduces the utilization by 49% and vice versa. Using YouTube values (bs=128, depth=1) causes a 65% drop.

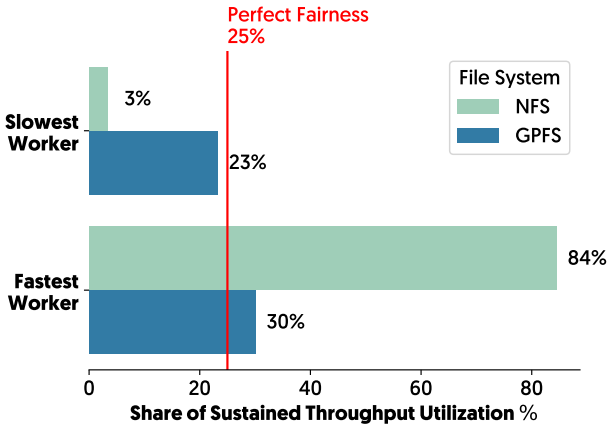

Figure 5.6: I/O Delivery fairness among workers.
ImageNet (training) dataset on 4 Workers.

		Training		I/O	
Domain	**Framework**	**Model**	**BatchSize**	**Depth**	**Batching**
Emotion Detection	TensorFlow	DenseNet	64	1	No
Image Processing	Pytorch	VGG-16	64	4	No
Image Processing	Pytorch	Custom	64	2	No
Unsupervised Image translation	Pytorch	DeepLab	1	4	No
Image Processing	Pytorch	VGG-16	4	12	No
Automobile	Pytorch	Resnet-50 + RNN	64	36	No
Image Segmentation	Pytorch	Boundary-Aware Network	4	4	Yes
Astronomy	TensorFlow	Custom	32	4	Yes
Video Processing	Pytorch	EmotionDetect	4	12	Yes
Image Processing	Pytorch	Resent-50	128	96	Yes

Table 5.1: Example Size Distribution in select Datasets

5.3.4 Delivery Fairness

The I/O throughput is not always shared equally among active workers. Figure 5.6 compares the sharing of I/O throughput over multiple workers. GPFS with a fair scheduling mechanism has a nearly perfect I/O sharing among four workers. On the contrary, all NFS workloads in our evaluations demonstrate a high divergence from perfect I/O sharing, where one worker takes a significant share of the I/O.

5.3.5 I/O Tuning in Practice

To get insight on I/O optimization in practice, we have studied job on NCSA HAL Cluster: a specialized cluster for deep learning research at the University of Illinois at Urbana-Champaign. Table 5.1 shows the results of surveying the top ten jobs by computation hours.

Out of 10 jobs, six do not use I/O batching at all, and six use a small I/O depth (¡=4). Only in 2 jobs, both I/O batch and depth are set significantly beyond the default behavior.

5.4 CONCLUSION

In this chapter, we show that I/O tuning has a huge impact on the I/O throughput, which could be as wide as three orders of magnitude improvement on throughput. Optimized settings do not hold across all datasets and storages, and simply maximizing I/O parameters does not usually lead to optimal throughput. Lastly, our user survey shows that users in practice are not properly tuning the I/O.

We propose Diot to automate the I/O tuning for modern ML workloads by accelerating the parameter grid search. Diot improves the I/O throughput up to 3 orders of magnitude compared to default I/O settings.

CHAPTER 6: COMMUNICATION SCHEDULING OF CAUSAL DEPENDENCIES

State-of-the-art deep learning systems rely on iterative distributed training to tackle the increasing complexity of models and input data. In this work, we identify an opportunity for accelerating distributed DNN training in systems that rely on graph representation for computation, such as TensorFlow and PyTorch, through communication scheduling. We develop a system, TicTac, that reduces the iteration time by identifying and enforcing parameter transfers in the order in which the parameters are consumed by the underlying computational model, thereby guaranteeing near-optimal overlap of communication and computation. Our system is implemented over TensorFlow and enforces the optimal ordering by prioritization of parameter transfers at the Parameter Server in data parallel training. TicTac requires no changes to the model or developer inputs and improves the throughput by up to 37.7% in inference and 19.2% in training, while also reducing straggler effect by up to 2.3×. Our code is publicly available.

6.1 INTRODUCTION

Deep learning has grown significantly in the past decade, fuelled by the flexibility of development offered by machine learning frameworks, availability of rich data, and readily accessible distributed high-performance computing. The computational cost of training sophisticated deep learning models has long outgrown the capabilities of a single high-end machine, leading to distributed training being the norm in a typical AI pipeline. Training a deep learning model is an iterative job which may take days to weeks in high-end clusters today.

Computational graphs are used to represent the training jobs in state-of-the-art systems [1, 21, 80]. In the commonly-used Model Replica or data parallel mode of training, the input data is partitioned and processed at participating workers using identical computational graphs. Each iteration typically lasts milliseconds to seconds. At the end of each iteration, servers exchange a relatively large amount of data associated with parameter updates to aggregate the results of the iteration. This communication overhead has a substantial impact on throughput of the system and also limits its scalability [96, 5]. Even a small improvement in communication overhead can improve the learning time by hours in these long-running learning jobs.

The iteration time in deep learning systems depends on the time taken by (i) computation, (ii) communication and (iii) the overlap between the two. When workers receive the param-

eters from the parameter server at the beginning of each iteration, all parameters are not used simultaneously; they are consumed based on the dependencies in the underlying DAG. While one particular schedule of parameter transfers (over the complete set of parameters in a given model in a single iteration) may facilitate faster computation, another may cause blockage. Hence, identifying the best schedule of parameter transfers is critical for reducing the blocking on computation (determined by DAG dependencies), and in turn improving the overlap and the iteration time.

We observe that the schedule of data transfers in current systems [1, 21, 80] is determined arbitrarily during execution without considering the impact on overlap. We quantify the observed combinations in TensorFlow and find that in a trial with 1000 iterations on ResNet-V2-50, every iteration had a unique order of received parameters which has not been observed previously. This random order of parameter transfers at workers has two performance implications. First, the iteration time, and in turn throughput (number of samples processed per second), suffers significantly due to sub-optimal overlap. Second, even in the same iteration, multiple workers might follow different schedules of data transfers, leading to stragglers during synchronized training.

Past work has attempted to address this issue by enforcing the same order of parameter transfers at all workers. However, these solutions are restricted to earlier systems with layer-by-layer model representation [8, 29, 116] where finding the optimal order of execution is trivial [28]. In modern systems with DAG representation [1, 80], this is a non-trivial challenge.

In this work, we devise a systematic methodology for deriving near-optimal schedules of parameter transfers through critical path analysis on the underlying computational graph. This allows maximal overlap of computation and communication and prevents stragglers arising from random order of parameter transfers at workers. We also develop a lightweight resource-level enforcement mechanism over TensorFlow [1]. These techniques form the core of our system, TicTac, which achieves substantial performance improvement while requiring no changes in the model or developer inputs.

In summary, we make the following contributions:

- We identify an opportunity for improving performance in state-of-the-art deep learning systems with Parameter Server-based aggregation through prioritized parameter transfers (§6.2).
- We define a metric to quantify the efficiency of a given execution: the overlap coefficient (§6.3).
- We propose two heuristics, TIC and TAC, for near-optimal scheduling of computation and

communication in Model Replica with Parameter Server.

- We implement our system over TensorFlow (§ 6.5). The code is publicly available[1].
- We extensively evaluate the performance of our system in GPU and high-end CPU environments under training and inference of DNN models and show that throughput can be improved by up to 37% (§6.6).

6.2 BACKGROUND AND MOTIVATION

Our system focuses on network optimization in deep learning frameworks with DAG representation of computational graphs [1, 80], Model Replica (MR) mode of distribution and Parameter Servers. The performance improvement provided by TicTac is beneficial in two key environments. First, it improves throughput and iteration time in clud environment with commodity hardware or on-demand clusters where high resiliency is critical (workers may be preempted). Second, in online reinforcement learning with workers for training and separate active agents for inference, enforced ordering can improve the inference time. In this environment, the active agents are reading parameters from the PS or decentralized workers as shown in Figure 6.3. While decentralized aggregation techniques (such as all-reduce and Horovod [90]) are gaining traction in high performance networking, TicTac does not address such systems and is focused on PS.

In this section, we give a brief overview of deep learning systems, prior techniques proposed in these systems to mitigate network overhead, and opportunities for further optimization.

6.2.1 Network Optimization in DNN training

In deep learning systems, high GPU utilization can be achieved in two ways: (i) when total communication time is less than or equal to the computation time and (ii) with efficient overlap of communication and computation. Several techniques have been proposed to improve GPU utilization.

Increasing computation time: The fraction of computation time relative to communication time can be increased by increasing the batch size [52]. However, this approach suffers from decreased accuracy [60] and may not be generally applicable under resource constraints. [37, 25, 113, 4].

Decreasing communication time: Solutions for reducing network communication have

[1] https://github.com/xldrx/tictac

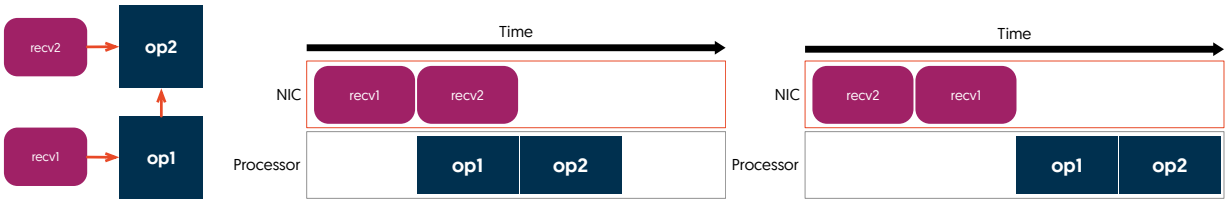

(a) DataFlow Graph (b) Good Execution Order (c) Bad Execution Order

Figure 6.1: Impact of multi-resource operation ordering on performance

taken multiple approaches — modifying the machine learning algorithm to reduce communication cost [5, 109, 116], reducing the precision of parameter representation [105, 27, 41], changing the network primitives to collective (e.g. all reduce) [37, 25, 7, 113, 4] or broadcast [116].

Smarter interleaving of computation and communication: Several layer-by-layer systems [8, 29, 116], where the models are sequential and obtaining the order is trivial [28], adopt this approach. These solutions are not applicable to current DAG-based systems such as TensorFlow [1] and PyTorch [80]. The inter-resource dependency considered in [29] (with GPU memory) and in [116] (with network) is constrained to layer-by-layer models.

In this work, we focus on *improving the iteration time through better and predictable overlap of communication and computation.* Techniques for optimizing communication and communication time are orthogonal to our system and may be used in parallel with TicTac.

6.2.2 Opportunity for Optimization

We demonstrate the opportunity for accelerating DNN training through a better understanding of the internal computational model in TensorFlow which is a Directed Acyclic Graph (DAG). The parameter transfers are denoted by *send* and *recv* operations in the DAG. In MR, each worker has an identical copy of the computational DAG. In the **worker DAG**, all `recv` ops are roots and *send* ops are leaves. Thus *recv* ops can block the initialization of a computation branch in the DAG. Since the activation of various branches of computation in the DAG is dependent on the *recv* at the root of the branch, the ordering in MR can be reduced to the ordering of `recv` ops in workers. DAG at the PS is different from that at workers. **PS DAG** has five ops per parameter: aggregation, *send*, *recv*, read, and update. Since *send* and *recv* at the PS are not blocked by computation, our focus is on the worker DAG.

In the simple DAG shown in Figure 6.1a, a sample worker DAG, there are two possible schedules for parameter transfers. If $recv_1$ (parameter 1 transfer from PS to the worker)

happens before $recv_2$ (parameter 2 transfer), it reduces the blocking on computation time and improves the overlap. The reverse order results in increased iteration time due to blocking on computation. Thus, in a distributed environment, network can block computation based on dependencies in the DAG. This can lead to under-utilization of computational capacity, in turn resulting in sub-optimal performance. In addition, variation in iteration time caused by random order of parameter transfers across multiple workers can lead to straggling effect.

The impact of poor overlap can be significant in DNN training due to complexity of state-of-the-art models. For instance, ResNet-v2-152 [50] has 363 parameters with an aggregate size of 229.5MB. The computational graph associated with this neural network has 4655 operations in the TensorFlow framework. Finding the optimal schedule in this complex DAG involves evaluating 363! combinations. We run 1000 iterations of learning over ResNet-v2-50, Inception-v3 and VGG-16 networks and observe the order of network transfers at a single worker. The observed order of parameter transfer is unique in ResNet-v2-50 and Inception-v3 networks across the 1000 runs. In VGG-16, we observe 493 unique combinations across 1000 runs.

6.2.3 Comparison with Other Distributed Systems

It is worth noting that deep learning systems with computational graphs are fundamentally different from graph processing systems [70, 51, 110]. In deep learning, the graph is a representation of the computation to be done on the input data. In graph processing systems, the graph itself is the input to the computation. As a result, graphs in DNN frameworks are a few orders of magnitude smaller than a typical large-scale graph processing system. Iterations in DNN frameworks are identical, and network communication pattern is fixed. This may not be true for graph processing systems.

In stream processing systems, the relationship between processing elements are represented using graphs. These systems allow pipelining, with different partitions of input data being processed in different elements along the pipeline at the same time. In contrast, DNN frameworks process the entire batch of input at a processing element at a worker. Pipelining is not employed in this environment. Hence, optimizations proposed for stream processing cannot be borrowed here.

6.3 QUANTIFYING PERFORMANCE

In this section, we explore methods for quantitatively comparing the efficiency of multiple schedules. Towards this goal, we formally define the scheduling problem and investigate the

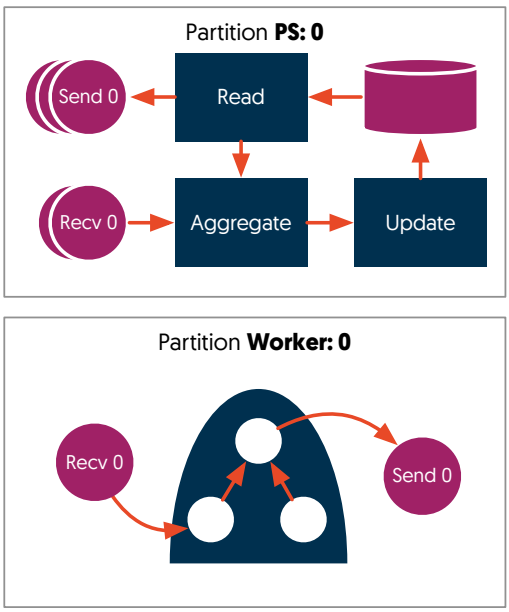

Figure 6.2: Distributed execution of Model-Replica with Parameter Server

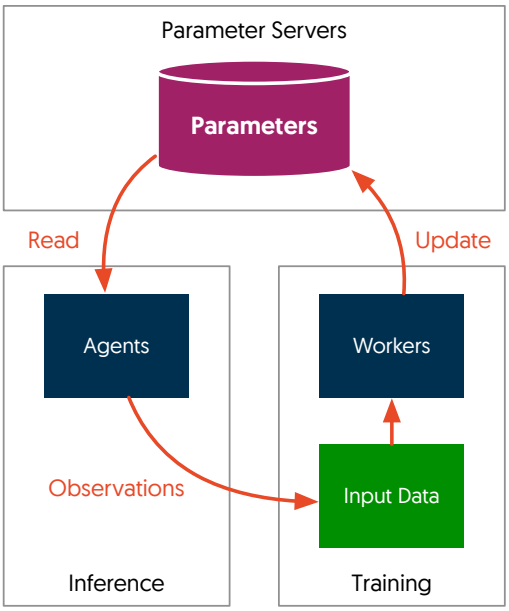

Figure 6.3: A general reinforcement learning setup

feasibility of finding an optimal solution. Finally, we define a metric that is used to quantify the efficiency of a schedule.

6.3.1 Scheduling Problem

The objective is to find the optimal schedule of network transfers that minimizes the iteration time by improving the communication/computation overlap. The network transfers of parameters (*recv* ops) are roots in the computational graph at the worker. The branch of computation ops dependent on a *recv* op can be executed only after the network transfer is completed. Thus, the order of network transfers can determine the order of computation as well as the extent of overlap. We focus on improving the overlap, and in turn the iteration time, by choosing a near-optimal schedule of parameter transfers.

The inputs to this optimization problem are: (a) *the worker DAG*, and (b) *a time oracle*. The time oracle ($Time(op)$) predicts the execution time of a given op. For computation ops, this indicates the elapsed time on a computation resource. For communication ops, this represents the transfer time on the communication medium. We compute the time assuming that the resource is dedicated to the op under consideration.

The output of the scheduling algorithm is a feasible schedule of ops in the DAG tagger by priorities. Ops in a computational DAG may have multiple feasible topological orders. However, some of them may result in a bad iteration time (as explained in Figure 6.1). We

want to limit the execution path to take the one that improves the training performance. We achieve this with priority numbers. Priority number is a positive integer assigned to an op in the DAG. A higher priority op is given a lower priority number. An op may not be assigned a priority if it need not be ordered. Multiple ops may be assigned the same priority if their relative order is insignificant.

The order is enforced in the following manner. When we need to select a new op from the ready-to-execute queue, we randomly choose from among the set of ops that contain the lowest priority number and those without any priority number. It is worth noting that priority only specifies relative order among candidate ops in the ready-to-execute queue at a given resource, and the resulting order will still respect the topological order specified by the DAG.

The problem of finding the optimal schedule is NP-hard. A simpler version of the optimal execution problem with homogeneous hardware can be formally defined as follow (Using notation in [83]): $P_m|M_i, prec|C_{max}$

In this formulation, P_m represents multiple parallel resources with identical performance. M_i assigns the operations to specific resources, i.e., computation ops vs. communication. $prec$ describes the dependency relation of ops in the DAG. The C_{max} represents the goal of scheduling is to minimize the last node completion time.

This problem is still open [19] and simpler cases are proven to be NP-Hard. While there exist approximations for relaxed versions of this problem, to the best of our knowledge, there is no solution or approximation with guaranteed bounds for our original problem.

6.3.2 Defining Overlap Coefficient

The two major contributors to total DNN iteration time (T) are network transfer time or the communication time (N) and the computation time (C). Since the computation and communication may overlap, the total time $T \leq N + C$. Given a GPU/CPU/TPU environment, we assume the computation time, C, to be constant. We ignore the case of computation stragglers and focus on communication.

We define two metrics that define the DNN iteration time: (a) the communication/computation ratio, ρ and (b) the overlap coefficient, α. The ratio of communication to computation, denoted by ρ, determines the extent of benefits achievable. When $\rho < 1$, communication time is smaller than the total computation time, providing ample opportunity for running GPUs at high utilization.

The second factor affecting the GPU utilization is the overlap coefficient, $\alpha = \frac{N+C-T}{min(N,C)}$. $N+C$ is the iteration time when there is no overlap, and T is the actual iteration time. The

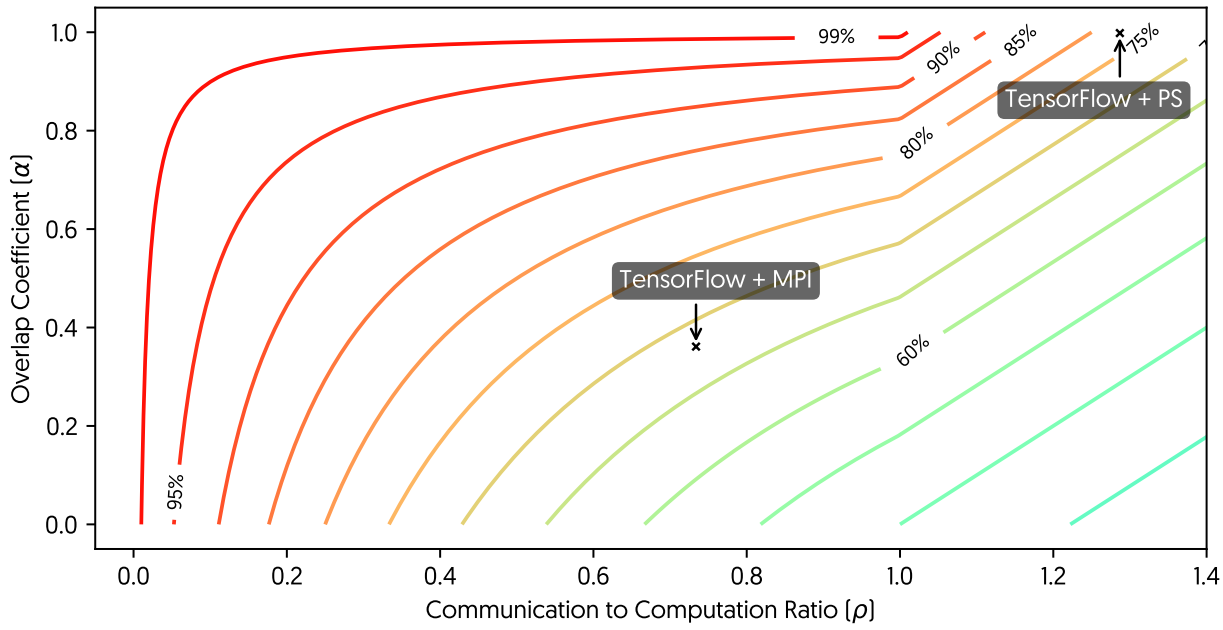

Figure 6.4: Improvement in GPU utilization with TicTac

difference between these quantities is the extent of overlap. The maximum overlap possible is given by $min(N, C)$, which is achieved when the smaller quantity completely overlaps with the large quantity. The difference is normalized by this factor to obtain the overlap coefficient, $\alpha \in [0, 1]$.

The GPU utilization ($U = \frac{C}{T}$) can be represented in terms of these coefficients:

$$U = \frac{C}{N + C - \alpha * min(N, C)} = \frac{1}{1 + \rho - \alpha * min(\rho, 1)} \tag{6.1}$$

The goal of our scheduling algorithms is to achieve high GPU efficiency by maximizing α, i.e., increasing the overlap of communication and computation. The impact of our scheduling algorithm on α, and in turn the GPU utilization is plotted in Figure 6.4 using Inception v3 with 2 workers and 1 PS as an example.

6.4 SCHEDULING ALGORITHMS

In this section, we present two heuristics to derive the optimal schedule of *recv* ops using a given worker DAG (§6.3). The intuition behind our heuristics is to prioritize transfers that speed up the critical path in the DAG by reducing blocking on computation caused by parameter transfers.

Timing-Independent Communication scheduling (TIC): In TIC, we assign priorities based only on vertex dependencies in the DAG (ignoring the execution time of each op). Higher priorities are given to transfers which are least blocking on computation. In this algorithm, we ignore the time oracle, $Time$, and assume all ops have equal cost.

Timing-Aware Communication scheduling (TAC): In this algorithm, we prioritize transfers that maximize α by using information on (a) vertex dependencies among ops specified by the computational DAG, and (b) execution time of each op estimated with time oracle.

6.4.1 Op properties

Before delving into the algorithms, we define properties associated with ops that are used in the scheduling algorithms. The inputs are the worker dataflow DAG (G), a time oracle ($Time$), available communication channels on a device (C) and a set of outstanding (to-be-activated) $recv$s ops (R). We assume that $recv$ ops not in R have their corresponding transfers completed. These properties are updated using the algorithm 6.1.

Communication Dependency (op.dep): This is the set of $recv$ ops that an op is directly or transitively dependent on. For example, in figure 6.1a, $op_2.dep = \{recv_1, recv_2\}$. We extract the communication dependencies using a depth-first post-fix graph traversal on the DAG.

Communication Time (Op.M): Communication time of an op is the total network transfer time required to complete that op. For a $recv$ op, this is the time required to complete its corresponding transfer, given by $Time(recvOp)$. For other ops, this is the total time to complete all outstanding dependent transfers, given by $\sum_{r \in op.dep \cap R} Time(r)$. For example, in Figure 6.1a, $op_1.M = Time(recv_1)$ and $op_2.M = Time(recv_1) + Time(recv_2)$.

For **recv ops**, we define two additional properties.

Directly-Dependent Compute Load (recvOp.P): This property represents the computational benefit of completing a $recv$ op. More specifically, it is the total $Time(op)$ for all ops that can be activated only by completing this $recvOp$, but not without it. These ops are those whose communication dependencies contain only this outstanding $recvOp$ (it is admissible to have communication dependencies on other completed $recv$ operations). For example, in Figure 6.1a, $recv_1.P = Time(op_1)$ and $recv_2.P = 0$ since no op can execute with completion of only $recv_2$.

Algorithm 6.1: Property Update Algorithm

```
   // Update properties for the given the set of outstanding read ops R
 1 Function UpdateProperties(G, Time, R):
 2     foreach op ∈ G do
 3         op.M ← ∑_{∀r∈op.dep∩R} Time(r);
 4     end
 5     foreach op ∈ R do
 6         op.P ← 0;
 7         op.M+ ← +∞;
 8     end
 9     foreach op ∈ G − R do
10         D ← op.dep ∩ R;
11         if |D| = 1 then
12             ∀r ∈ D : r.P ← r.P + Time(op);
13         end
14         if |D| > 1 then
15             ∀r ∈ D : r.M+ ← min{r.M+, op.M};
16         end
17     end
18 end
```

Impending Communication Load (recvOp.M^+): This property helps us to identify candidate *recv* ops to be activated, given the current *recv* is completed. In more detail, it is the minimum communication cost to activate a computation op which has multiple *recv* dependencies including the one under consideration. For example, in Figure 6.1a, $read_1.M^+ = read_2.M^+ = Cost(read_1) + Cost(read_2)$. Please note that $recvOp.M^+$ includes the communication time of that recvOp.

6.4.2 Timing-Independent Communication Scheduling (TIC)

The goal of this algorithm is to prioritize those transfers which reduce blocking on network transfers. Our intuition is that information on DAG structure alone can provide significant improvement.

To achieve this goal, we define a generic time function which only uses the number of communication ops instead of time taken by an op. We use this simple cost function to generate the schedule in Timing-Independent Communication scheduling (TIC).

Algorithm 6.2: Timing-Independent Communication Scheduling (TIC)

```
1 Function TIC(G)
2 |  FindDependencies(G) ;
3 |  UpdateProperties(G,R,Time={Computation: 0, Communication: 1});
4 |  ∀op in G, if op is recv : op.priority ← op.M+;
5 end
```

General Time Oracle: We define a simple universal time oracle as follows:

$$Time_{General}(op) = \begin{cases} 0 & \text{if } op \text{ is not recv} \\ 1 & \text{if } op \text{ is recv} \end{cases} \tag{6.2}$$

The complete solution is given in Algorithm 6.2.

6.4.3 Timing-Aware Communication Scheduling (TAC)

The goal of this algorithm is to prioritize those transfers which reduces the blocking of computation, i.e., speeding up transfers on the critical path. To achieve this goal, the algorithm focuses on two cases. First, it considers the opportunity for overlapping communication and computation. Second, in the case of equal overlap or absence of it, it looks at the impending transfers to choose one which eliminates the computation block sooner.

To better describe the logic, we begin with an example for each case.

Case 1: In Figure 6.5a, when deciding between two read ops, A and B, A should precede B iff:

$$\begin{aligned} \mathbf{A \prec B} &\iff T(A \rightarrow B) < T(B \rightarrow A) \\ &\iff M_A + \max\{P_A, M_B\} + P_B < M_B + \max\{P_B, M_A\} + P_A \\ &\iff M_A + P_A + M_B - \min\{P_A, M_B\} + P_B < \\ &\qquad M_B + P_B + M_A - \min\{P_B, M_A\} + P_A \\ &\iff \min\{P_B, M_A\} < \min\{P_A, M_B\} \end{aligned} \tag{6.3}$$

Therefore:

$$A \prec B \rightarrow \min\{P_B, M_A\} < \min\{P_A, M_B\} \tag{6.4}$$

Case 2: In Figure 6.5b, when all *recv* ops are outstanding, their P is 0, making them equivalent under the comparison in Equation 6.4. Obviously, $recv_A$ and $recv_B$ should precede

(a) Case 1 (b) Case 2

Figure 6.5: Sample DAG

other *recv*s. Hence, we use M^+ to break the ties: $recv_A.M^+ = recv_B.M^+ = Time(recv_A) + Time(recv_B) < recv_C.M^+ < recv_D.M^+$.

Comparator: We combine results from the two cases to make a comparator that extends to multiple read ops. This is an approximate induction, which may not be correct in general. The result is the `Comparator` function in algorithm 6.3. It is easy to prove that this function is transitive and can be used for partial ordering.

The ordering algorithm takes a partition graph on a worker, calculates the communication dependencies, then while there is an outstanding *recv* op, it updates properties, finds the smallest *recv* op with respect to the comparator (The heuristic to this greedy algorithm) and then removes the *recv* from the outstanding set and assign it a higher priority relative to others.

6.5 SYSTEM DESIGN

In this section, we provide a brief overview of the system design and implementation. The system has four main components: the tracing module, the time oracle estimator, the ordering wizard, and the enforcement module (shown in Figure 6.6).

Tracing Module: This module collects runtime stats from an execution, which is later fed to the time oracle estimator.

Time Oracle: The time oracle is responsible for estimating the runtime of each op in the system based on the execution timing stats. Note that the runtime may vary depending on the platform, device characteristics, input data and even across iterations on the same hardware/software. We execute each operation 5 times and measure the time taken in each

Algorithm 6.3: Timing-Aware Communication Scheduling (TAC)

```
   // Compare two given recv ops
 1 Function Comparator(Op_A,Op_B): Bool
 2     A ← min(P_A, M_B);
 3     B ← min(P_B, M_A);
 4     if A ≠ B then
 5         return A < B
 6     else
 7         return M_A^+ < M_B^+
 8     end
 9 end
10 Function TAC(G,Time)
11     FindDependencies(G) ;
12     R ← {op|∀op in G, op is recv};
13     count ← 0;
14     while R is not empty do
15         UpdateProperties(G,R,Time);
16         Find the minimum op from R wrt Comparator;
17         Remove op from R;
18         op.priority ← count;
19         count ← count + 1;
20     end
21 end
```

run. Our Time Oracle implementation chooses the minimum of all measured runs for a given op as the time for that op.

Ordering Wizard: This module is responsible for assigning priorities to recv ops on a single worker. The schedule may be computed based on TIC or TAC. In TAC, the ordering module relies on the time estimated by the time oracle. In TIC, the order is determined based on the DAG alone. The estimated priorities are sent to the enforcement module. The priority list is calculated offline before the execution; all iterations follow the same order.

Enforcement Module: This module takes as input the priority list computed by the ordering module and enforces this order on the network transfers per worker.

6.5.1 Implementation

We implement our system over TensorFlow 1.8. We describe our implementation in detail.

Time Oracle: We use the TensorFlow internal tracer to measure the time of computation ops. We extend the capability (115 LOC C++) of this tracer to collect information on network transfer at all workers. Our code is publicly available (https://github.com/xldrx/tictac).

Ordering Wizard: We implement TIC and TAC as offline analyzers (250 LOC in Python).

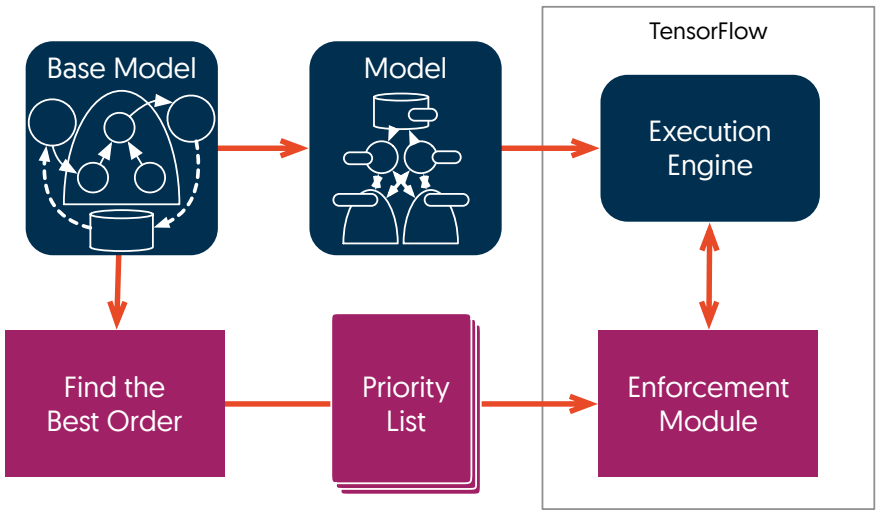

Figure 6.6: System Design. Components of TicTac are in purple rectangles.

The implementation takes time oracle and base model in the TensorFlow DAG format and generates the priority of recv ops.

Enforcing: The enforcement module is implemented over the gRPC submodule of TensorFlow (40LOC in C++).

gRPC provides one channel per worker-PS pair with all transfers between the pair sent to the same queue. Only one transfer can be active at a given moment for each channel. A network transfer over gRPC in TensorFlow involves multiple stages as shown in Figure 6.7. When a *recv* op is activated at the receiver, it sends a request for transfer to the sender. If the *send* op is also active at the sender, the transfer may be initiated by gRPC. In this dataflow, there are three possible candidate locations for enforcing ordering — at the receiver before the request is initiated, at the sender before the *send* op is activated or at the sender before the transfer is sent to gRPC. Alternatively, this may also be enforced as a direct dependency in the DAG.

We implement the enforcement module at the sender, i.e. the PS, before the transfer is sent to gRPC. This choice is guided by several practical concerns. Enforcing directly on the DAG is conservative since each transfer has to wait for the completion of the previous transfer. This prevents pipelining and drastically reduces the communication throughput. Ordering the activation of recv or *send* ops is not sufficient since it could change throughout the data flow. For example, a larger transfer request may take longer to reach the response state on the sender side. During this interval, a smaller transfer with lower priority may catch up.

For the purpose of enforcement, the priorities are sequentially assigned to an integer in the

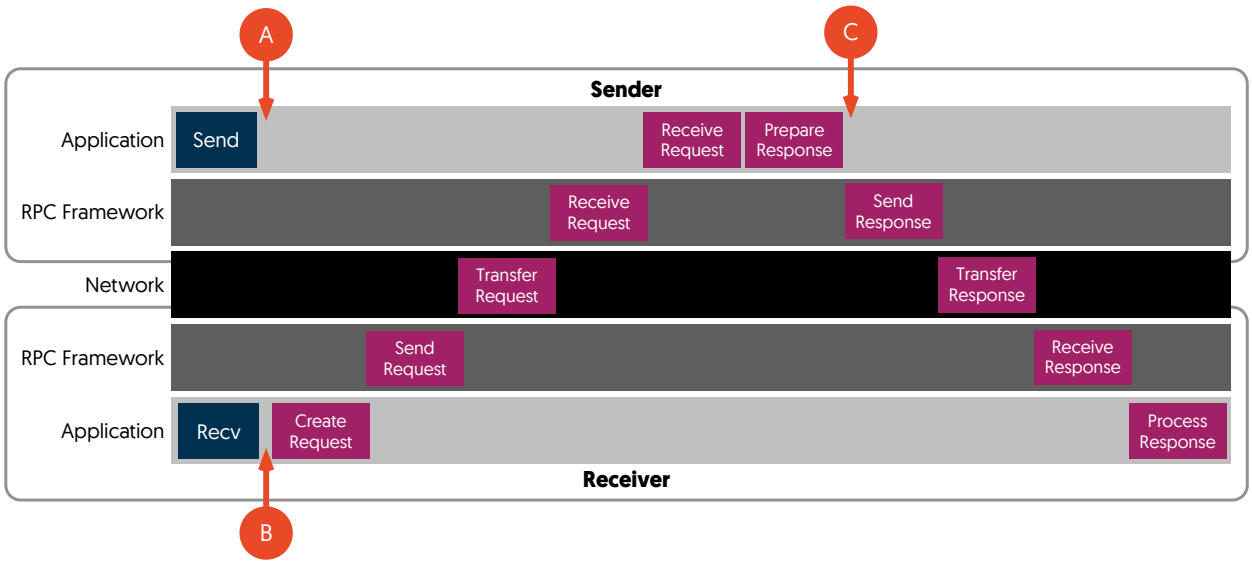

Figure 6.7: Life time of a network transfer.

range of $[0, n)$. Thus, the priority number of a transfer represents the number of transfers that have to complete before it. The sender (PS server) maintains a counter for each worker per iteration which is incremented when a corresponding transfer is handed to the gRPC. Before a transfer is handed to the gRPC, it is blocked until the corresponding counter reaches the normalized priority number.

During experiments, we notice that gRPC may not always process transfers in the order they are queued. This affects the performance of our ordering in some cases. However, the number of such occurrences at the gRPC level are very few. In Inception model (one of the tested models), this error was 0.5% in TIC and 0.4% in TAC.

6.6 RESULTS

In this section, we evaluate TicTac under a wide range of inputs/system parameters to answer the following questions:

- How does TicTac perform with scale out of workers?
- How is TicTac affected by the number of parameter servers?
- How does the benefits accrued with TicTac change with the communication and computation cost?
- How well do the proposed heuristics perform in terms of consistency and straggler mitigation?

Setup: We use in-graph replication for Distributed TensorFlow [17] with synchronized training and synthetic input data.

We test TicTac under two environments:

1. **Cloud GPU environment(env_G):** We use Standard NC6 virtual machines (6 cores, 56 GB memory, 1 X Nvidia K80 GPU with 12GB memory) on Azure cloud environment. For parameter servers we used Standard F64s v2 (CPU Only, 64 cores, 128 GB memory).

2. **High-end CPU cluster (env_C):** We use a commodity cluster (32 core, 64GB memory, 1GbE network).

In both environments, we test 2 to 16 workers and 1 to 4 PS. For understanding the impact of batch size, we test the networks with the standard batch size multiplied by factors [0.5, 1, 2]. We tested our method on 10 well-known models (Table 6.1).

We evaluate the performance under two workloads: training and inference. In training, we use Stochastic Gradient Descent (SGD) as optimizer. The training workload is identical to the training jobs used in practice. We emulate the inference workload of agents in reinforcement learning with online training. In this environment, parameter servers store the parameters which are updated by a set of training worker nodes (which we do not consider in the inference workload). The inference agents are responsible for reading the parameters from the PS and running the inference (this is the phase we evaluate in this workload).

In each test, we discard the first 2 iterations to limit the warm-up effect (initialization of GPUs, cache etc). This is necessary since the first iteration takes much longer compared to the rest. We record the next 10 iterations. For throughput, we report the mean across 10 iterations; for straggler effect and overlap coefficient we report the maximum. Computing the TIC and TAC heuristics takes approximately 10 seconds. Note that these heuristics are computed *before* the training/inference begins. Hence, this will not add overhead during the execution.

We use Imagenet Dataset for our experiments. We evaluated both synthetic and real data and observed less than 3% difference in iteration time on a single machine. The data is read in the TFRecord format from a shared NFS-connected Azure storage, samples are resized, augmented, and prefetched during training. TicTac does not alter the computational flow of the model; it only chooses one of the feasible orders of network transfers. Hence, it does not affect the accuracy of training (shown in Figure 6.8).

Next, we compare the performance metrics across various heuristics. Specifically, we evaluate throughput, overlap coefficient, and prevalence of stragglers (slow workers that

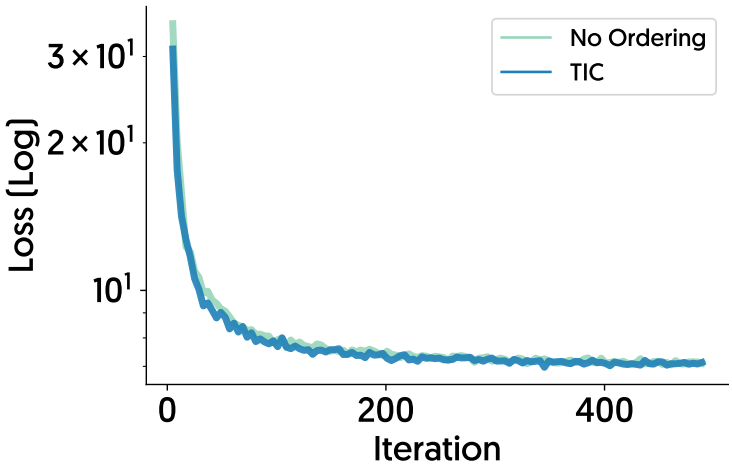

Figure 6.8: Loss value throughout the first 500 iterations of training InceptionV3 on ImageNet.

force others to wait, thereby increasing the iteration time). Performance of TIC is only marginally worse compared to TAC (shown in Figure 6.9 in Appendix). This indicates that, for current models, DAG-level information is sufficient for obtaining a near-optimal scheduling. However, we expect the gap between TIC and TAC to increase as complexity of models increases.

We attempted to compare TicTac with Poseidon [116]. However, only the binaries of Poseidon are publicly available. In our experiments, Poseidon performed extremely poorly compared to TicTac, and even vanilla TensorFlow 1.8. Since Poseidon is based on older version of TensorFlow (TensorFlow 1.0) and CUDA (8.0), we were unable to account the poor performance to their methodology. Hence, we exclude the results since the comparison is inconclusive. Additionally, since order extraction is not explained in their paper, we were unable to reimplement their strategy.

6.7 TIC VS. TAC

In Figure 6.9, we plot the increase in throughput achieved with scheduling in env_C with and without the scheduling schemes (TIC and TAC). We observe that both TIC and TAC offer significant speedup compared to the baseline (no scheduling). Performance of TIC is comparable to that of TAC indicating that we can achieve improved performance without relying on runtime statistics in current models.

Due to the simplicity of TIC algorithm, we use it as the representative algorithm for scheduling in the cloud GPU environment (env_G).

Neural Network Model	#Par	Total Par Size (MiB)	#Ops Inference/Training	Batch Size
AlexNet v2 [63]	16	191.89	235/483	512
Inception v1 [97]	116	25.24	1114/2246	128
Inception v2 [55]	141	42.64	1369/2706	128
Inception v3 [98]	196	103.54	1904/3672	32
ResNet-50 v1 [49]	108	97.39	1114/2096	32
ResNet-101 v1 [49]	210	169.74	2083/3898	64
ResNet-50 v2 [50]	125	97.45	1423/2813	64
ResNet-101 v2 [50]	244	169.86	2749/5380	32
VGG-16 [95]	32	527.79	388/758	32
VGG-19 [95]	38	548.05	442/857	32

Table 6.1: DNN model characteristics

6.7.1 Throughput

Scaling the number of workers: In Figure 6.10, we evaluate the impact of scaling the number of workers with the number of PS to workers fixed to the ratio 1:4. We obtain up to 37.7% of speed up in throughput across networks. The gains are measured relative to the baseline — no scheduling. Larger networks have higher performance gains. The speed up depends on two factors — communication load and extent of overlap. As the number of workers increases, the communication load increases in PS. When the communication load increases, scheduling can provide benefits through better overlap until a threshold. When the communication load is much higher than the computation load, the impact of overlap diminishes. Hence, beyond this threshold, the benefits accrued with scheduling reduces. This threshold varies across models. Also, the gains are measured with respect to the baseline which chooses a random schedule, leading to variations in performance. Hence, we observe varying trends across networks based on the network-specific characteristics. In small networks, with small number of workers and parameter servers, the overhead associated with scheduling may overshadow the benefits of better overlap. In such rare cases, we observe a slow down of up to 4.2%. This shows that scheduling network transfers may be disabled in small networks at small training and inference sizes.

Scaling the number of Parameter Servers: In Figure 6.11, we evaluate the impact of scaling the number of parameter servers with 8 workers in env_G (Cloud with GPU) across various networks. In general, we obtain higher gains in the inference phase than training. Even in the presence of multiple parameter servers, enforcing ordering with TicTac provides significant performance improvement.

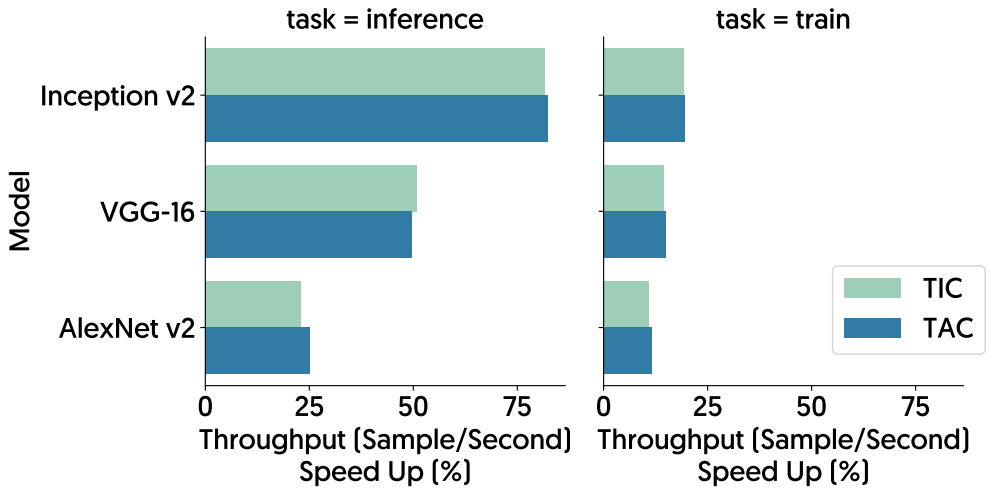

Figure 6.9: Increase in throughput with the scheduling schemes (TIC and TAC) compared to the baseline (no scheduling). Measured on env_C (CPU-Only).

Scaling the computational load: In Figure 6.12, we show the impact of varying computational load by testing each model with the prescribed batch size multiplied by three factors — 0.5, 1, 2. There are two factors affecting the scaling of computation load — computation time and opportunity for overlap. The relative ratio of communication and computation determines the opportunity for overlap. As the batch size increases, the computation time increases. If the communication time is higher (compared to the computation time), increase in computation time increases the opportunity for overlap. If communication time is smaller than computation time, scaling will reduce throughput as the opportunity for overlap reduces.

Scalability with network size:: We show the improvement in throughput (samples/second) achieved with TIC compared to the baseline with no scheduling in Figure 6.14. We observe that larger networks obtain higher gains. This can be attributed to larger variance in parameter transfer orders in larger DAGs in the absence of scheduling.

6.7.2 Overlap Coefficient

To validate the overlap coefficient metric, we run training of Inception v2 1000 times each with and without the scheduling algorithm, TAC in env_C. The overlap coefficient can predict step time accurately, with a high R^2 score of 0.98, as seen in Figure 6.15 (a). This proves that most of the variation in iteration time arises from random schedules in parameter transfers. We also observe that in the absence of enforced scheduling, the step time and overlap coefficient have a large variance. With scheduling, the step time is reduced

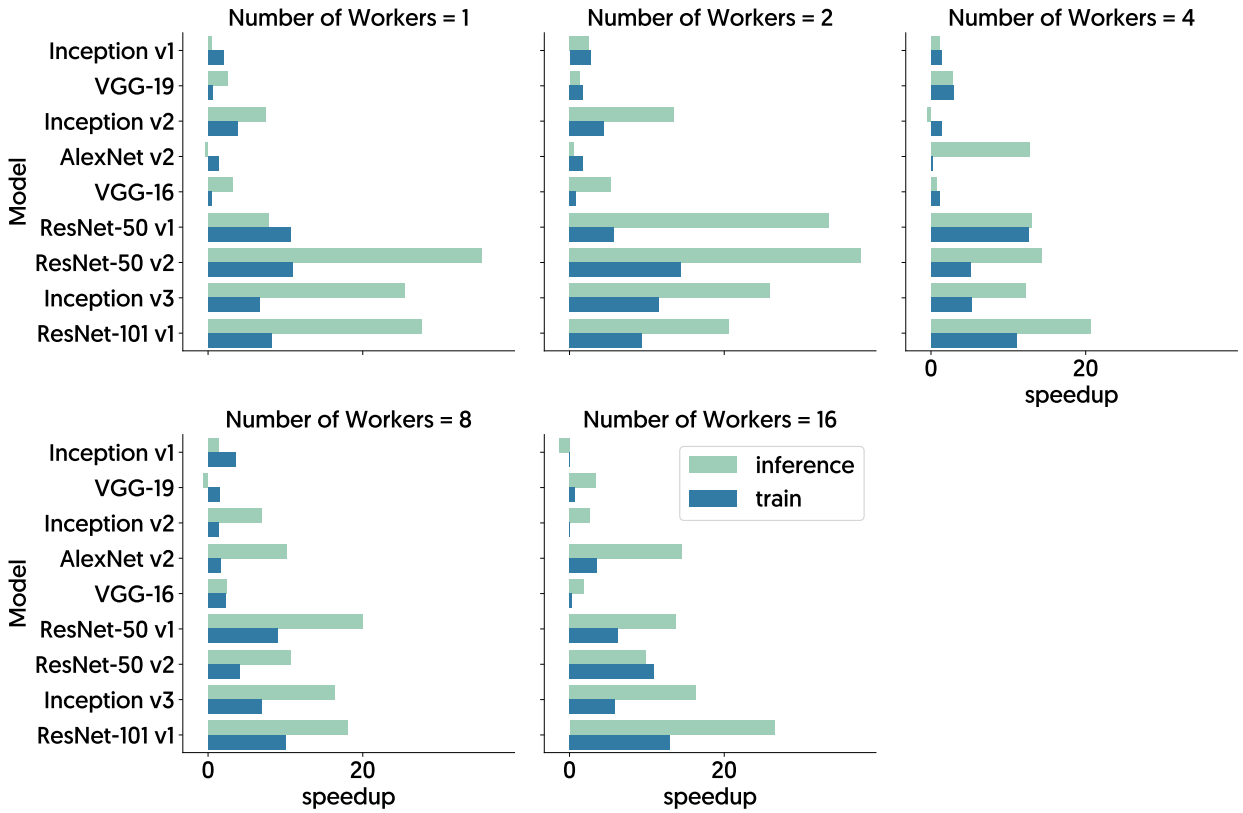

Figure 6.10: Impact of scaling the number of workers on throughput.
Gains are measure with respect to the baseline (no scheduling).
Measured on env_G with PS:Workers in the ratio 1:4.

and the variance is minimal. Moreover, most runs have an overlap coefficient approaching 1, indicating near-optimal scheduling in TAC.

6.7.3 Performance Consistency

In Figure 6.15 (b), we compare the consistency in performance obtained with and without scheduling (TAC) in inference on InceptionV2 with 1000 runs in env_C. We see that TAC has consistent performance, denoted by a sharp curve in the CDF. The baseline (no scheduling), on the other hand, has a large variance. For comparison, 95^{th} percentile of normalized step time in the baseline and TAC are respectively 0.63403 and 0.99825.

Straggler Effect: : Performance inconsistency creates straggling worker effect when multiple workers have different makespan. As a result, all workers have to wait for the slowest one. We quantify the straggler time as the maximum time spent by any worker in waiting to the total iteration time (represented in percentage).

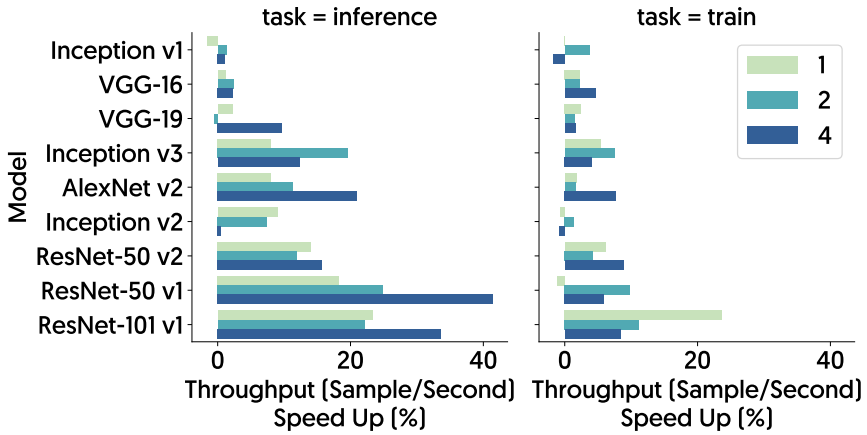

Figure 6.11: Impact of scaling the number of Parameter Servers on env_G cloud GPU environment with 8 workers.

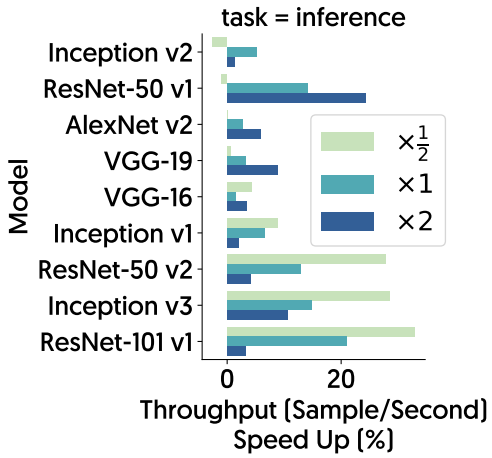

Figure 6.12: Impact of scaling the computational load on env_G cloud GPU environment with 4 workers.

In Figure 6.13, we show the impact of stragglers. Straggler effect is caused by two factors: system-level performance variations and efficiency of scheduling on individual workers. In the baseline, workers follow arbitrary scheduling. Hence, a worker with a bad order forces other workers into a long wait, more than 50% of the total iteration time in some cases. On average, scheduling limits straggler effect with larger benefits in bigger DNNs (higher number of ops). Enforcing *any* order reduces straggler effect regardless of the quality of the chosen order.

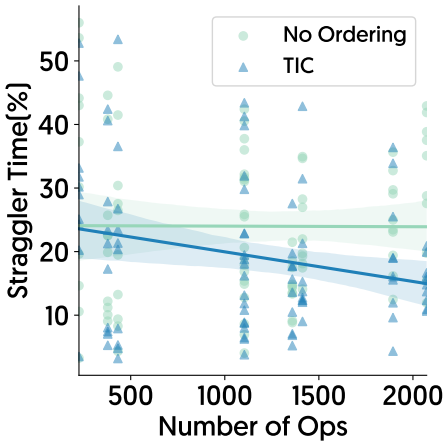

Figure 6.13: Effect of stragglers with TIC in the GPU environment, env_G.

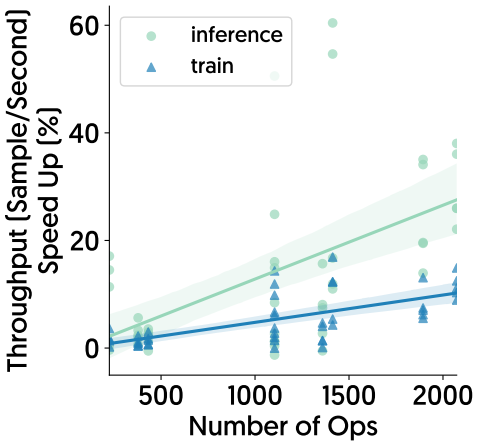

Figure 6.14: Throughput speedup with training and inference as a function of DAG size represented in number of ops

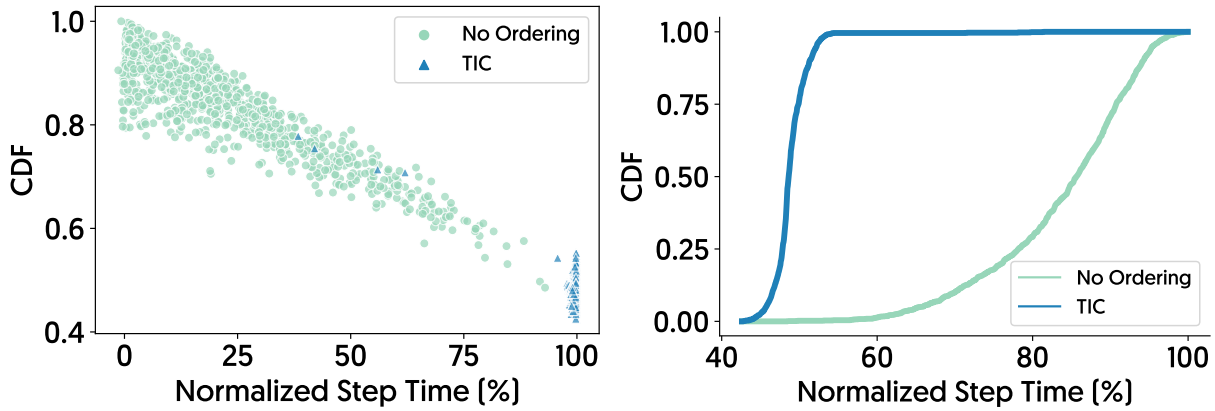

Figure 6.15: In env_C, on Inception v2, (a) Regression test of Scheduling Efficiency and Normalized Step Time, (b) Step Time Comparison across Scheduling Mechanisms.

6.8 CONCLUSION

In this work, we elucidate the importance of communication scheduling in distributed deep learning systems. We devised a metric for quantifying the efficiency of a given schedule of data transfers and developed two heuristics for efficient scheduling. Through extensive testing of these heuristics across a variety of workloads, we demonstrated that significant gains are achievable through communication scheduling. For a typical DNN training which runs for days to weeks, 20% improvement in iteration time can save significant compute power.

Our study encourages further research in network scheduling for parameter server as well as other unexplored aggregation techniques such as all reduce. In future, we can also take

into account additional metrics such as congestion from the network fabric for better network performance. These results also provide motivation for extending the scheduling to additional resources types such as memory and storage.

CHAPTER 7: ACHIEVING NETWORK EFFICIENCY THROUGH COMPUTATION SCHEDULING

7.1 INTRODUCTION

Deep Neural Networks (DNNs) form the crux of advanced solutions in a variety of fields such as computer vision and natural language processing. In frameworks such as TensorFlow [1], interdependence of computation and communication operations involved in training a model is represented using a dataflow graph which is a Directed Acyclic Graph (DAG). The state of the DNN is represented by a vector of parameters. Each iteration involves the computation of parameter updates, followed by its exchange between the participating nodes.

Today, performance and scalability of distributed DNN training in the cloud is bottlenecked by this parameter aggregation [52, 61]. Recently, decentralized aggregation schemes [13, 102, 32], initially introduced in the HPC environment [7, 89], have emerged as a popular choice of aggregation in many frameworks [11, 90, 101]. In these schemes, unlike in the Parameter Server model, all workers store a copy of parameters which are aggregated through collective transfers such as `MPI_allreduce()` in MPI [40] or `ncclAllReduce()` in Nvidia's NCCL. However, in spite of recent optimizations [37], current decentralized implementations fail to achieve the guaranteed performance gains since they overlook interdependency of communication and computation, especially in the cloud, which can leave GPUs idle for a significant fraction of time.

In this paper, we introduce CARAMEL to improve efficiency of decentralized DNN training, in terms of iteration time and GPU utilization, through model-aware dataflow DAG optimizations. CARAMEL achieves this goal by (a) expanding the feasible window of transfer for each parameter (*transfer boundaries*) and (b) improving the network efficiency by smoothening the load.

The transfer boundaries of a parameter represent the window when that parameter can be aggregated without blocking the computation. When the transfer boundaries are farther apart, the performance is less sensitive to slow network. CARAMEL expands these boundaries through precise computation scheduling where it (i) moves the start boundaries earlier while also reducing variance and (ii) pushes the end boundary by postponing the execution of some computation operations to the next iteration.

Optimizations for smoothening the network load include (iii) batching of small parameters to reduce the network overhead, and (iv) adaptive splitting and pipelining of parameters to accelerate aggregation of large data which involves multi-stage network transfers with

intermediate aggregation computation at workers.

Optimizations in CARAMEL are motivated by our observations of shortcomings in state-of-the-art decentralized aggregation systems and our *transfer boundary* model.

First, a dataflow model (DAG) may have multiple feasible traversals, i.e., different orderings for computation operations in the DAG which are all valid. Network transfers are leaf nodes in this dataflow DAG. Based on the schedule chosen for computation operations, network transfers may be activated (i.e., parameters being ready for aggregation) in different orders across multiple workers. This can prove detrimental in decentralized aggregation where all workers should activate the same parameter before its transfer can be initiated and bad schedules can delay transfers. To solve this problem, CARAMEL enforces a schedule on network transfers by adding additional dependencies in the DAG to force all workers to follow the best schedule that activates network transfers as early as possible. Note that this does not affect the correctness of the initial model as CARAMEL is choosing one of the valid schedules in the initial DAG, but it reduces the variance in start boundary.

Second, we identify opportunity for increasing the window of network transfer during an iteration by pushing the end boundary. An iteration has two phases: forward pass and backpropagation phase. Currently, transfers are restricted to the backpropagation phase. We propose techniques for extending network transfers to forward pass in CARAMEL by posponding execution of some operations to the next iteration in the dataflow DAG.

Third, all DNNs we analyzed have a large number of small parameters which incur significant overhead during network transfer. To tackle the small-parameter overhead, we implement model-aware batching in CARAMEL, while also ensuring that the batched parameters are ready at nearly the same time to avoid waiting.

Fourth, transfer of large parameters can be accelerated by splitting a single large aggregation operation into multiple smaller aggregations over partitions of the data and pipelining computation and communication stages of each sub-operation. CARAMEL adaptively chooses the optimal level of splitting them.

We implement CARAMEL over TensorFlow and demonstrate that the iteration time can be reduced by up to 3.62×, with up to 73% network cost reduction. In summary, we make the following contributions:

- We identify opportunities for improving efficiency of decentralized distributed DNN training.
- We develop CARAMEL and implement it over TensorFlow with model-aware optimizations to expand *transfer boundaries* and smoothen network utilization.
- We extensively evaluate the performance of CARAMEL in the Azure cloud and show

that training iteration time can be improved by up to 3.83× and GPU utilization by up to 3× in 5 commonly used DNN models.

7.2 BACKGROUND

In this section, we give a brief overview of the distributed DNN training environment that we aim to optimize.

Popular machine learning frameworks such as TensorFlow [1] and PyTorch [80] represent the DNN training as a Directed Acyclic Graph (DAG). A toy model is given in Figure 7.1a. A DAG has two types of operations (ops): computation ops (multiplication, convolution etc.) and communication ops (read and update). Each parameter is read and updated independently. Each iteration has two stages: forward pass and backpropagation phase. In the forward pass, a loss function is calculated based on the input to the model. In the backpropagation phase, the model parameters are updated based on the calculated loss.

We target the commonly used model replica (MR) (also called data parallel) style of distributed training. In this style, each participating node called worker has a copy of the complete DAG. Input data is partitioned and fed in parallel to the workers. A worker computes updates (gradients) to model parameters based on its inputs. Update to a given parameter is of the same size (byte length) at all workers and the aggregation process is typically a commutative operation (mainly addition). In synchronized training in model replica there is a barrier at the end of iteration to ensure all the workers have their updates aggregated.

Parameter aggregation can be done in several ways. In Parameter Server (PS) mode, there are one or more centralized servers responsible for aggregating parameters. In this paper, our focus is on **decentralized aggregation** techniques (Bucket or Ring algorithm [13], Vector Halving and Distance Doubling Algorithm (HD) [102], Shuffle [32], etc.). In all decentralized patterns, aggregation of a parameter is initiated only after it is activated at all workers. Unlike PS, all workers are involved in the process with communication and computation load related to aggregation distributed across nodes based on the pattern selected. Currently, decentralized aggregation is initiated for each parameter in the backpropagation phase after the parameter is updated.

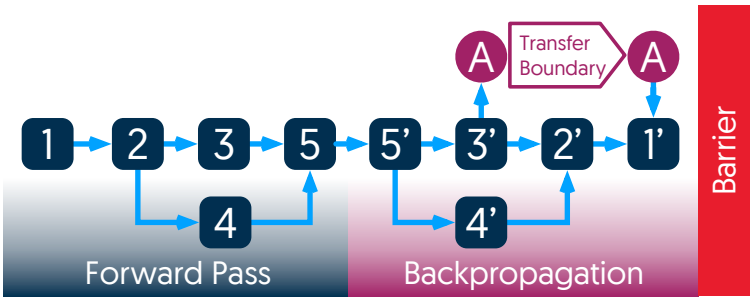

(a) Example DAG

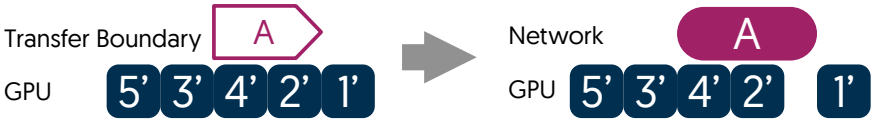

(b) Best Schedule

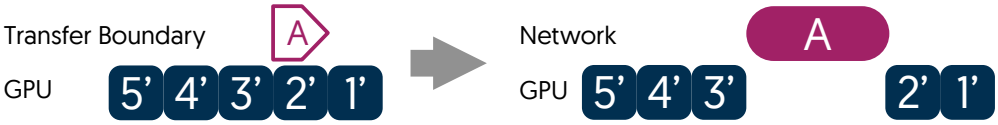

(c) Worst Schedule

Figure 7.1: Impact of Transfer Window on Performance

7.3 MOTIVATION

In distributed DNN training, GPUs are forced to be idle when waiting for network transfers to complete. In this section, we define transfer boundaries of a parameter and analyze various factors causing delays in DNN training.

7.3.1 Defining the Environment

The total iteration time (T), communication time (N), and the computation time (C) are related as $T \leq N + C$ since the computation and communication may overlap. As shown in [46], the communication/computation ratio, ρ, the overlap coefficient, α, and the GPU utilization, U, are related as follows: $U = \frac{1}{1+\rho-\alpha*min(\rho,1)}$. When $\rho < 1$, communication time is smaller than the total computation time, providing ample opportunity for running GPUs at high utilization. Poor overlap of communication and computation can result in low GPU utilization.

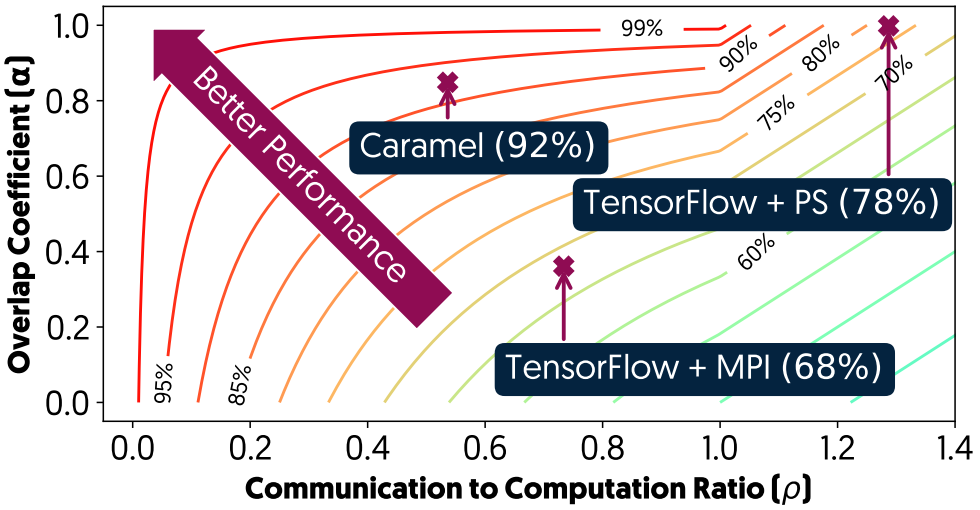

Figure 7.2: Overlap coefficient and communication/computation ratio for different frameworks with GPU utilization contours in the background (using Inception-v3 with 8 workers).

7.3.2 Performance of current systems

Similar to PS comparisons in [46], we plot the contour curves for GPU utilization with respect to α and ρ to understand the performance of MPI implementation in the state-of-the-art decentralized aggregation with Horovod [90]. We observe that TensorFlow with Horovod suffers from poor overlap of communication and computation, and hence poor GPU utilization. In this paper, we will identify causes for this poor performance and design optimizations in CARAMEL that help us improve GPU utilization significantly.

7.3.3 Understanding Model Characteristics

Next, we define transfer window of a parameter and identify causes of low GPU utilization based on this characteristic and other well-known attributes of a model.

Transfer Boundary: We define **transfer boundary** of a parameter based on the window where its aggregation is feasible. The start boundary is determined by the completion of the computation operation that updates the parameter. The end boundary is the computation operation that reads the parameter. Given a schedule of computation operations, start and end boundaries of a parameter are fixed. For example, in Figure 7.1a, start boundary is at $3'$ where parameter A is updated and end boundary is at $1'$ where parameter A is read.

Opportunities for Performance Improvement:

(A) Randomness in transfer boundaries: In decentralized aggregation, all workers

(a) Parameter Server

(b) Decentralized aggregation

Figure 7.3: Comparison of transfer boundaries in a single iteration of distributed training with PS and decentralized aggregation. Data collected from training VGG-16 with batch size of 256.

should have the parameter available for aggregation before the transfer can be initiated. However, there are multiple feasible orders for executing operations in a DAG. As a result, parameters may become available at different workers in varying orders. For example, Figures 7.1b and 7.1c show two schedules of computation operations which are both feasible according to Figure 7.1a. In the best schedule, transfer boundaries are farther apart, allowing better overlap of computation and communication, which will in turn improve GPU utilization. In the worst schedule, the overlap is significantly reduced due to the shorter window available. Thus, we can increase the window between transfer boundaries through better scheduling of computation operations.

(B) Restrictions on network transfers: In PS, the parameters are updated at the backpropogation phase of an iteration and read in the forward pass of next iteration. However, current implementations of decentralized schemes restrict these network transfers to the backpropagation phase. As a result, the network is not utilized during the forward pass as shown in Figure 7.3. In common models, forward pass accounts for about 30% of the computation time (Figure 7.4(a)) which is currently not utilized for network transfers.

(C) Large overhead for small parameters: PDF of parameter sizes across 5 popular models are given in Figure 7.4 (b). We observe that there are a large number of small parameters, with 50% of parameters smaller than 20KB in all models. This observation also holds for 15 other models that we evaluated. Next, we study the impact of small

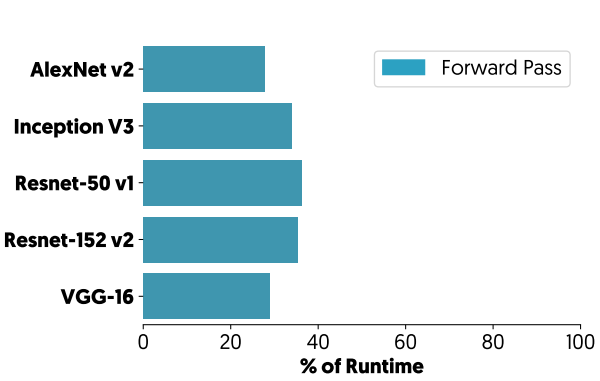

(a) Percentage of Forward Pass in common DNN models

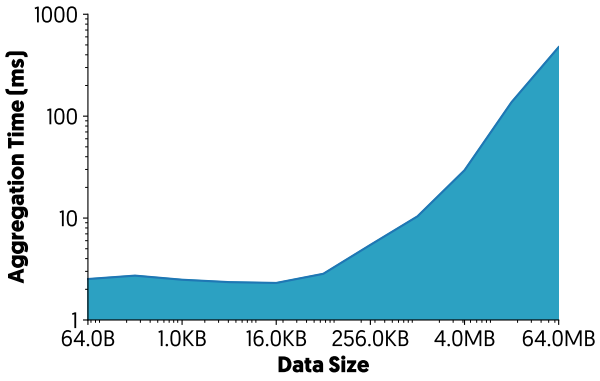

(b) End-to-end transfer time within TensorFlow at different data sizes

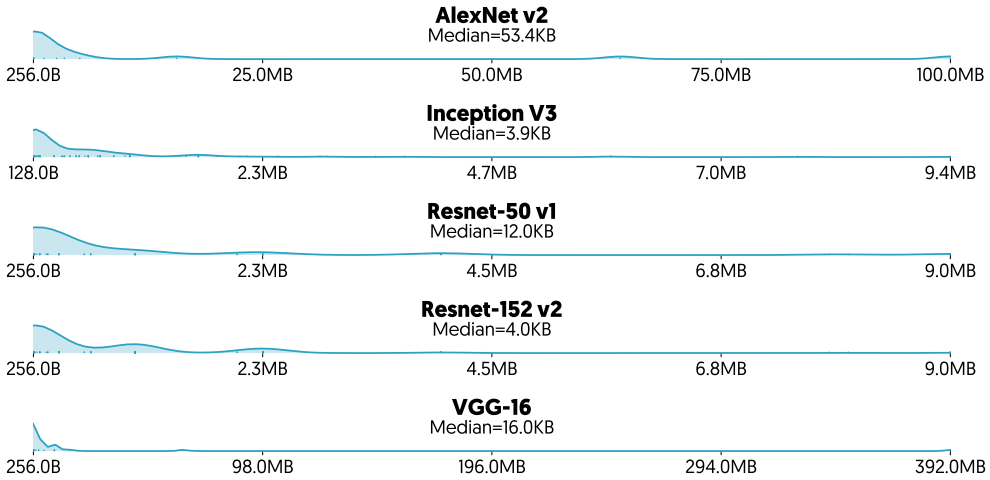

(c) Parameter Size distribution in 5 DNN models

Figure 7.4: Understanding model characteristics: opportunities for optimization (a) significant duration of forward pass which is not used for transfers, (b) large network overhead at small data sizes, (c) large number of small parameters

parameters by measuring the time to receive a small parameter within the TensorFlow framework. This is the end-to-end time from the application perspective which includes the network transfer time and the time for serialization/deserialization, kernel to user-space delay etc. In Figure 7.4 (c), we show the end-to-end transfer time from within TensorFlow for different data sizes with recursive doubling-halving algorithm on 16 workers. We observe that small parameters incur a large delay due to non-network overheads. Thus, we can improve performance by batching smaller parameters. Also, different parameters are read and updated at different times, based on their order of activation in the DAG. This opens the door for smart parameter batching and scheduling based on their transfer boundaries.

(a) Before (b) After

Figure 7.5: DAG Optimization in Caramel

7.4 Caramel DESIGN

Network transfer optimization in Caramel involves four functionalities: (i) dataflow DAG optimizer, (ii) small-parameter batcher, (iii) network transfer scheduler, and (iv) adaptive depth enforcer.

7.4.1 Dataflow DAG Optimizer

In decentralized aggregation patterns, it is necessary to have a parameter ready for aggregation at all workers before it can be aggregated (§ 7.3.3 B). This module is responsible for (i) determining the best executing order of ops in the DAG and (ii) adding additional dependencies in the model to ensure that there is only a single feasible order of execution.

Stage 1 — Determining the best order: To maximize the overlap coefficient, α, the computations should be prioritized in a manner that activates the communication operations as early as possible (early start boundary for parameters). We add the minimal number of additional dependencies to ensure desired ordering on the parameter updates/activation.

First, we trace execution of an iteration on a single machine 10 times. The execution time of a computation operation is determined as the minimum observed time across all runs. Empirically, we find that our method can accurately predict the computation time of execution (with less than 3% error in the worst case) with only 5 runs.

Next, we use an iterative greedy algorithm to find the best order of parameter updates. In each step, we calculate the total time taken by computation ops that need to be completed before each parameter can be activated. The parameter with the least cost of computation required to activate it is chosen and the computation ops that it depends on are marked as completed (their are not counted as dependencies in the next iterations). This process is repeated until all parameter updates are visited.

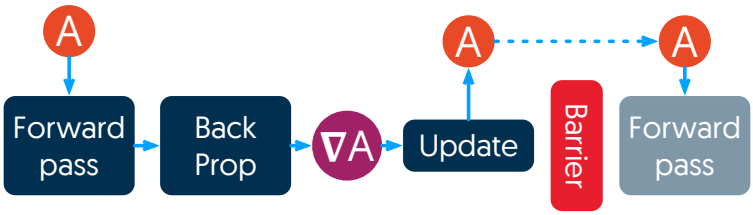

(a) Before

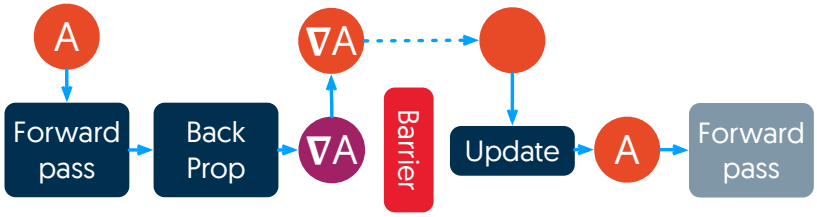

(b) After

Figure 7.6: Transfer Scheduling in Caramel

Stage 2 — Enforcing the best order: This is an iterative process where parameters are activated in the best order chosen in the previous stage. In each step, we find the list of all ops that the chosen parameter directly or indirectly depends on. We define the *free set* as the set of all ready-to-execute ops, i.e., ops with no dependencies on any unexecuted ops. The *end set* is the list of ops which the target parameter update depends on directly. New dependencies are added between end set of parameter with tag i and free set of parameter with tag $i + 1$. Parameters are executed in the increasing order of their tags (based on the chosen order).

This ensures that at each given time, only ops needed for the target parameter update can be executed. It is worth noting that adding additional control dependencies to the dataflow model does not change the underlying logic of the DAG. The enforced order is one of the feasible orders in which the DAG may be executed, even without the additional dependencies.

7.4.2 Parameter Batcher

Small parameters incur large overhead (§ 7.3.3). Hence, the goal of parameter batching is to reduce this overhead by combining parameters in to groups. In our implementation, we focus on grouping small parameters only. Larger parameters, larger than a certain threshold determined by the network characteristics, are transferred without batching.

We begin with the order we obtained (§ 7.4.1) and calculate the expected parameter update time. For each parameter, in the ascending order of the estimated update time,

we determine whether to batch it or not. If the size of the parameter is larger than the threshold (the choice of the threshold explained in the next paragraph), it is transferred without batching. If the parameter is smaller than the threshold, we decide whether to transfer immediately (effectively, putting the transfer in a queue to transfer eventually) or add to the current active batch. The current batch is transferred when the active batch size exceeds the threshold or if the transfers in the queue are done before the next parameter update.

This algorithm ensures that parameters are batched whenever there is an opportunity, i.e., the network is busy with other transfers. The threshold plays an important role in this algorithm. If the threshold is too small, too few parameters will be batched. If it is too large, the batching overhead will exceed the benefit. The threshold can be set manually.

We use a network model to predict the total transfer time for a given data size. Empirically, we find that a simple linear regression model can accurately predict the transfer time for a given data size in the network. In order to generate this model, we run two sets of network microbenchmarks for two data sizes: $64B$, and $4MB$. The choice of data size is arbitrary; we get very similar results with different combinations. For each chosen data size, we run sequential aggregation transfers and record the time. Next, we fit this data to a linear model. Using this network model, we estimate the best threshold as follows:

$$Threshold = min_x \frac{f(2x)}{2f(x)} > 0.8 \tag{7.1}$$

where $f(d)$ is the network transfer time for data size d. We obtain the minimum overhead using this threshold.

7.4.3 Network Transfer Scheduler

The network transfer scheduler is responsible for increasing the overlap coefficient by scheduling parameter transfers efficiently. Transfers are scheduled in both backward pass and forward pass to overcome the shortcomings discussed in § 7.3.3, without affecting the computation (Figure 7.6).

Moving a network transfer to the forward pass has the possibility of causing delay in computation. We avoid this problem through model-awareness. A parameter cannot be updated beyond its transfer boundaries. For batched parameters, this boundary is determined by the parameter that is read at the earliest time/updated at the latest time.

We implement a greedy 2D-Bin packing algorithm to pack the parameters based on their feasible window. The two dimensions are time and data size. The algorithm proceeds as

follows. First, we sort the batched groups in the descending order of size. Second, for each group, we attempt to pack the group in parallel with computation, first in the backward pass (any time after the end of the batch); if that is not feasible, next, in the forward pass (any time before the start of the batch). At the end of this stage, we have a few groups which are allocated a transfer time and some that are unassigned.

In the third stage, we repeat the same process on unassigned items, but allowing transfers beyond the computation time, i.e., after the end of the backward pass, or before the start of the forward pass. For each item, we compare the additional time added to iteration time by placing the group in FP and BP, and we choose the one with the smallest overhead.

7.4.4 Adaptive Depth Enforcer

In decentralized algorithms, there are two or more stages where data is transferred and aggregated across participating nodes. In each step, data is transferred on the network, and is sent to application to be reduced, before the result is sent again over the network. This back and forth between network and application reduces the network utilization since the network is not utilized during the reduction at the application layer. One solution for avoiding this network under-utilization is to chunk (or break) the data in to a few pieces, and transfer each chunk independently in parallel. The number of chunks is called *depth* of algorithm. In this case, while one chunk is being reduced on the CPU, another chunk can be sent over the network, i.e., this enables pipelining of network transfer and application-level processing across various chunks. The choice of depth in some DL systems is fixed. For example in [37] a fixed depth of 2 is used. Throughout the experimentation we observe that the depth has a conflicting effect on transfer performance. As shown in Figure 7.13, transfer time of small parameters increases with increasing depth. In the worst case, we observe 3× slow down going from depth of 1 to 8. For large parameters, however, the transfer time decreases by increasing the depth. At the peak, we observer 60% decrease in transfer time going from depth of 1 to 8.

We choose the depth of transfer adaptively, starting from a depth of 1 at smaller parameter sizes to a maximum of 8 at larger sizes. The depth is determined based on the data size and a threshold, (this is same as the parameter batching threshold in 7.4.2). As shown in Figure 7.13, our adaptive depth gets the best performance; smallest transfer time at all sizes.

In-Graph Implementation In contrast to other implementations of decentralized aggregation in deep learning systems such as Horovod (in TensorFlow and PyTorch) and Gloo (in Caffe2) where the aggregation pattern is abstracted as a single op in the dataflow model, we

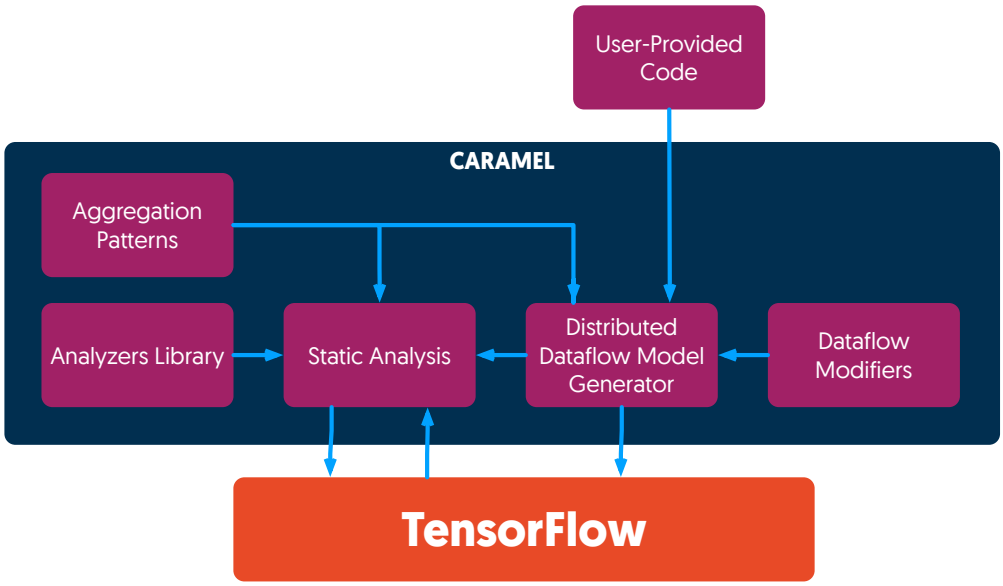

Figure 7.7: Caramel Implementation

implement the aggregation pattern as a part of the DAG. In other words, the data conversion, transfer, and aggregation are defined as standard dataflow ops. This allows the aggregation pattern to take advantage of further optimizations by the framework such as op fusing, XLA [66]. Additionally, in-Graph implementation does not dependent on external dependencies such as MPI, making it more accessible and easier to deploy in the cloud environment.

7.5 IMPLEMENTATION

We implement Caramel as a Python library over TensorFlow. The code is publicly available (obfuscated for review). The library takes user code dataflow model intended for a single device, and generates an In-Graph distributed dataflow model. Caramel API declaration is as follows:

```
def ARModel(context,
            number_of_workers,
            serialization = True,
            batching = True,
            scheduling = True,
            analyzers = None,
            device_list = None)
```

The functionality of Caramel is divided in two: 1) extracting information from the environment and calculating the best network schedule based on the user-provided code, 2)

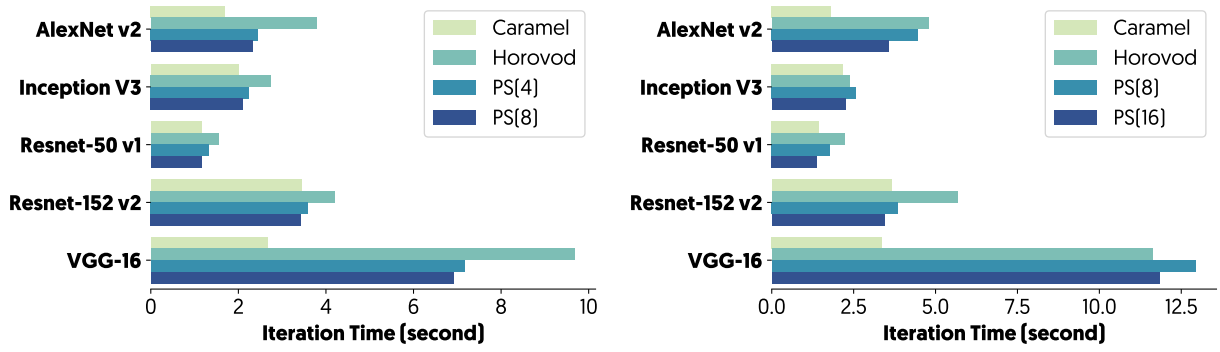

(a) 8-Worker

(b) 16-Worker

Figure 7.8: Comparison of Iteration Time in Caramel with PS and Horovod. Lower is better.

generating a new distributed TensorFlow dataflow model with the added optimizations.

Figure 7.7 shows the main components of Caramel. **Distributed Dataflow Model Generator** is the component which glues together all the other components in the system and provides an interface to the user to interact with CARAMEL. The ultimate goal of this component is to generate a network-optimized distributed model. This component generates a distributed dataflow model using the **aggregation pattern** as the network primitive. Next, it applies the optimizations on the dataflow model through **Dataflow Modifiers**. Each modifier applies an optimization on the dataflow graph. For example, the DAG optimizer takes a list of control dependencies and adds it to the dataflow model. The behavior of the modifiers and the choice of aggregation pattern is controlled by the **analyzers**. Each analyzer generates a piece of information to be used by other analyzers or modifiers. **Static Analysis** component is responsible for figuring out the data dependencies between analyzers and executing them. The **Distributed Dataflow Model Generator** automatically selects the set of analyzers based on optimizations. However, the user can send a custom list of analyzers.

7.6 EXPERIMENTS

In this section, we evaluate the efficiency of Caramel system implemented over TensorFlow.

Experiment settings: We run our tests on Azure cloud environment using Standard NC6 virtual machines (6 cores, 56 GB memory, 1 X Nvidia K80 GPU with 12GB memory). The bandwidth is 10 Gbps. Our evaluations use 8 to 16 workers.

We use *Microsoft Data Science Virtual Machine for Linux (Ubuntu)* image on our VMs

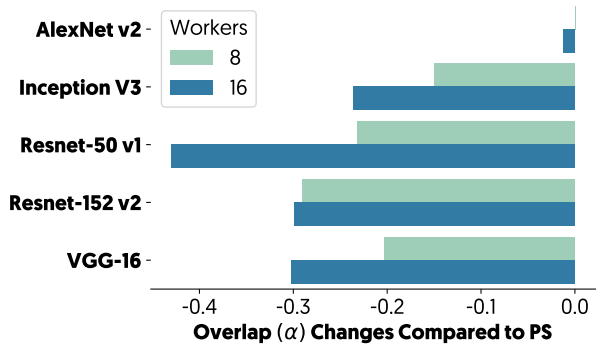

(a) Overlap vs PS

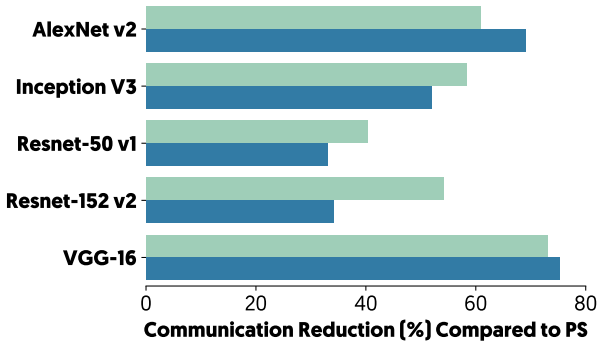

(b) Network Cost vs PS

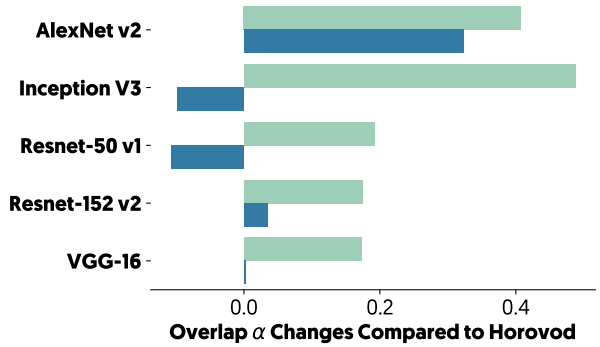

(c) Overlap vs Horovod

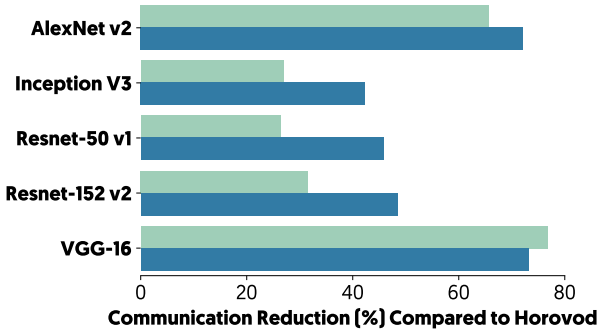

(d) Network Cost vs Horovod

Figure 7.9: Micro Comparison of Caramel with PS and Horovod. Higher is Better.

which comes with CUDA 9.0, cuDNN 7.0.5, Anaconda Python 3.5.4, Open MPI 1.10.2, and Horovod 0.11.3. We upgrade the TensorFlow to the GPU-enabled binary release of 1.8 from *pip* repository.

DNN models: We analyze 16 models and select 5 representative neural networks for our experiments. (Model, number of parameters, total parameter size (MiB)) are as follows: (AlexNet-v2 [63], 16, 191.9), (Inception-v3 [98], 196, 103.5), ResNet-v1-50 [49], 108, 97.4), (ResNet-v2-152 [50], 363, 229.5), and (VGG-16 [95], 32, 527.8). We use the reference implementation in `github.com/tensorflow/models`.

We evaluated both synthetic and real data based training. For real data, we read the Imagenet Dataset in TFRecord format from a shared NFS-connected Azure storage, resize it with augmentation and prefetch the data during the training. This initial evaluation showed that we have less than 1% iteration time difference between experiments with synthetic data and real data (except in AlexNet-v2 with 3% error). Hence, for the rest of the experiments, we rely on synthetic data.

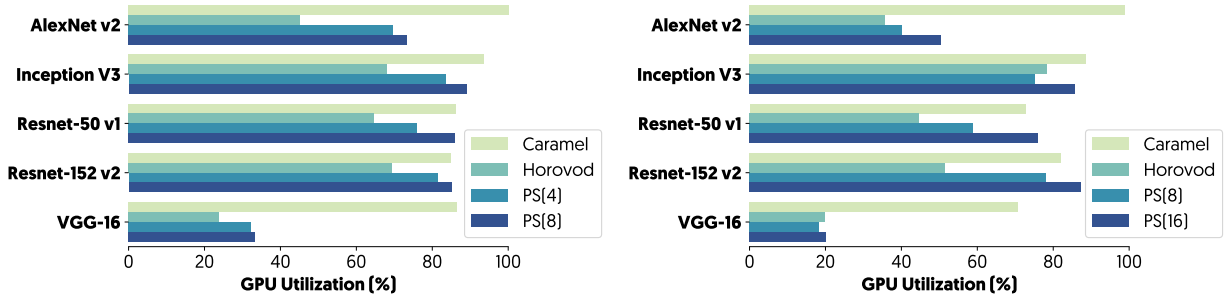

(a) 8-Worker

(b) 16-Worker

Figure 7.10: Comparison of GPU Utilization in Caramel with PS and Horovod. Higher is better.

7.6.1 Comparison with other systems

We compare performance of Caramel with Parameter Server scheme (with #Parameter servers = #workers and #workers/2) and Horovod (state-of-the-art decentralized aggregation scheme). We evaluate two metrics: iteration time (Figure 7.8) and GPU utilization (Figure 7.10) with 8 and 16 workers. We observe that performance of Caramel is consistently better than PS and Horovod with lower iteration time and higher GPU utilization across all configurations tested. The largest improvement is observed with VGG-16 at 16 workers with 3.62× improvement in iteration time and 3.5× in GPU utilization. This highest benefit is observed for DNNs with largest variance in parameter sizes. We also observe that Caramel optimizations result in a GPU utilization of atleast 70% in all networks tested.

To understand the performance better, we trace the execution of each iteration using `tensorflow-tracer` [48]. We measure α and ρ from the traces (Inception-v3 example in Figure 7.2). In Figure 7.9, we observe that at all sizes tested, Caramel results in reduced communication cost compared to the baselines due to adaptive depth and batching. The benefits accrued by Caramel over PS is due to reduced network cost and over Horovod is due to better overlap. While overlap of Caramel is better than Horovod, it is still worse than PS. However, this is compensated by significant reduction in network cost.

7.6.2 Impact of Caramel Optimizations

In this section, we quantify the contribution of each of the optimizations in terms of overlap coefficient (α) and communication cost in Caramel towards the performance benefits achieved. In Figure 7.11, we see the impact of putting these optimizations together on a single model, Inception-v3 with 8 workers. ***Adaptive All Reduce:*** Compared to the MPI

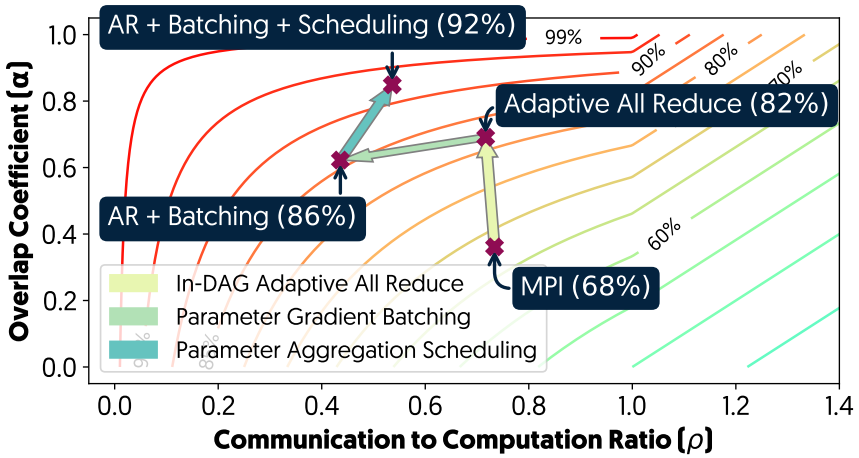

Figure 7.11: Caramel Components Contributions on Performance of Inception v3

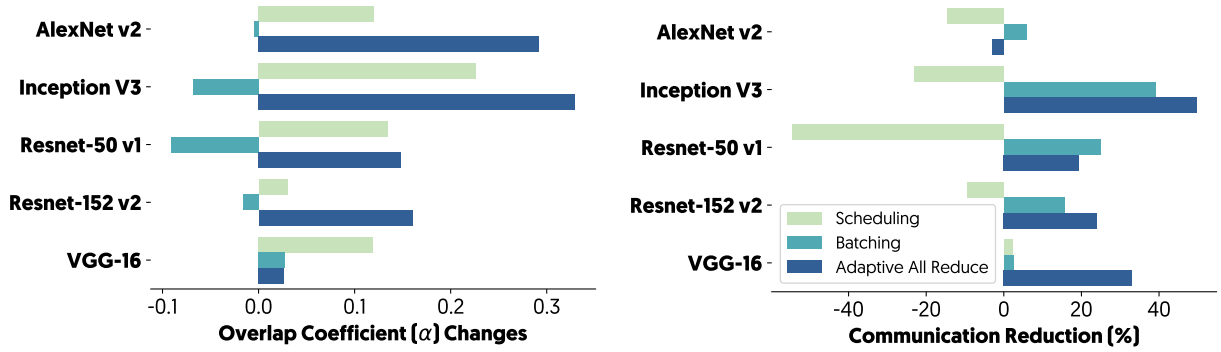

(a) Overlap

(b) Network Cost

Figure 7.12: Contribution of each module in Caramel to performance. Higher is better.

implementation in Horovod, the adaptive all reduce significantly improves the overlap and cost, thereby the GPU utilization by 14%. ***Batching:*** Implementation reduces the overlap slightly. However, significant reduction in communication overhead further improves the GPU utilization by 4%. ***Transfer Boundaries:*** Adding the computation scheduling, increases communication cost, but improves overlap significantly. As a result, the GPU utilization increases by 24% (92% in CARAMEL vs. 68% in MPI implementation of Horovod). Similar trends hold in training of other networks as shown in Figure 7.12.

7.6.3 Evaluation of Adaptive Decentralized Schemes

We test constant depth and adaptive depth schemes at different data sizes (shown in Figure 7.13. At smaller data sizes, splitting the data to be aggregated into smaller chunks results in increased transfer time. This is caused by the high overhead in each chunk. Hence,

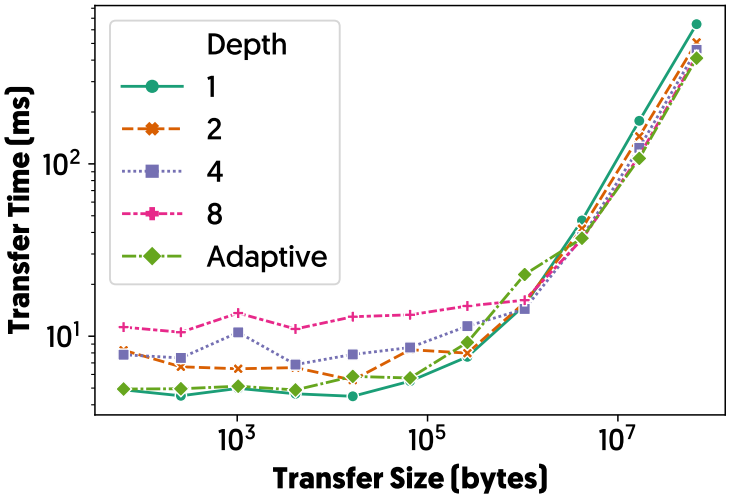

Figure 7.13: Impact of depth on transfer time

a smaller value of depth works better for small data transfers. At large data sizes, on the other hand, a larger depth allows pipelining of multiple transfers, particularly the processing at nodes. The adaptive scheme in CARAMEL chooses depth of 1 at small data sizes and a depth of 8 at the largest size tested. Note that the y-axis is logscale; the adaptive scheme achieves 60% lower transfer time compared with depth 1 at 100 MB.

All results until the previous subsection are based on shuffle mode of decentralized aggregation. However, CARAMEL optimizations are applicable to all decentralized aggregation schemes. In Figure 7.14, we show the iteration time with two other decentralized schemes: ring and halving-doubling at two transfer sizes representating small and large transfers. Shuffle has the highest performance benefit with less number of workers, hence we showed results for this scheme. As the number of workers increase, halving-doubling has better performance. The choice of the best aggregation scheme depends on the number of workers, network bandwidth available, etc.

In summary, we have shown that CARAMEL offers the following performance benefits:

- CARAMEL improves iteration time by up to 3.62× and GPU utilization by up to 3.5× compared with Horovod in 5 popular DNNs.
- Optimizations in CARAMEL reduces communication cost and improves the communication/computation overlap.
- Small parameter batching and adaptive depth allows CARAMEL to choose the optimal chunk size for transmission with minimal overhead.
- CARAMEL is the first system implementing decentrilized aggregation to support network

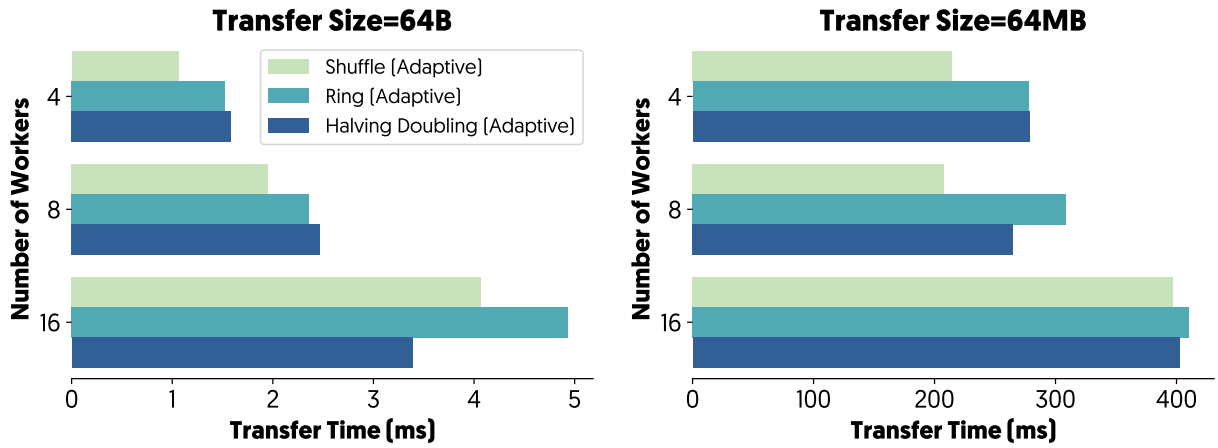

(a) Small Transfers

(b) Large Transfers

Figure 7.14: Performance Comparison of Different Collective Transfer Implementation in Caramel. Lower is better.

transfers during the forward pass of computation, thereby increasing overlap significantly.

7.7 DISCUSSION

In this section, we discuss limitations of CARAMEL and avenues for future work.

Dynamic and variable models: CARAMEL cannot accurately predict the timing of dataflow models with Dynamic control flow [114] or models with highly variable input sizes (e.g. DeepSpeech2 [7]) since our model relies on the iterative nature of the DNN training. In such environments, inaccurate prediction can lead to higher iteration time.

Extending network optimization to multiple GPUs: CARAMEL focuses on optimizing network transfers over the cloud network. Our implementation does not rely on Nvidia's NCCL or other GPU-to-GPU libraries to aggregate the data on a single machine. In future, CARAMEL can be extended with additional optimization for network aggregation between multiple GPUs within a single machine.

Alternative implementations: Our implementation currently generates an In-Graph dataflow model, where the dataflow at all workers is represented in a single large DAG and later partitioned. The size of this graph grows as the number of workers increases, which may increase the TensorFlow processing time at large graph sizes. Note that we have not hit this limit with the current models. In contrast, Horovod uses a Between-Graph dataflow model, where each worker's version of dataflow model is generated separately. Since none of the optimizations in CARAMEL is dependent on the type of the dataflow model, CARAMEL

components may also be implemented as a "between-graph" dataflow model.

Extending to other frameworks: CARAMEL is currently implemented over TensorFlow. However, the optimizations are independent of the choice of framework, and can be adapted to other systems (similar to porting Horovod from TensorFlow to PyTorch [80]).

7.8 ENFORCING THE EXECUTION TIMING THROUGH TIMED RPC

Remote Procedure Call (RPC) encapsulates the kernel networking APIs in a procedural programming abstract. RPC frameworks are an essential part of distributed systems. gRPC in TensorFlow, netty in Giraph, Gloo in Caffe2, and NCCL2 in Horovod to name some examples. Having a separate layer between makes it easier to better adapt the workload to the specification of underlying hardware without changing the application.

7.8.1 Problem

Timing of RPC call execution by the frameworks may impact the overall performance significantly when the execution is blocked waiting for a call to finish. Figure 7.15 demonstrates this problem in an overly simplified example representing an iterative system (similar to a TensorFlow workload). The execusion DAG has two RPC calls: `A` and `B` where `A` is called after operator #5 and the response is sent to the operator # 1 of the next iteration. As it is shown in timelines different RPC call ordering causes different iteration time.

Obviously, this problem impacts workloads with tightly-coupled network and processing dependencies such as iterative systems and gets worse as as the size of the workload grows, or in the presence of multiple services.

In our measurement on a set of "Deep Learning" workloads on TensorFlow with "gRPC", the best timing has a 60% higher throughput than the worst timing, and 23% than average of gRPC timing[1].

7.8.2 Current Solutions

The root cause of this problem is the lack of application information in lower layers. Some works such as Naiad enforces the ordering in the application layer. While effective for one application, these works could not properly react to the presence of other services.

[1]We tested AlexNet v2, Inception V3, Resnet-50 v1, and VGG16 on a 4-worker cluster with P100 GPUs

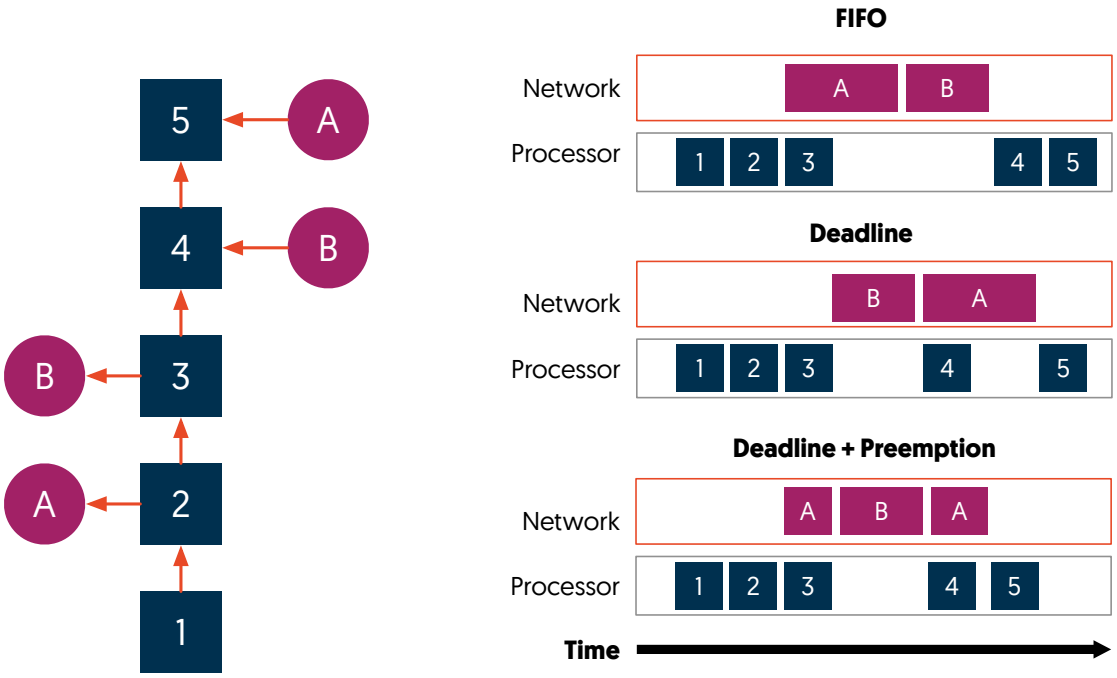

(a) DAG (b) Timelines

Figure 7.15: Impact of RPC call orders on Performance

Other approaches such as CoFlow, try to communicate the application needs to lower layers. There have works that assign priorities to RPCs, mark related IP packets, or mark related network flows.

While we are taking the second approach in our ongoing solution, we argue that much richer information has to be communicated since none of the previous suggestions could fully address the aforementioned problem.

7.8.3 Design

In our proposed system (Figure 7.16), the application communicates the absolute deadline of an RPC call as well as an objective function. If the deadline of a call is passed, the application suffers a delay in the execution, however, there is no performance benefit in finishing up earlier. An objective function quantitatively measures the performance penalty of a passed deadline. For example "$\max_{call}(max(end_{call} - deadline_{call}, 0))$" represents a TensorFlow like system where the delay in iteration is equally when just one or all calls get delayed by a certain time.

The deadlines can be explicitly assigned to calls or be inferred automatically in iterative workloads using `Timing Oracle`. The scheduler then optimizes the calls using the objective

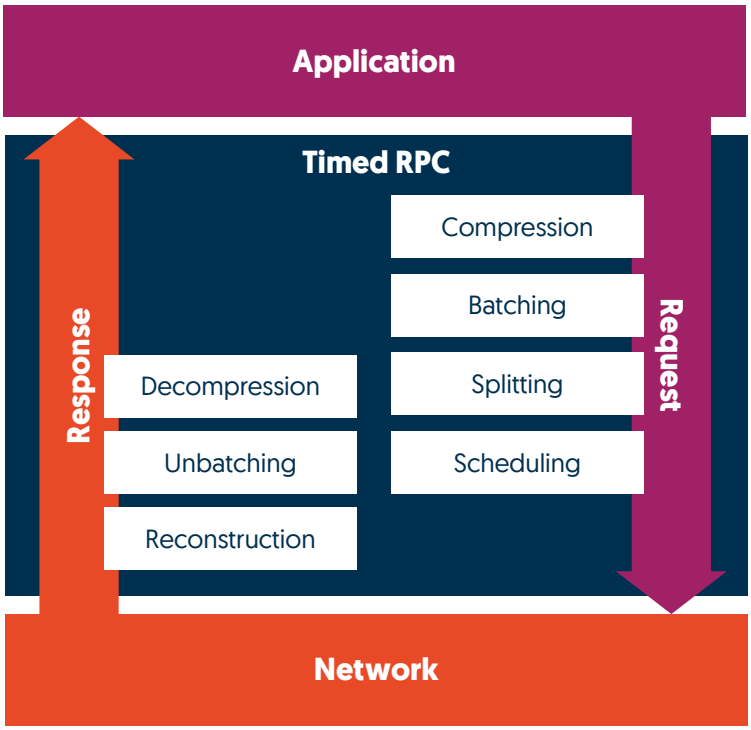

Figure 7.16: Timed RPC Architecture

function.

7.8.4 Results

We have implemented an RPC framework simulator and replaced it with gRPC in TensorFlow. In our implementation deadlines are pre-calculated from analyzing the data flow DAG. We split the large RPC calls to make the bin packing problem in scheduling easier. Our results show that our RPC framework achieves up to 20% higher throughput compares to default gRPC.

7.9 RELATED WORK

Several solutions have been proposed for reducing iteration time through network acceleration in distributed DNN training. The first category focuses on modifying the machine learning algorithm with the objective of optimizing network tranfers [5, 109, 116]. CARAMEL does not change the DNN; it only adds additional dependencies in the dataflow DAG without altering the underlying logic. The second class of solutions decreases network overhead by reducing the precision of parameters [105, 27, 41]. CARAMEL does not change the parame-

ters of the DNN. The third approach is to optimize the aggregation pattern for accelerated DNN training [37, 25, 7, 113, 4, 116]. CARAMEL belongs to this category.

However, prior solutions for improving communication/computation overlap [8, 29, 116] developed for earlier layer-by-layer systems where the model is sequential cannot be adapted to modern DAG-based systems. CARAMEL algorithms are not related to these prior solutions. Solutions for improving communication/computation overlap in Parameter Server (PS) based systems cannot optimize Collective communication (AR) due to significant differences in the execution model. PS has three steps: "Push" gradients to PS, "Update" parameters on PS, and "Pull" parameters to workers. Poseidon [116], P3 [56], and TicTac [46] overlap Pull, Update, and Push across different parameters at the same time in PS-based aggregation. AllReduce (which CARAMEL tackles) has only 2 steps: "collective reduce" of gradients followed by "Update" parameters at each worker (Fig 1). More importantly, similar techniques are used differently in Caramel and past work. E.g., CARAMEL splits transfers to overlap "time on the wire" with kernel context switching and aggregation op within a single transfer. P3 splits a transfer to overlap Push and Pull of subparts. CARAMEL transfers all subparts in parallel while P3 transfers sequentially.

Finally, some systems focus on increasing the communication/computation overlap. However, these solutions [8, 29, 116] were developed for earlier layer-by-layer systems where the model is sequential. These techniques cannot be adapted to modern DAG-based systems. CARAMEL algorithms are not related to these prior solutions.

Kylix [117] proposed the use of allreduce primitives (such as recursive halving-doubling used by CARAMEL) in commodity clusters primarily for big data processing systems such as Hadoop and PowerGraph. It leverages the sparsity of data to optimize network transfers. While CARAMEL relies on the same primitives, we implement additional optimizations tailored to the TensorFlow framework. Moreover, CARAMEL chooses *when* to do the aggregation and on *what data size* based on the model and network characteristics. Another work [69] that optimizes allreduce for machine learning frameworks is tailored for the HPC environment with high speeds and not suitable for the cloud environment (InfiniBand is 54+Gbps, and Azure cloud environment provides the highest cloud bandwidth of 10Gbps.)

Horovod [90], built atop an earlier work [11], uses a decentralized aggregation pattern with model-replica training jobs similar to CARAMEL. Horovod also adds communication ops to dataflow DAG of TensorFlow. However, it redirects the communication to MPI or NCCL allreduce implementations with limited optimizations on transfer. In contrast with Horovod, CARAMEL involves significant optimization for overlap improvement and communication cost reduction using fine-grained scheduling and batching. The large performance benefits of CARAMEL over Horovod is due to these model- and network-aware optimizations.

ByteScheduler [82], a generic scheduler for both PS and AllReduce with network-only optimizations, has limitations for AllReduce workloads. It needs custom implementation for every accelerator and network fabric. Currently, it only supports NVIDIA GPUs but not CPU/TPU. Caramel works with all hardware supported by TensorFlow out of the box. ByteScheduler also requires an out-of-DAG implementation of parameter optimization and only supports SGD, Adam and RMSprop currently[2]. Caramel supports all TensorFlow optimizers and auxiliary services such as checkpointing without any modification. The random execution order of transfers, which could cause deadlock and underutilized network and pipelining of parameters, are other problems in AllReduce that only Caramel tackles.

More importantly, prior work in this space requires changes to the underlying framework: P3 [56] modified KVServer in MXNet, TicTac [46] modified WorkerService in TensorFlow, ByteScheduler [82] uses out-of-DAG scheduler. Caramel works with vanilla TensorFlow without any changes to the underlying framework.

7.10 CONCLUSION

Iteration time in distributed DNN training in cloud environment is often bottlenecked by network transfers. In this paper, we develop Caramel to accelerate DNN training through network transfer optimizations. Caramel identifies the appropriate aggregation pattern for a given network environment to reduce the communication cost. The communication/computation overlap is improved with model- and network-aware optimizations. High performance gains achieved by decentralized aggregation patterns in Caramel motivates further research in decentralized aggregation mechanisms tailored for cloud environments.

[2] https://github.com/bytedance/byteps/blob/e4bbd24747470941bb5b76f542d4e8b2a9d02e1a/example/pytorch/benchmark_bytescheduler.py#L26

CHAPTER 8: CONCLUSION

This dissertation investigates the performance challenges of scaling out ML jobs which stem from resource interdependency. We show how poor timing of the network transfers may lead to accelerator underutilization, changes to workflow DAG could improve network utilization while prevent network congestion, an untuned I/O pipeline blocks the computation, and I/O delivery unfairness could cause the struggling worker effect.

Several systems and toolkits are introduced in this work to address these challenges:

First, we have developed a set of performance observability toolkit to bring transparency to the execution. Our distributed tracing expands the application-level performance tracing to multi-machine jobs. Our visualization framework facilities the data exploration while retaining the details of events. `tensorflow-tracer` brings the observability to production.

Second, we have developed `diot` to automatically find the best configuration to maximize I/O throughput and examine I/O delivery fairness in a distributed file storage.

Third, `TicTac` addresses the problem of network transfer poor timing. We introduce a performance model to evaluate the execution order quantitatively. Later, we design two approximation algorithms to find the near-optimal order. Finally, we modify the TensorFlow to enforce the order on the RPC calls.

Forth, `Caramel` addresses the network underutilization problem by making changes to the DAG and the order of computation. Our system chooses the best aggregation network primitive for the load, batches the parameters before handing them over to the network, and move parameter updates to forward-pass to extends network activity throughout the iteration.

Lastly, `TimedRPC` addresses the problem of adequately enforcing an order to the execution. We show that correct order enforcing is achievable by priority-based scheduling with network transfer preemption. Our RPC framework implements this scheduling strategy and approximately provides the preemption by splitting transfers into smaller pieces.

8.1 LIMITATIONS

This thesis studies the effect of enforcing the right timing of resource in the workloads with tightly-coupled resource dependencies. However, disproportional resource load where only a single resource dominates the execution time, fades the benefit of right timing. Figure 8.1 shows two examples where computation to network ratio is either extremely small or extremely large. In both cases, the difference between the best-case scenario and the

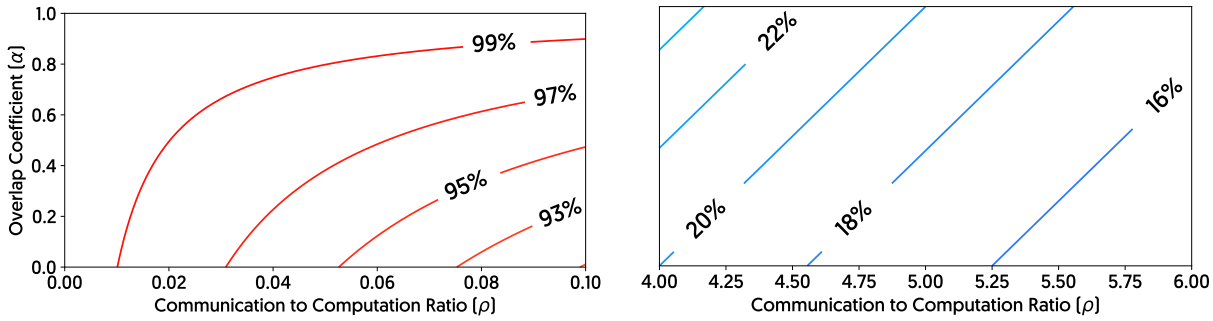

(a) Extreme Computation Load

(b) Extreme Network Load

Figure 8.1: Demonstration of Disproportional Resource Load

worth-case is less than 5%.

Furthermore, many of the assumptions and solutions in this dissertation presume workload is presented in a DAG form. However, this work needs to revisit if a more general representation replaces DAG.

8.2 FUTURE WORKS

Explicitly timing the execution of distributed ML workload is the central idea in this dissertation. This section discusses multiple directions to expand upon this idea:

Resources: This dissertation has explored the timing of I/O, network transfers, computation, and their interplay. An organic expansion to this work is to explore other critical resources in an ML workload such as host memory, accelerator memory, caches, and accelerator-host data bus. For example, timing can enforce the execution to reduce memory utilization or increases cache efficiency. Moreover, a generalized solution could combine the efficiency of multiple resources and their inter-dependency to introduce a holistic execution executor in complex machine learning systems.

Timing Representation: DAG is an established workload representation for ML workloads, which clearly expresses the data and control dependencies. However, this representation leaves the runtime to choose an execution path from multiple options with very different performance outcomes. To help the runtime to take the more performant path, in this work we include additional data in the DAG representing the timing dependencies: TicTac used per node priority metadata, and Caramel overloaded the control dependencies to put more restrictions on the execution.

A research direction toward addressing this issue is a universal language to express the timing dependencies between nodes. This language needs to be expressive enough to be able

to represent the complex resource inter-dependencies while keeps the runtime performance in mind. Ultimately this universal timing language could decouple the process of finding an optimal execution timing from the enforcing of such execution path in runtime.

Heuristics: The optimization problems in the execution timing are often NP-Hard or harder. In this work, we used mostly empirical hand-crafted heuristics to approximate the optimal solutions. Future researches could look at alternative approaches to solve these hard problems. For example, with the current advancement in Deep Reinforcement Learning, it seems ML could find approximations that are better suited for the workload in hand. Equally important, this ML-driven approach could result in cost reduction in grid search optimization methods such as one we used in Diot.

Workloads: This thesis mainly focuses on distributed training workloads with expensive computation and frequent communication between steps. There are other classes of distributed ML workloads with vastly different characteristics that can benefit from execution timing. Examples of such workloads are embarrassingly parallel jobs such as Hyperparameter tuning or batch inferences.

REFERENCES

[1] Martin Abadi, Paul Barham, Jianmin Chen, Zhifeng Chen, Andy Davis, Jeffrey Dean, Matthieu Devin, Sanjay Ghemawat, Geoffrey Irving, Michael Isard, Manjunath Kudlur, Josh Levenberg, Rajat Monga, Sherry Moore, Derek G. Murray, Benoit Steiner, Paul Tucker, Vijay Vasudevan, Pete Warden, Martin Wicke, Yuan Yu, and Xiaoqiang Zheng. 2016. TensorFlow: A system for large-scale machine learning. In *12th USENIX Symposium on Operating Systems Design and Implementation (OSDI 16)*. 265–283.

[2] Sami Abu-El-Haija, Nisarg Kothari, Joonseok Lee, Paul Natsev, George Toderici, Balakrishnan Varadarajan, and Sudheendra Vijayanarasimhan. 2016. Youtube-8m: A large-scale video classification benchmark. *arXiv preprint arXiv:1609.08675* (2016).

[3] Akshay Agrawal, Akshay Naresh Modi, Alexandre Passos, Allen Lavoie, Ashish Agarwal, Asim Shankar, Igor Ganichev, Josh Levenberg, Mingsheng Hong, Rajat Monga, and Shanqing Cai. 2019. TensorFlow Eager: A Multi-Stage, Python-Embedded DSL for Machine Learning. *arXiv e-prints*, Article arXiv:1903.01855 (Feb. 2019), arXiv:1903.01855 pages. arXiv:cs.PL/1903.01855

[4] Takuya Akiba, Shuji Suzuki, and Keisuke Fukuda. 2017. Extremely Large Minibatch SGD: Training ResNet-50 on ImageNet in 15 Minutes. *CoRR* abs/1711.04325 (2017). arXiv:1711.04325 `http://arxiv.org/abs/1711.04325`

[5] Dan Alistarh, Demjan Grubic, Jerry Li, Ryota Tomioka, and Milan Vojnovic. 2017. QSGD: Communication-Efficient SGD via Gradient Quantization and Encoding. In *Advances in Neural Information Processing Systems*. 1707–1718.

[6] Gene M Amdahl. 1967. Validity of the single processor approach to achieving large scale computing capabilities. In *Proceedings of the April 18-20, 1967, spring joint computer conference*. ACM, 483–485.

[7] Dario Amodei, Rishita Anubhai, Eric Battenberg, Carl Case, Jared Casper, Bryan Catanzaro, Jingdong Chen, Mike Chrzanowski, Adam Coates, Greg Diamos, Erich Elsen, Jesse Engel, Linxi Fan, Christopher Fougner, Tony Han, Awni Y. Hannun, Billy Jun, Patrick LeGresley, Libby Lin, Sharan Narang, Andrew Y. Ng, Sherjil Ozair, Ryan Prenger, Jonathan Raiman, Sanjeev Satheesh, David Seetapun, Shubho Sengupta, Yi Wang, Zhiqian Wang, Chong Wang, Bo Xiao, Dani Yogatama, Jun Zhan, and Zhenyao Zhu. 2015. Deep Speech 2: End-to-End Speech Recognition in English and Mandarin. *CoRR* abs/1512.02595 (2015). `http://arxiv.org/abs/1512.02595`

[8] Sebastien Arnold. 2016. An Introduction to Distributed Deep Learning. `https://seba1511.com/dist_blog/`.

[9] Jens Axboe. 2019. Flexible I/O tester. *Retrieved Augest* (2019).

[10] Mohammad Babaeizadeh, Chelsea Finn, Dumitru Erhan, Roy Campbell, and Sergey Levine. 2018. Stochastic Variational Video Prediction. `https://openreview.net/pdf?id=rk49Mg-CW`

[11] Baidu Research. 2016. baidu-allreduce. `https://github.com/baidu-research/baidu-allreduce`.

[12] Paul Barham and Michael Isard. 2019. Machine Learning Systems Are Stuck in a Rut. In *Proceedings of the Workshop on Hot Topics in Operating Systems (HotOS '19)*. ACM, New York, NY, USA, 177–183. `https://doi.org/10.1145/3317550.3321441`

[13] Mike Barnett, Lance Shuler, Robert van De Geijn, Satya Gupta, David G Payne, and Jerrell Watts. 1994. Interprocessor collective communication library (InterCom). In *Scalable High-Performance Computing Conference, 1994., Proceedings of the*. IEEE, 357–364.

[14] Tal Ben-Nun and Torsten Hoefler. 2018. Demystifying parallel and distributed deep learning: An in-depth concurrency analysis. *arXiv preprint arXiv:1802.09941* (2018).

[15] Léon Bottou. 2010. Large-Scale Machine Learning with Stochastic Gradient Descent. In *Proceedings of COMPSTAT'2010*, Yves Lechevallier and Gilbert Saporta (Eds.). Physica-Verlag HD, Heidelberg, 177–186.

[16] Léon Bottou and Olivier Bousquet. 2008. The tradeoffs of large scale learning. In *Advances in neural information processing systems*. 161–168.

[17] Google Brain. [n. d.]. Distributed TensorFlow. `https://www.tensorflow.org/deploy/distributed`.

[18] Google Brain. Accessed: February 15, 2019. TensorBoard: Visualizing Learning. `https://www.tensorflow.org/guide/summaries_and_tensorboard`.

[19] Peter Brucker and Sigrid Knust. 2007. Complexity results for scheduling problems.

[20] Liang-Chieh Chen, Yukun Zhu, George Papandreou, Florian Schroff, and Hartwig Adam. 2018. Encoder-decoder with atrous separable convolution for semantic image segmentation. In *Proceedings of the European conference on computer vision (ECCV)*. 801–818.

[21] Tianqi Chen, Mu Li, Yutian Li, Min Lin, Naiyan Wang, Minjie Wang, Tianjun Xiao, Bing Xu, Chiyuan Zhang, and Zheng Zhang. 2015. Mxnet: A flexible and efficient machine learning library for heterogeneous distributed systems. *arXiv preprint arXiv:1512.01274* (2015).

[22] Tianqi Chen, Thierry Moreau, Ziheng Jiang, Haichen Shen, Eddie Q Yan, Leyuan Wang, Yuwei Hu, Luis Ceze, Carlos Guestrin, and Arvind Krishnamurthy. 2018. TVM: end-to-end optimization stack for deep learning. *arXiv preprint arXiv:1802.04799* (2018), 1–15.

[23] Yanpei Chen, Rean Griffith, Junda Liu, Randy H Katz, and Anthony D Joseph. 2009. Understanding TCP incast throughput collapse in datacenter networks. In *Proceedings of the 1st ACM workshop on Research on enterprise networking*. ACM, 73–82.

[24] Trishul M Chilimbi, Yutaka Suzue, Johnson Apacible, and Karthik Kalyanaraman. 2014. Project Adam: Building an Efficient and Scalable Deep Learning Training System.. In *OSDI*, Vol. 14. 571–582.

[25] Minsik Cho, Ulrich Finkler, Sameer Kumar, David Kung, Vaibhav Saxena, and Dheeraj Sreedhar. 2017. PowerAI DDL. *arXiv preprint arXiv:1708.02188* (2017).

[26] François Chollet. 2015. Keras: Deep Learning for humans. `https://keras.io`.

[27] Matthieu Courbariaux, Yoshua Bengio, and Jean-Pierre David. 2015. Binaryconnect: Training deep neural networks with binary weights during propagations. In *Advances in neural information processing systems*. 3123–3131.

[28] Henggang Cui, Alexey Tumanov, Jinliang Wei, Lianghong Xu, Wei Dai, Jesse Haber-Kucharsky, Qirong Ho, Gregory R Ganger, Phillip B Gibbons, Garth A Gibson, et al. 2014. Exploiting iterative-ness for parallel ML computations. In *Proceedings of the ACM Symposium on Cloud Computing*. ACM, 1–14.

[29] Henggang Cui, Hao Zhang, Gregory R Ganger, Phillip B Gibbons, and Eric P Xing. 2016. GeePS: Scalable deep learning on distributed GPUs with a GPU-specialized parameter server. In *Proceedings of the Eleventh European Conference on Computer Systems*. ACM, 4.

[30] Abdul Dakkak, Cheng Li, Abhishek Srivastava, Jinjun Xiong, and Wen-Mei Hwu. 2018. MLModelScope: Evaluate and Measure ML Models within AI Pipelines. *arXiv preprint arXiv:1811.09737* (2018).

[31] Jeffrey Dean, Greg Corrado, Rajat Monga, Kai Chen, Matthieu Devin, Mark Mao, Andrew Senior, Paul Tucker, Ke Yang, Quoc V Le, et al. 2012. Large scale distributed deep networks. In *Advances in neural information processing systems*. 1223–1231.

[32] Jeffrey Dean and Sanjay Ghemawat. 2004. MapReduce: Simplified Data Processing on Large Clusters. In *Proceedings of the 6th Conference on Symposium on Opearting Systems Design & Implementation - Volume 6 (OSDI'04)*. USENIX Association, Berkeley, CA, USA, 10–10. `http://dl.acm.org/citation.cfm?id=1251254.1251264`

[33] Jia Deng, Wei Dong, Richard Socher, Li-Jia Li, Kai Li, and Li Fei-Fei. 2009. Imagenet: A large-scale hierarchical image database. In *2009 IEEE conference on computer vision and pattern recognition*. Ieee, 248–255.

[34] National Center for Supercomputing Applications (NCSA) at the University of Illinois. 2018. Deep Learning Major Research Instrument Project. `http://www.ncsa.illinois.edu/enabling/data/deep_learning`

[35] Sanjay Ghemawat, Howard Gobioff, and Shun-Tak Leung. 2003. The Google file system. (2003).

[36] Ian Goodfellow, Yoshua Bengio, and Aaron Courville. 2016. *Deep learning*. MIT press.

[37] Priya Goyal, Piotr Dollár, Ross Girshick, Pieter Noordhuis, Lukasz Wesolowski, Aapo Kyrola, Andrew Tulloch, Yangqing Jia, and Kaiming He. 2017. Accurate, Large Minibatch SGD: Training ImageNet in 1 Hour. *arXiv preprint arXiv:1706.02677* (2017).

[38] Richard L Graham, Timothy S Woodall, and Jeffrey M Squyres. 2005. Open MPI: A flexible high performance MPI. In *International Conference on Parallel Processing and Applied Mathematics*. Springer, 228–239.

[39] Brendan Gregg. 2013. *Systems performance: enterprise and the cloud*. Pearson Education.

[40] William Gropp, Ewing Lusk, and Anthony Skjellum. 1999. *Using MPI: portable parallel programming with the message-passing interface*. Vol. 1. MIT press.

[41] Suyog Gupta, Ankur Agrawal, Kailash Gopalakrishnan, and Pritish Narayanan. 2015. Deep learning with limited numerical precision. In *International Conference on Machine Learning*. 1737–1746.

[42] Sayed Hadi Hashemi. 2018. TensorFlow Runtime Tracing Metadata Visualization. `https://github.com/xldrx/tensorflow-runtime-metadata-visualization`.

[43] Sayed Hadi Hashemi and Roy Campbell. 2018. Making a Case for Timed RPCs in Iterative Systems. *Poster Presentation in USENIX Symposium on Operating Systems Design and Implementation (OSDI)*.

[44] Sayed Hadi Hashemi, Sangeetha Abdu Jyothi, and Roy Campbell. 2018. Network Efficiency through Model-Awareness in Distributed Machine Learning Systems. *Poster Presentation in USENIX Symposium on Networked Systems Design and Implementation (NSDI)*.

[45] Sayed Hadi Hashemi, Sangeetha Abdu Jyothi, and Roy Campbell. 2018. On The Importance of Execution Ordering in Graph-Based Distributed Machine Learning Systems. *The Conference of Systems and Machine Learning*.

[46] Sayed Hadi Hashemi, Sangeetha Abdu Jyothi, and Roy H Campbell. 2019. TicTac: Improving Distributed Deep Learning with Communication Scheduling. *The Conference of Systems and Machine Learning*.

[47] Sayed Hadi Hashemi, Shadi A. Noghabi, William Gropp, and Roy H. Campbell. 2016. Performance Modeling of Distributed Deep Neural Networks. *CoRR* abs/1612.00521 (2016). arXiv:1612.00521 `http://arxiv.org/abs/1612.00521`

[48] Sayed Hadi Hashemi, Paul Rausch, Benjamin Rabe, Kuan-Yen Chou, Simeng Liu, Volodymyr Kindratenko, and Roy H Campbell. 2019. tensorflow-tracing: A Performance Tuning Framework for Production. In *2019 {USENIX} Conference on Operational Machine Learning (OpML 19)*. 31–33.

[49] Kaiming He, Xiangyu Zhang, Shaoqing Ren, and Jian Sun. 2015. Deep Residual Learning for Image Recognition. *CoRR* abs/1512.03385 (2015). arXiv:1512.03385 `http://arxiv.org/abs/1512.03385`

[50] Kaiming He, Xiangyu Zhang, Shaoqing Ren, and Jian Sun. 2016. Identity Mappings in Deep Residual Networks. *CoRR* abs/1603.05027 (2016). arXiv:1603.05027 `http://arxiv.org/abs/1603.05027`

[51] Imranul Hoque and Indranil Gupta. 2013. LFGraph: Simple and fast distributed graph analytics. In *Proceedings of the First ACM SIGOPS Conference on Timely Results in Operating Systems*. ACM, 9.

[52] Forrest N. Iandola, Matthew W. Moskewicz, Khalid Ashraf, and Kurt Keutzer. 2016. FireCaffe: Near-Linear Acceleration of Deep Neural Network Training on Compute Clusters. In *2016 IEEE Conference on Computer Vision and Pattern Recognition, CVPR 2016, Las Vegas, NV, USA, June 27-30, 2016*. 2592–2600. `https://doi.org/10.1109/CVPR.2016.284`

[53] Grant Ingersoll. 2009. Introducing apache mahout. *Scalable, commercialfriendly machine learning for building intelligent applications. IBM* (2009).

[54] Intel. 2019. PlaidML: a platform for making deep learning work everywhere. `https://ai.intel.com/plaidml`

[55] Sergey Ioffe and Christian Szegedy. 2015. Batch Normalization: Accelerating Deep Network Training by Reducing Internal Covariate Shift. *CoRR* abs/1502.03167 (2015). arXiv:1502.03167 `http://arxiv.org/abs/1502.03167`

[56] Anand Jayarajan, Jinliang Wei, Alexandra Fedorova, and Gennady Pekhimenko. 2019. Priority-based Parameter Propagation for Distributed DNN Training. *The Conference of Systems and Machine Learning*.

[57] Xianyan Jia, Shutao Song, Wei He, Yangzihao Wang, Haidong Rong, Feihu Zhou, Liqiang Xie, Zhenyu Guo, Yuanzhou Yang, Liwei Yu, et al. 2018. Highly scalable deep learning training system with mixed-precision: Training imagenet in four minutes. *arXiv preprint arXiv:1807.11205* (2018).

[58] Yangqing Jia, Evan Shelhamer, Jeff Donahue, Sergey Karayev, Jonathan Long, Ross Girshick, Sergio Guadarrama, and Trevor Darrell. 2014. Caffe: Convolutional architecture for fast feature embedding. In *Proceedings of the 22nd ACM international conference on Multimedia*. ACM, 675–678.

[59] Norman P Jouppi, Cliff Young, Nishant Patil, David Patterson, Gaurav Agrawal, Raminder Bajwa, Sarah Bates, Suresh Bhatia, Nan Boden, Al Borchers, et al. 2017. In-datacenter performance analysis of a tensor processing unit. In *2017 ACM/IEEE 44th Annual International Symposium on Computer Architecture (ISCA)*. IEEE, 1–12.

[60] Nitish Shirish Keskar, Dheevatsa Mudigere, Jorge Nocedal, Mikhail Smelyanskiy, and Ping Tak Peter Tang. 2016. On large-batch training for deep learning: Generalization gap and sharp minima. *arXiv preprint arXiv:1609.04836* (2016).

[61] Janis Keuper. 2016. Distributed Training of Deep Neuronal Networks: Theoretical and Practical Limits of Parallel Scalability. *CoRR* abs/1609.06870 (2016). arXiv:1609.06870 `http://arxiv.org/abs/1609.06870`

[62] Jack Kiefer, Jacob Wolfowitz, et al. 1952. Stochastic estimation of the maximum of a regression function. *The Annals of Mathematical Statistics* 23, 3 (1952), 462–466.

[63] Alex Krizhevsky. 2014. One weird trick for parallelizing convolutional neural networks. *arXiv preprint arXiv:1404.5997* (2014).

[64] Alex Krizhevsky, Ilya Sutskever, and Geoffrey E Hinton. 2012. Imagenet classification with deep convolutional neural networks. In *Advances in neural information processing systems*. 1097–1105.

[65] Thorsten Kurth, Sean Treichler, Joshua Romero, Mayur Mudigonda, Nathan Luehr, Everett H. Phillips, Ankur Mahesh, Michael Matheson, Jack Deslippe, Massimiliano Fatica, Prabhat, and Michael Houston. 2018. Exascale Deep Learning for Climate Analytics. *CoRR* abs/1810.01993 (2018). arXiv:1810.01993 `http://arxiv.org/abs/1810.01993`

[66] Chris Leary and Todd Wang. 2017. XLA: TensorFlow, compiled. *TensorFlow Dev Summit* (2017).

[67] Yann LeCun, Yoshua Bengio, and Geoffrey Hinton. 2015. Deep learning. *nature* 521, 7553 (2015), 436.

[68] Mu Li, David G. Andersen, Jun Woo Park, Alexander J. Smola, Amr Ahmed, Vanja Josifovski, James Long, Eugene J. Shekita, and Bor-Yiing Su. 2014. Scaling Distributed Machine Learning with the Parameter Server. In *11th USENIX Symposium on Operating Systems Design and Implementation (OSDI 14)*. USENIX Association, Broomfield, CO, 583–598. `https://www.usenix.org/conference/osdi14/technical-sessions/presentation/li_mu`

[69] Zhenyu Li, James Davis, and Stephen Jarvis. 2017. An Efficient Task-based All-Reduce for Machine Learning Applications. In *Proceedings of the Machine Learning on HPC Environments (MLHPC'17)*. ACM, New York, NY, USA, Article 2, 8 pages. `https://doi.org/10.1145/3146347.3146350`

[70] Grzegorz Malewicz, Matthew H Austern, Aart JC Bik, James C Dehnert, Ilan Horn, Naty Leiser, and Grzegorz Czajkowski. 2010. Pregel: a system for large-scale graph processing. In *Proceedings of the 2010 ACM SIGMOD International Conference on Management of data*. ACM, 135–146.

[71] D. Martin, C. Fowlkes, D. Tal, and J. Malik. 2001. A Database of Human Segmented Natural Images and its Application to Evaluating Segmentation Algorithms and Measuring Ecological Statistics. In *Proc. 8th Int'l Conf. Computer Vision*, Vol. 2. 416–423.

[72] Xiangrui Meng, Joseph Bradley, Burak Yavuz, Evan Sparks, Shivaram Venkataraman, Davies Liu, Jeremy Freeman, DB Tsai, Manish Amde, Sean Owen, et al. 2016. Mllib: Machine learning in apache spark. *The Journal of Machine Learning Research* 17, 1 (2016), 1235–1241.

[73] A. Metzger, P. Leitner, D. Ivanović, E. Schmieders, R. Franklin, M. Carro, S. Dustdar, and K. Pohl. 2015. Comparing and Combining Predictive Business Process Monitoring Techniques. *IEEE Transactions on Systems, Man, and Cybernetics: Systems* 45, 2 (2015), 276–290.

[74] Azalia Mirhoseini, Anna Goldie, Hieu Pham, Benoit Steiner, Quoc V. Le, and Jeff Dean. 2018. Hierarchical Planning for Device Placement. `https://openreview.net/pdf?id=Hkc-TeZ0W`

[75] Azalia Mirhoseini, Hieu Pham, Quoc Le, Mohammad Norouzi, Samy Bengio, Benoit Steiner, Yuefeng Zhou, Naveen Kumar, Rasmus Larsen, and Jeff Dean. 2017. Device Placement Optimization with Reinforcement Learning. `https://arxiv.org/abs/1706.04972`

[76] Tom M Mitchell et al. 1997. Machine learning. 1997. *Burr Ridge, IL: McGraw Hill* 45, 37 (1997), 870–877.

[77] Dan Moldovan, James Decker, Fei Wang, Andrew Johnson, Brian Lee, Zack Nado, D Sculley, Tiark Rompf, and Alexander B Wiltschko. 2019. AutoGraph: Imperative-style Coding with Graph-based Performance. In *SysML*.

[78] Yuval Netzer, Tao Wang, Adam Coates, Alessandro Bissacco, Bo Wu, and Andrew Y Ng. 2011. Reading digits in natural images with unsupervised feature learning. (2011).

[79] University of Illinois at Urbana-Champaign. 2013. Illinois Campus Cluster Program. `https://campuscluster.illinois.edu`

[80] Adam Paszke, Sam Gross, Soumith Chintala, and Gregory Chanan. 2017. PyTorch: Tensors and dynamic neural networks in Python with strong GPU acceleration.

[81] Adam Paszke, Sam Gross, Soumith Chintala, Gregory Chanan, Edward Yang, Zachary DeVito, Zeming Lin, Alban Desmaison, Luca Antiga, and Adam Lerer. 2017. Automatic differentiation in pytorch. (2017).

[82] Yanghua Peng, Yibo Zhu, Yangrui Chen, Yixin Bao, Bairen Yi, Chang Lan, Chuan Wu, and Chuanxiong Guo. 2019. A Generic Communication Scheduler for Distributed DNN Training Acceleration. In *Proceedings of the 27th ACM Symposium on Operating Systems Principles (SOSP '19)*. Association for Computing Machinery, New York, NY, USA, 16–29. `https://doi.org/10.1145/3341301.3359642`

[83] Michael L. Pinedo. 2008. *Scheduling: Theory, Algorithms, and Systems* (3rd ed.). Springer Publishing Company, Incorporated.

[84] Bryan A Plummer, Liwei Wang, Chris M Cervantes, Juan C Caicedo, Julia Hockenmaier, and Svetlana Lazebnik. 2015. Flickr30k entities: Collecting region-to-phrase correspondences for richer image-to-sentence models. In *Proceedings of the IEEE international conference on computer vision*. 2641–2649.

[85] Herbert Robbins and Sutton Monro. 1951. A stochastic approximation method. *The annals of mathematical statistics* (1951), 400–407.

[86] David E Rumelhart, Geoffrey E Hinton, Ronald J Williams, et al. 1988. Learning representations by back-propagating errors. *Cognitive modeling* 5, 3 (1988), 1.

[87] Frank B Schmuck and Roger L Haskin. 2002. GPFS: A Shared-Disk File System for Large Computing Clusters.. In *FAST*, Vol. 2.

[88] Philip Schwan et al. 2003. Lustre: Building a file system for 1000-node clusters. In *Proceedings of the 2003 Linux symposium*, Vol. 2003. 380–386.

[89] Frank Seide and Amit Agarwal. 2016. CNTK: Microsoft's open-source deep-learning toolkit. In *Proceedings of the 22nd ACM SIGKDD International Conference on Knowledge Discovery and Data Mining*. ACM, 2135–2135.

[90] Alexander Sergeev and Mike Del Balso. 2018. Horovod: fast and easy distributed deep learning in TensorFlow. *CoRR* abs/1802.05799 (2018). arXiv:1802.05799 `http://arxiv.org/abs/1802.05799`

[91] Spencer Shepler, Mike Eisler, David Robinson, Brent Callaghan, Robert Thurlow, David Noveck, and Carl Beame. 2003. Network file system (NFS) version 4 protocol. *Network* (2003).

[92] Ben Shneiderman. 2003. The eyes have it: A task by data type taxonomy for information visualizations. In *The craft of information visualization*. Elsevier, 364–371.

[93] Konstantin Shvachko, Hairong Kuang, Sanjay Radia, Robert Chansler, et al. 2010. The hadoop distributed file system.. In *MSST*, Vol. 10. 1–10.

[94] Svetlana Sicular and Kenneth Brant. 2018. Hype Cycle for Artificial Intelligence, 2018. (July 2018).

[95] Karen Simonyan and Andrew Zisserman. 2014. Very deep convolutional networks for large-scale image recognition. *arXiv preprint arXiv:1409.1556* (2014).

[96] Srinivas Sridharan, Karthikeyan Vaidyanathan, Dhiraj Kalamkar, Dipankar Das, Mikhail E Smorkalov, Mikhail Shiryaev, Dheevatsa Mudigere, Naveen Mellempudi, Sasikanth Avancha, Bharat Kaul, et al. 2018. On Scale-out Deep Learning Training for Cloud and HPC. *arXiv preprint arXiv:1801.08030* (2018).

[97] Christian Szegedy, Wei Liu, Yangqing Jia, Pierre Sermanet, Scott E. Reed, Dragomir Anguelov, Dumitru Erhan, Vincent Vanhoucke, and Andrew Rabinovich. 2014. Going Deeper with Convolutions. *CoRR* abs/1409.4842 (2014). arXiv:1409.4842 `http://arxiv.org/abs/1409.4842`

[98] Christian Szegedy, Vincent Vanhoucke, Sergey Ioffe, Jonathon Shlens, and Zbigniew Wojna. 2015. Rethinking the Inception Architecture for Computer Vision. *CoRR* abs/1512.00567 (2015). arXiv:1512.00567 `http://arxiv.org/abs/1512.00567`

[99] Christian Szegedy, Vincent Vanhoucke, Sergey Ioffe, Jon Shlens, and Zbigniew Wojna. 2016. Rethinking the inception architecture for computer vision. In *Proceedings of the IEEE conference on computer vision and pattern recognition*. 2818–2826.

[100] Bokeh Development Team. 2014. Bokeh: Python library for interactive visualization. (2014).

[101] TensorFlow. 2019. tf.distribute.experimental.MultiWorkerMirroredStrategy. `https://www.tensorflow.org/api_docs/python/tf/distribute/experimental/MultiWorkerMirroredStrategy`. (Accessed on 09/09/2019).

[102] Rajeev Thakur and William D Gropp. 2003. Improving the performance of collective operations in MPICH. In *European Parallel Virtual Machine/Message Passing Interface Users' Group Meeting*. Springer, 257–267.

[103] Philippe Tillet, HT Kung, and David Cox. 2019. Triton: an intermediate language and compiler for tiled neural network computations. In *Proceedings of the 3rd ACM SIGPLAN International Workshop on Machine Learning and Programming Languages*. ACM, 10–19.

[104] Seiya Tokui, Kenta Oono, Shohei Hido, and Justin Clayton. 2015. Chainer: a next-generation open source framework for deep learning. In *Proceedings of workshop on machine learning systems (LearningSys) in the twenty-ninth annual conference on neural information processing systems (NIPS)*, Vol. 5. 1–6.

[105] Vincent Vanhoucke, Andrew Senior, and Mark Z Mao. 2011. Improving the speed of neural networks on CPUs. In *Proc. Deep Learning and Unsupervised Feature Learning NIPS Workshop*, Vol. 1. Citeseer, 4.

[106] Ashish Vaswani, Samy Bengio, Eugene Brevdo, Francois Chollet, Aidan N Gomez, Stephan Gouws, Llion Jones, Łukasz Kaiser, Nal Kalchbrenner, Niki Parmar, et al. 2018. Tensor2tensor for neural machine translation. *arXiv preprint arXiv:1803.07416* (2018).

[107] Vinod Kumar Vavilapalli, Arun C Murthy, Chris Douglas, Sharad Agarwal, Mahadev Konar, Robert Evans, Thomas Graves, Jason Lowe, Hitesh Shah, Siddharth Seth, et al. 2013. Apache hadoop yarn: Yet another resource negotiator. In *Proceedings of the 4th annual Symposium on Cloud Computing*. ACM, 5.

[108] Abhishek Verma, Luis Pedrosa, Madhukar Korupolu, David Oppenheimer, Eric Tune, and John Wilkes. 2015. Large-scale cluster management at Google with Borg. In *Proceedings of the Tenth European Conference on Computer Systems*. ACM, 18.

[109] Wei Wen, Cong Xu, Feng Yan, Chunpeng Wu, Yandan Wang, Yiran Chen, and Hai Li. 2017. Terngrad: Ternary gradients to reduce communication in distributed deep learning. In *Advances in Neural Information Processing Systems*. 1508–1518.

[110] Reynold S Xin, Joseph E Gonzalez, Michael J Franklin, and Ion Stoica. 2013. Graphx: A resilient distributed graph system on spark. In *First International Workshop on Graph Data Management Experiences and Systems*. ACM, 2.

[111] Arvind Thiagarajan Yi Zhuang and Tim Sweeney. 2019. Ranking Tweets with TensorFlow. `https://medium.com/tensorflow/ranking-tweets-with-tensorflow-932d449b7c4`

[112] Yang You, Igor Gitman, and Boris Ginsburg. 2017. Scaling sgd batch size to 32k for imagenet training. *arXiv preprint arXiv:1708.03888* 6 (2017).

[113] Yang You, Zhao Zhang, Cho-Jui Hsieh, and James Demmel. 2017. 100-epoch ImageNet Training with AlexNet in 24 Minutes. *CoRR* abs/1709.05011 (2017). arXiv:1709.05011 `http://arxiv.org/abs/1709.05011`

[114] Yuan Yu, Martín Abadi, Paul Barham, Eugene Brevdo, Mike Burrows, Andy Davis, Jeff Dean, Sanjay Ghemawat, Tim Harley, Peter Hawkins, Michael Isard, Manjunath Kudlur, Rajat Monga, Derek Murray, and Xiaoqiang Zheng. 2018. Dynamic Control Flow in Large-scale Machine Learning. In *Proceedings of the Thirteenth EuroSys Conference (EuroSys '18)*. ACM, New York, NY, USA, Article 18, 15 pages. `https://doi.org/10.1145/3190508.3190551`

[115] Matei Zaharia, Mosharaf Chowdhury, Michael J Franklin, Scott Shenker, and Ion Stoica. 2010. Spark: Cluster computing with working sets. *HotCloud* 10, 10-10 (2010), 95.

[116] Hao Zhang, Zeyu Zheng, Shizhen Xu, Wei Dai, Qirong Ho, Xiaodan Liang, Zhiting Hu, Jinliang Wei, Pengtao Xie, and Eric P. Xing. 2017. Poseidon: An Efficient Communication Architecture for Distributed Deep Learning on GPU Clusters. In *2017 USENIX Annual Technical Conference (USENIX ATC 17)*. USENIX Association, Santa Clara, CA, 181–193. `https://www.usenix.org/conference/atc17/technical-sessions/presentation/zhang`

[117] H. Zhao and J. Canny. 2014. Kylix: A Sparse Allreduce for Commodity Clusters. In *43rd International Conference on Parallel Processing*. 273–282. `https://doi.org/10.1109/ICPP.2014.36`